ECOLOGY AND EVOLUTION OF PLANT PHYSIOLOGICAL STRATEGIES USING LEAF STABLE ISOTOPES

A Dissertation

Presented to the Faculty of the Graduate School

of Cornell University

In Partial Fulfillment of the Requirements for the Degree of

Doctor of Philosophy

by

Elissa Marie Goud

May 2020

ECOLOGY AND EVOLUTION OF PLANT PHYSIOLOGICAL STRATEGIES USING LEAF STABLE ISOTOPES

Elissa Marie Goud, Ph. D.

Cornell University 2020

ABSTRACT

Determining the mechanisms that shape biodiversity is a central question in ecology and evolutionary biology. Presumably, environmental challenges exert important influences on organismal growth and survival, leading to diverse ecological strategies. One such challenge that terrestrial plants face is how to gain carbon for photosynthesis without losing too much water. This challenge arises from the fact that as carbon dioxide (CO_2) diffuses into leaves, water vapor simultaneously diffuses out, resulting in a tradeoff between leaf-level carbon gain and water loss. The need to maximize carbon gain while minimizing water loss has long been presumed to drive the evolution of diverse strategies by which plants adapt to variable environments. In this dissertation, I explore the macroevolution and ecological consequences of variation in plant physiological strategies, with a focus on leaf-level carbon and water exchange. In the first chapter, I introduce the concept of 'integrated metabolic strategy' (IMS) to describe the ratio between leaf carbon isotope composition ($\delta^{13}C$) and oxygen isotope composition above source water ($\Delta^{18}O$). IMS is a novel way of representing leaf carbon-water tradeoffs that are integrated over the lifespan of a leaf, thus avoiding problematic comparisons between instantaneous point measurements of metabolic fluctuations. I tested how metabolic strategies evolve among closely related yet ecologically diverse milkweed species, and subsequently addressed phenotypic plasticity in response to water availability in species with divergent strategies. In the second

chapter, I asked whether metabolic strategies vary among co-occurring species in a successional old field community in Ithaca, NY. I found considerable variation in $\delta^{13}C$, $\Delta^{18}O$, and IMS values among 18 perennial angiosperm species. Changes in species abundance over two years suggested that temporal variation in water availability (i.e., inter-annual precipitation) may be an important mechanism structuring functional diversity and species composition in this community. In the third chapter, I formally tested the hypothesis that inter-annual variation in growing season precipitation promotes metabolic diversity among old field Asteraceae species. Through the use of rainout shelters, I subjected the community to five water treatments to simulate the range of growing season water availabilities based on the long-term average in the region. Species differentially responded to variation in growing season water availability and, importantly, how they responded could be explained by differences in metabolism. Water-conservative species grew best in the dry treatments and had their minimal growth in wet treatments. Carbon-acquisitive species displayed the opposite pattern, with maximal growth in wet treatments and steep declines in dry treatments. Metabolic differences among co-occurring species may help explain temporal variation in growth, and could provide an underlying physiological mechanism for long-term dynamics that promote biodiversity. In the fourth chapter, I assessed the relative roles of phylogenetic history and environment on patterns of leaf $\delta^{13}C$ and nitrogen stable isotope ratios ($\delta^{15}N$) as integrators of physiological processes in a diverse group of Ericaceae species native to North America. The signal of phylogeny was generally stronger than that of the local environment, suggesting that close relatives have similar physiological strategies across this plant family. Examining ecological and evolutionary patterns of leaf stable isotopes across plant clades and within communities illustrates a previously under-appreciated role of metabolism for species distributions and community diversity.

BIOGRAPHICAL SKETCH

Elissa Marie Goud grew up in Quispamsis, New Brunswick, Canada and obtained a Bachelors of Agricultural and Environmental Sciences from McGill University in 2011 with a Major in Botanical Sciences. She obtained a Masters of Science in Geography from McGill University in 2015.

DEDICATION

This dissertation is dedicated to my son Aryeh.

ACKNOWLEDGEMENTS

I would like to thank my major advisor Dr. Jed Sparks for introducing me to the science and community of stable isotope ecology, for teaching me how to be a more thorough and conscientious scientist, and for showing me the kind of collaborator and educator I want to be. Thank you for your generosity in supporting my graduate research at Cornell, for giving me the opportunity to attend IsoCamp, and for welcoming me and my family into your home. I would also like to thank my doctoral advisory committee Dr. Monica Geber and Dr. Anurag Agrawal for their guidance and support. Monica, for your valuable perspective and feedback, for your attention to detail, and for your unending patience and steady hand. Thank you for caring so much about the growth and development of every graduate student in the department. Anurag, for sharing your enthusiastic approach to scientific inquiry, for your encouragement through the excitements and challenges over the years, and for teaching me how to be more accountable in all aspects of my science. Thank you for giving me the opportunity to work with and fall in love with milkweeds.

Great appreciation is given to Kim Sparks for her immeasurable help in the lab. I am indebted to my fellow graduate students at Cornell, and my lab and office mates for their help, valuable discussions and great friendship. Thanks to Drs Tim Moore and Marcia Waterway for their continued support and perspective on my academic journey and professional development. Countless thanks to my incredible friends, fellow musicians, and family for their love and encouragement and to my son, Aryeh, who is my greatest joy and motivator. Finally, I would like to express my special appreciation and thanks to my husband Michael. I am so grateful for all of his love, encouragement, and constant support throughout this process.

TABLE OF CONTENTS

ABSTRACT iii
LIST OF FIGURES vii
LIST OF TABLES x
CHAPTER ONE 1
Integrated metabolic strategy: A mechanistic framework for predicting carbon-water tradeoffs within plant clades 1
Abstract 1
Introduction 3
Methods 10
Results 17
Discussion 24
Literature Cited 33
CHAPTER TWO 43
Metabolic diversity: an important mechanism contributing to species diversity in ecological communities? 43
Abstract 43
Introduction 44
Material and methods 47
Results 53
Discussion 65
Literature Cited 72
CHAPTER THREE 76
Is variation in inter-annual precipitation a mechanism for maintaining plant metabolic diversity? 76
Abstract 76
Introduction 77
Methods 81
Results 86
Discussion 96
Literature Cited 105
CHAPTER FOUR 110
Leaf stable isotopes suggest shared ancestry is an important driver of functional diversity 110
Abstract 110
Introduction 111
Materials and methods 115
Results 119
Discussion 125
Literature Cited 131
APPENDIX 138
Appendix 1.1 138
Appendix 2.1 143
Appendix 3.1 145

LIST OF FIGURES

Figure 1.1: Conceptual model for variation in (A) leaf-level $\delta^{13}C$ and $\Delta^{18}O$ and (B) associated IMS values for different hypothetical plant species or individuals. 7
Figure 1.2: Maximum likelihood chronogram based on plastome sequences from 19 *Asclepias* taxa and the range of associated integrated metabolic strategies (IMS). Bootstrap values less than 100% are indicated at nodes. IMS colors among taxa correspond to the average IMS value of each Tukey post-hoc group, ranging from the lowest IMS values (0.39, black circles) to the largest IMS values (0.51, white circles). This phylogeny is missing *A. fascicularis* (see Methods), which would be placed in the clade containing *A. perennis* and *A. mexicana* (Fishbein et al. 2011).....15
Figure 1.3: Diversity in leaf morphology among juvenile *Asclepias* species used in this study. A) *A. curassavica*; B) *A. incarnata*; C) *A. californica*; D) *A. eriocarpa*; E) *A. pumila*; F) *A. verticillata*.....16
Figure 1.4: Relationships between A) $\delta^{13}C$ and $\Delta^{18}O$ of leaf cellulose ($p = 0.3$); B) integrated metabolic strategy (IMS) values, in order from lowest to highest IMS values; C) IMS values and $\delta^{13}C$ ($R^2 = 0.91$, $p < 0.0001$); and D) IMS and $\Delta^{18}O$ of leaf cellulose ($R^2 = 0.23$, $p = 0.033$) for 20 *Asclepias* taxa grown under common conditions. Larger IMS values indicate higher metabolic efficiency. Data are species means with standard error. Colors correspond to four distinct groups in mean IMS values based on Tukey post-hoc comparisons. 1 = *A. brachystephana*, 2 = *A. californica*, 3 = *A. curassavica*, 4 = *A. eriocarpa*, 5 = *A. fascicularis*, 6 = *A. incarnata* subsp. *incarnata*, 7 = *A. labriformis*, 8 = *A. latifolia*, 9 = *A. linaria*, 10 = *A. mexicana*, 11 = *A. perennis*, 12 = *A. incarnata* subsp. *pulchra*, 13 = *A. pumila*, 14 = *A. speciosa*, 15 = *A. subulata*, 16 = *A. subverticillata*, 17 = *A. syriaca*, 18 = *A. tuberosa*, 19 = *A. verticillata*, 20 = *A. viridis*. 21
Figure 1.5: Linear relationships based on ordinary least squares regressions (OLS, solid lines) and phylogenetic independent contrasts (PIC, dashed lines) between IMS and A) leaf size (OLS $R^2 = 0.26$*, PIC $R^2 = 0.36$*); B) stomatal conductance, g_s (OLS $R^2 = 0.06$, PIC $R^2 = 0.13$*); C) nitrogen content (OLS $R^2 = 0.23$*, PIC $R^2 = 0.45$**); and D) maximum rate of carboxylation, Vc_{max} (OLS $R^2 = 0.13$*, PIC $R^2 = 0.13$*) for 20 *Asclepias* taxa grown under common conditions. Data are raw species means, * $p < 0.05$, ** $p < 0.01$, *** $p < 0.0001$. 22
Figure 1.6: Results of one-way ANOVAs between A) IMS, B) biomass, C) $\delta^{13}C$, and D) $\Delta^{18}O$ for four *Asclepias* species grown under three different soil water treatments: dry (one-third field capacity), mesic (field capacity), and wet (twice field capacity). Data are means ± standard error (n=6). Asterisks indicate significant differences between water levels ($P < 0.05$), based on post-hoc Tukey tests. 23
Figure 2.1: Species composition and evolutionary relationships for 18 perennial angiosperm species co-occurring in a successional old field community in Ithaca, NY. Relative abundance (% cover) for each species, indicated at the tips, is the average % cover (2017 and 2018). Phylogenetic branch supports are > 0.95 unless otherwise indicated. 52
Figure 2.2: Relationships over a normal (open circles, 2017) and a dry (grey circles, 2018) growing season between (A) $\delta^{13}C$ and $\Delta^{18}O$ of bulk leaf material ($R^2 = 0.53$, $P < 0.0001$); (B) average IMS values calculated from bulk leaf material, (C) $\delta^{13}C$ and $\Delta^{18}O$ of leaf cellulose ($R^2 = 0.34$, $P = 0.0002$); and (D) average integrated metabolic strategy (IMS) values calculated from leaf cellulose. Data are species means ± standard error (n=5 per species, per year) for 18 co-occurring old field species: 1 = *A. syriaca*, 2 = *C. arvense*, 3 = *C. vulgare*, 4 = *D. carota*, 5 = *E. philadelphicus*, 6 = *E. graminifolia*, 7 = *G. triflorum*, 8 = *G. macrophyllum*, 9 = *L. morrowii*, 10 = *L. salicaria*, 11 = *M. moschata*, 12 = *P. pratense*, 13 = *R. multiflora*, 14 = *S. altissima*, 15 = *S. arvensis*, 16 = *S. juncea*, 17 = *S. rugosa*, 18 = *T. officinale*. Species that share the same letters in (B) and (D) are statistically indistinguishable based on ANOVA Tukey post-hoc tests. Species full names are in Figure 2.1.....62
Figure 2.3: Species responses in (A-B) bulk leaf $\delta^{13}C$ and $\Delta^{18}O$; (C-D) IMS between average growing season conditions (2017) and a dry growing season (2018) for (A) species with a coupled gas exchange response (linear correlation), and (B) species with an uncoupled gas exchange response (no correlation). Average IMS across all species with a (C) coupled and (D) uncoupled response are shown for each year. Data are species means ± standard error (n=5 per species, per year) for 18 co-occurring old field species: 1 = *A. syriaca*, 2 = *C. arvense*, 3 = *C. vulgare*, 4 = *D. carota*, 5 = *E. philadelphicus*, 6 = *E. graminifolia*, 7 = *G. triflorum*, 8 = *G. macrophyllum*, 9 = *L. morrowii*, 10 = *L. salicaria*, 11 = *M. moschata*, 12 = *P. pratense*, 13 = *R. multiflora*, 14 = *S. altissima*, 15 = *S. arvensis*, 16 = *S. juncea*, 17 = *S. rugosa*, 18 = *T. officinale*. Species full names are in Figure 2.1. 63
Figure 2.4: Relationships between the change in species relative abundance (% cover) in a drier year (2018) and (A) average integrated metabolic strategy (IMS) values between years ($R^2 = 0.18$, $P = 0.047$); (B) the extent to which a species has coupled or uncoupled gas exchange (i.e., the slope of the $\delta^{13}C$-$\Delta^{18}O$ correlation between years; $R^2 = 0.11$, $P = 0.048$). Data are species means ± standard error (both years combined, n=5 per species, per year) of bulk leaf material for 18 co-occurring old field species: 1 = *A. syriaca*, 2 = *C. arvense*, 3 = *C. vulgare*, 4 = *D. carota*, 5 = *E. philadelphicus*, 6 = *E. graminifolia*, 7 = *G. triflorum*, 8 = *G. macrophyllum*, 9 = *L. morrowii*, 10 = *L. salicaria*, 11

= *M. moschata*, 12 = *P. pratense*, 13 = *R. multiflora*, 14 = *S. altissima*, 15 = *S. arvensis*, 16 = *S. juncea*, 17 = *S. rugosa*, 18 = *T. officinale*. Species full names are in Figure 2.1. Correlations for leaf cellulose data and for additional variables are in Table A2.1. 64
Figure 3.1: Variation within and among seven co-occurring Asteraceae species in (A) leaf carbon isotope composition (δ13C) and leaf oxygen isotope enrichment above source water (Δ18O). δ13C and Δ18O were positively correlated across all species and water treatments (R2 = 0.73, p < 0.0001, slope = 0.65). Linear regression slopes and significance (within-species values reported in the inset) were calculated from linear mixed effects models with 'block' as a random effect. (B) Inter-specific variation in integrated metabolic strategy (IMS) values. Data are species means across five experimental water treatments ± standard error (n = 45 per species). Species that share the same letter are statistically indistinguishable, based on Tukey post-hoc tests. Species abbreviations are the first two letters of the genus and species epithet given in Materials and Methods. Asterisks indicate non-native species. 93
Figure 3.2: Observed changes in (A) aboveground biomass (g, standardized), (B) integrated metabolic strategy (IMS) values, (C) leaf carbon isotope composition ($\delta^{13}C$) and (D) leaf oxygen isotope enrichment above source water ($\Delta^{18}O$) across five experimental water treatments that span a gradient from the driest ('treatment 1') to the wettest ('treatment 5') year on record from the last 30 years in Ithaca, NY. Data are species means ± standard error for seven co-occurring Asteraceae species (n = 9 per species, per treatment). Species abbreviations are the first two letters of the genus and species epithet given in *Materials and Methods*....94
Figure 3.3: The change in biomass between the driest and wettest treatments in relation to (A) average integrated metabolic strategy (IMS) values across all treatments (t=-0.42, p = 0.69), and (B) the extent of coupling between carbon and water leaf gas exchange, measured as the linear regression slope between leaf carbon isotope composition ($\delta^{13}C$) and leaf oxygen isotope enrichment above source water ($\Delta^{18}O$) (t = 0.22, p = 0.83). Linear regression slopes were calculated from linear mixed effects models with 'block' as a random effect. Data are species means across five experimental water treatments ± standard error (n = 45 per species)....95
Figure 4.1 Geographic locations of herbarium specimen collection sites across North America for 57 Ericaceae species (n=225). The legend shows phylogenetic relationships among the 12 genera represented in this study. The phylogeny was constructed by maximum likelihood analyses using sequence data from mat*K*, *nr*ITS and rbcL gene regions from GenBank. This figure is available in color in the online version. 122
Figure 4.2 Relationships between (a) phylogenetic similarity and similarity in leaf $\delta^{15}N$ (r^2=0.32, $P < 0.0001$), (b) phylogenetic similarity and similarity in leaf $\delta^{13}C$ (r^2=0.20, $P < 0.0001$), (c) environmental similarity and similarity in leaf $\delta^{15}N$ (r^2=0.002, $P = 0.02$), and (d) environmental similarity and similarity in leaf $\delta^{13}C$ (r^2=0.01, $P < 0.0001$) for 57 Ericaceae species (n = 225). Phylogenetic similarity is derived from species pair-wise comparisons of phylogenetic branch lengths. Environmental similarity is derived from species pair-wise comparisons of average July vapor pressure deficits. Similarities range from 0 to 1, with 1 being completely similar and 0 being completely different. 123
Figure 4.3 Results of a one-way analysis of variance between leaf (a) $\delta^{13}C$ and (b) $\delta^{15}N$ and three mycorrhizal associations (Arbutoid, Ericoid, Monotropoid) for 57 Ericaceae species (n = 225). Asterisks indicate significant differences among mycorrhizal types ($P < 0.0001$). 124
Figure A1.1: Summary of leaf-level and whole-plant traits across 20 *Asclepias* taxa grown under common conditions, grouped by IMS (see Figure 4B for species identities); A) maximum rate of photosynthesis (A_{max}), B) stomatal conductance (g_s), C) plant height, D) total leaf area, E) leaf size, F) leaf nitrogen content root/shoot, G) maximum rate of carboxylation (Vc_{max}), and H) root/shoot. Data are means ± standard error (n=6). 139
Figure A1.2: Relationships between $\delta^{13}C$ and $\Delta^{18}O$ of leaf cellulose for *A. curassavica* (circles), *A. incarnata* (squares), *A. pumila* (diamonds) and *A. verticillata* (triangles) grown under three different soil water treatments: dry (one-third field capacity), mesic (field capacity), and wet (twice field capacity). Data are means based on six replicates. Arrows indicate the direction of change in $\delta^{13}C$ and $\Delta^{18}O$ between wet and dry treatments. 140
Figure A1.3: Summary of leaf-level and whole-plant traits across four *Asclepias* taxa grown under three soil water treatments: dry (red, one-third field capacity), mesic (green, field capacity), and wet (blue, twice field capacity). A) maximum rate of photosynthesis (A_{max}), B) stomatal conductance (g_s), C) plant height, D) total leaf area, E) leaf size, F) leaf nitrogen content root/shoot, G) maximum rate of carboxylation (Vc_{max}), and H) root/shoot. Data are means ± standard error (n=6). 141
Figure A1.4: Relationships between integrated metabolic strategy (IMS) and A) leaf size, B) stomatal conductance (g_s), C) leaf nitrogen content and D) maximum carboxylation rate (Vc_{max}) for *A. curassavica* (circles), *A. incarnata* (squares), *A. pumila* (diamonds) and *A. verticillata* (triangles) grown under three different soil water treatments: dry (one-third field capacity), mesic (field capacity), and wet (twice field capacity). Data are species means (n=6). 142

Figure A2.1: Patterns of soil water content (%) and soil water $\delta^{18}O$ (‰) with depth across two growing seasons, 2017 and 2018, in a successional old field in Ithaca, NY. Data are plot means (n=5 per plot, per year).....144
Figure A3.1: Changes in leaf area (LA, cm^2) across five experimental water treatments that span a gradient from the driest ('treatment 1') to the wettest ('treatment 5') year on record from the last 30 years in Ithaca, NY. Data are species means ± standard error for seven co-occurring Asteraceae species (n = 9 per species, per treatment). Species abbreviations are the first two letters of the genus and species epithet given in *Materials and Methods*. 145
Figure A3.2: Changes in plant height (cm) across five experimental water treatments that span a gradient from the driest ('treatment 1') to the wettest ('treatment 5') year on record from the last 30 years in Ithaca, NY. Data are species means ± standard error for seven co-occurring Asteraceae species (n = 9 per species, per treatment). Species abbreviations are the first two letters of the genus and species epithet given in *Materials and Methods*. 146
Figure A3.3: Changes in leaf nitrogen content (N, %) across five experimental water treatments that span a gradient from the driest ('treatment 1') to the wettest ('treatment 5') year on record from the last 30 years in Ithaca, NY. Data are species means ± standard error for seven co-occurring Asteraceae species (n = 9 per species, per treatment). Species abbreviations are the first two letters of the genus and species epithet given in *Materials and Methods*.....147
Figure A3.4: Changes in plant source water oxygen isotope composition ($\delta^{18}O$) across five experimental water treatments that span a gradient from the driest ('treatment 1') to the wettest ('treatment 5') year on record from the last 30 years in Ithaca, NY. Data are species means ± standard error for seven co-occurring Asteraceae species (n = 9 per species, per treatment). Species abbreviations are the first two letters of the genus and species epithet given in *Materials and Methods*. 148
Figure A3.5: Pair-wise species relationships between aboveground biomass (standardized) across five experimental water treatments that span a gradient from the driest ('treatment 1') to the wettest ('treatment 5') year on record from the last 30 years in Ithaca, NY. Data are species means ± standard error for seven co-occurring Asteraceae species (n = 9 per species, per treatment). Species abbreviations are the first two letters of the genus and species epithet given in *Materials and Methods*. 149

LIST OF TABLES

Table 1.1: Phylogenetic signal of isotopes and leaf traits using Pagel's λ and Blomberg's K. * $p < 0.05$, ** $p < 0.01$, *** $p < 0.0001$. Larger λ and K values indicate proportional phenotypic similarity to phylogenetic distance based on a Brownian Motion model. 20
Table 2.1: Growing season climate and soil properties in 2017 and 2018 for Ithaca, New York. Data were obtained from Ithaca Tompkins Regional Airport weather station. Asterisks indicate significant differences between years. * $p < 0.05$, ** $p < 0.01$, *** $p < 0.001$. 57
Table 2.2: Results of a linear mixed effects model analysis of variance showing the effects of species, year, and their interaction on leaf carbon isotope composition ($\delta^{13}C$), leaf oxygen isotope enrichment above source water ($\Delta^{18}O$), integrated metabolic strategy value (IMS), relative abundance (% cover), plant height, plant source water oxygen isotope composition ($\delta^{18}O$), and leaf nitrogen content (N). Data are for 18 species co-occurring in a temperate old field in Ithaca, NY (n=10 per species). 58
Table 2.3: Phylogenetic signal estimated by Pagel's λ and Blomberg's K of bulk leaf and cellulose carbon isotope composition ($\delta^{13}C$), bulk leaf and cellulose oxygen isotope enrichment above source water ($\Delta^{18}O$), bulk leaf and cellulose integrated metabolic strategy value (IMS), plant height, plant source water oxygen isotope composition ($\delta^{18}O$), leaf nitrogen content (% N), and relative abundance (% cover). Data are species means for two years ± standard error (n=10 per species). 60
Table 2.4: The extent to which species display coupled or uncoupled gas exchange responses between years: slopes and standard errors for the relationships between leaf carbon isotope ($\delta^{13}C$) and oxygen enrichment above source water ($\Delta^{18}O$), obtained from linear mixed effects models. 61
Table 3.1: Results of a linear mixed effects model analysis of variance showing the effects of species, water treatments, and their interaction on standardized total aboveground biomass, leaf carbon isotope composition ($\delta^{13}C$), leaf oxygen isotope enrichment above source water ($\Delta^{18}O$), integrated metabolic strategy value (IMS), total leaf area, plant height, plant source water oxygen isotope composition ($\delta^{18}O$), and leaf nitrogen content. Data are for seven Asteraceae species co-occurring in a temperate old field in Ithaca, NY (n=45 per species). 90
Table 3.2: Multiple linear regression model showing effects of leaf carbon isotope composition ($\delta^{13}C$), leaf oxygen isotope enrichment above source water ($\Delta^{18}O$), total leaf area, plant height, plant source water oxygen isotope composition ($\delta^{18}O$), and leaf nitrogen content on variation in aboveground biomass. Data are for seven Asteraceae species co-occurring in a temperate old field in Ithaca, NY (n=45 per species). Total model $R^2 = 0.782$, $p < 0.0001$. 92
Table 4.1: Phylogenetic signal using Pagel's λ of 10 leaf characteristics, average July vapor pressure deficits and mycorrhizal type (Arbutoid, Ericoid, Monotropoid) for 57 Ericaceae species (n = 225). Phylogenetic signal is significant at Pagel's $\lambda > 0.5$ ($\alpha = 0.05$), indicating variables that are more similar among close relatives than expected by chance. 120
Table 4.2: Phylogenetic signal and isotopic similarity among Ericaceae plants from specialized environments. Pagel's $\lambda > 0.5$ indicates phylogenetic signal. Isotopic similarity ranges from 0 to 1, with 1 being completely similar and 0 being completely different. The number of individuals from each environment is indicated in parentheses. .121
Table A1.1: Average leaf cellulose $\delta^{13}C$ and $\Delta^{18}O$, and associated integrated metabolic strategy (IMS) for ten Mediterranean plant species. Data are species' means and microhabitat means with standard error in parentheses from Moreno-Gutierrez *et al.* 2012. Asterisks indicate significant differences between mesic and xeric microhabitats determined by one-way analysis of variance. * $p < 0.05$, ** $p < 0.01$. 138
Table A2.1: Pearson correlations between the change in abundance (% cover) between two growing seasons (2017, 2018) and integrated metabolic strategy (IMS) values, leaf carbon isotope ($\delta^{13}C$), and oxygen isotope above source water ($\Delta^{18}O$) obtained from bulk leaf material and leaf cellulose of 18 old field plant species. Additional variables include plant height, leaf nitrogen content (N), and plant source water $\delta^{18}O$. * $p < 0.05$, ** $p < 0.01$, *** $p < 0.0001$. 143

CHAPTER ONE

Integrated metabolic strategy: A mechanistic framework for predicting carbon-water tradeoffs within plant clades[1]

Abstract

The fundamental tradeoff between carbon gain and water loss has long been predicted as an evolutionary driver of plant strategies across environments. Nonetheless, challenges in measuring carbon gain and water loss in ways that integrate over leaf lifetime have limited our understanding of the variation in and mechanistic bases of this tradeoff. Furthermore, the microevolution of plant traits within species versus the macroevolution of strategies among closely related species may not be the same, and accordingly, the latter must be addressed using comparative phylogenetic analyses. Here we introduce the concept of 'integrated metabolic strategy' (IMS) to describe the ratio between carbon isotope composition ($\delta^{13}C$) and oxygen isotope composition above source water ($\Delta^{18}O$) of leaf cellulose. IMS is a measure of leaf-level conditions that integrate several mechanisms contributing to carbon gain ($\delta^{13}C$) and water loss ($\Delta^{18}O$) over leaf lifespan, with larger values reflecting higher metabolic efficiency and hence less of a tradeoff. We tested how IMS evolves among closely related yet ecologically diverse milkweed species, and subsequently addressed phenotypic plasticity in response to water availability in species with divergent IMS. IMS varied strongly among 20 *Asclepias* species when grown under controlled conditions, and phylogenetic analyses demonstrate species-specific

[1] Goud, E.M., Sparks, J.P., Fishbein, M., and Agrawal, A.A. (2019) Integrated metabolic strategy: a mechanistic framework for predicting the evolution of carbon-water tradeoffs within plant clades. *Journal of Ecology* 107(4): 1-12.

tradeoffs between carbon gain and water loss. Larger IMS values were associated with species from dry habitats, with larger carboxylation capacity, smaller stomatal conductance and smaller leaves; smaller IMS was associated with wet habitats, smaller carboxylation capacity, larger stomatal conductance and larger leaves. The evolution of IMS was dominated by changes in species' demand for carbon ($\delta^{13}C$) more so than water conservation ($\Delta^{18}O$). Although some individual physiological traits showed phylogenetic signal, IMS did not. In response to experimental decreases in soil moisture, three species maintained similar IMS across levels of water availability because of proportional increases in $\delta^{13}C$ and $\Delta^{18}O$ (or little change in either), while one species increased IMS due to disproportional changes in $\delta^{13}C$ relative to $\Delta^{18}O$. IMS is a broadly applicable mechanistic tool; IMS variation among and within species may shed light on unresolved questions relating to evolution and ecology of plant ecophysiological strategies.

Introduction

The need to maximize carbon gain while minimizing water loss has long been presumed to drive the evolution of diverse strategies by which plants adapt to variable environments (Monson & Ehleringer 1993; Sage 2004). Such strategies include succulence and alternative photosynthetic pathways (e.g., CAM) that are evolutionarily convergent, coarse-grained metabolic solutions to the carbon-water dilemma. While closely related species typically share a defined coarse-grained strategy, more fine-grained solutions to balance carbon gain and water loss may be expressed via differences in traits, such as stomata, that affect the exchange rates of both carbon dioxide (CO_2) and water vapor (Farquhar & Sharkey 1982; O'Leary 1988). Additionally, the leaf's boundary layer, internal resistance to gaseous diffusion, and enzymatic activity driving CO_2 consumption contribute substantially to carbon and water flux, and are likely a concerted part of an overall plant strategy to manage the tradeoff between these two fluxes.

For decades, the tradeoff between carbon acquisition and water loss has been measured as the ratio of photosynthetic carbon gain to transpirational water loss, typically measured instantaneously and described as "water-use efficiency" (Osmond, Bjorkman & Anderson 1980; Keenan *et al.* 2013). Indeed, how this tradeoff varies among species and along environmental gradients is central to our understanding of plant ecology (Pugnaire & Valladares 1999; Lambers, Chapin & Pons 2008). Though empirical measures of this ratio are much more informative when integrated over longer periods of time, the measurements of long-term carbon gain and water loss are challenging. At the leaf level, photosynthetic carbon gain over time is driven by the average difference in leaf internal and air external CO_2 concentrations (c_i/c_a), which is influenced by the metabolic demand for CO_2 and the supply of CO_2 via diffusion through the stomata and leaf boundary layer. Similarly, water loss over time is defined by the

average difference in leaf internal and air external water vapor concentrations (e_a/e_i) where e_i varies with temperature and e_a varies with relative humidity (Caemmerer & Farquhar 1981; Farquhar & Sharkey 1982; Anyia 2004). As such, traditional measures of instantaneous leaf gas exchange of CO_2 and water vapor fail to account for continuous variation in light, humidity and air temperature, and thus may inaccurately reflect long-term carbon gain and water loss at the leaf level (Seibt *et al.* 2008).

Another approach is to use proxies (e.g., specific leaf area) to describe carbon and water exchange over a leaf's lifetime. Such measures are based on assumed relationships between traits and gas exchange (Wright *et al.* 2004; 2005) that may be inconsistent among closely-related species (Edwards *et al.* 2014; Mason & Donovan 2015), because leaf traits have multiple functions in addition to carbon gain and water regulation. A third approach has been to use the carbon stable isotope composition ($\delta^{13}C$) of leaf material as a proxy for water-use efficiency (Seibt *et al.* 2008). During carbon fixation, the Rubisco enzyme discriminates against the heavier ^{13}C-CO_2; when CO_2 is abundant (larger c_i/c_a), more discrimination results in tissues that are relatively depleted in ^{13}C. Thus, $\delta^{13}C$ reflects a measure of CO_2 supply and demand that integrates over the lifespan of the leaf and is proportional to c_i/c_a (Farquhar, Ehleringer & Hubick 1989). However, $\delta^{13}C$ cannot distinguish the individual influences of carboxylation rate and stomatal conductance (Ehleringer 1993).

An alternate methodology that has been applied recently is to integrate leaf carbon-water relations over time through the separate, concerted use of carbon and oxygen stable isotopes (Scheidegger *et al.* 2000; Grams *et al.* 2007; Roden & Farquhar 2012). The oxygen in cellulose comes from water, and the stable isotope composition ($\delta^{18}O$) of leaf cellulose is influenced by both source and leaf water $\delta^{18}O$. Source water $\delta^{18}O$ varies with temperature and evaporation,

while leaf water $\delta^{18}O$ primarily varies with evaporative enrichment during transpirational water loss, as well as leaf temperature, the degree of mixing between source and leaf waters within the plant, and the degree of isotopic exchange between organic molecules and water (Roden & Ehleringer 2000; Barbour *et al.* 2004). When calculated as an enrichment above source water ($\Delta^{18}O = \delta^{18}O_{cellulose} - \delta^{18}O_{source}$), $\Delta^{18}O$ reflects the evaporative environment at the time of cellulose production and is inversely proportional to e_a/e_i (Farquhar, Cernusak & Barnes 2007; Roden & Farquhar 2012). Although not a direct measure of fluxes, the relationship between $\delta^{13}C$ and $\Delta^{18}O$ of cellulose represents an endpoint integration of the tradeoff between carbon gain and water loss over the lifetime of a leaf.

Integrated metabolic strategy

Here, we introduce the concept of *integrated metabolic strategy* (IMS) to describe the relationship between carbon metabolism and leaf evaporative conditions using $\delta^{13}C$ and $\Delta^{18}O$ of leaf cellulose. There have been many attempts to describe the relationship between carbon gain and water loss, the most prominent being 'water-use efficiency'. Additionally, 'metabolic set point' has been used to describe long term c_i/c_a, similar to basal metabolism in animals (Ehleringer 1993). We purposefully don't redefine these terms in order to avoid confusion. Rather, we use the term 'integrated metabolic strategy' because it is a readily accessible and general term to describe a strategy to manage the tradeoff between carbon and water fluxes at the leaf-level.

The relationship between $\delta^{13}C$ and $\Delta^{18}O$ can be visualized by plotting these two variables in dual-isotope space (Figure 1.1A), providing a representation of integrated carbon metabolic set point and the evaporative state of the water used to form cellulose. As such, it is a gross

representation of the carbon for water tradeoff. Because the relationship between $\delta^{13}C$ and c_i/c_a is positive and the relationship between $\Delta^{18}O$ and e_a/e_i is negative (at least over the range of values of interest), it is convenient to rescale the denominator in order to 1) make all values positive, and 2) distort the values as little as possible without generating ratios larger than one. For our dataset, $\Delta^{18}O$ was subtracted from a constant of 100, and we define IMS as the following ratio:

$$IMS = \frac{|\delta^{13}C|}{100 - \Delta^{18}O}$$

Increasing IMS values correspond to increases in leaf-level metabolic efficiency (i.e., a higher metabolic carbon set point per unit of increasing evaporative condition in leaves; Figure 1.1B). We take the absolute value of $\delta^{13}C$ as the numerator to represent the general, positive relationship between $\delta^{13}C$ and c_i/c_a. In this dataset, IMS values range between 0 and 1, with 1 representing plants with the largest carbon set point at a minimum of evaporative water loss. Importantly, similar IMS values can be achieved by plants that differ in magnitudes of carbon metabolic set point and evaporative environment, if they have a similar ratio between the two. For example, species B and C (Figure 1.1A) differ in $\delta^{13}C$ and $\Delta^{18}O$ values, yet reach similar metabolic strategies because they exchange carbon and water in approximately the same 2/5 ratio. In contrast, plants differ in IMS when the ratio between these fluxes differ (species A and D, Figure 1.1B). We predict, then, that when responding to a driving force (e.g., water availability), plants with fixed IMS may differentially adjust anatomy and/or physiology, but $\delta^{13}C$ and $\Delta^{18}O$ will vary proportionally (e.g., movement between points C and B, Figure 1.1A). Alternatively, if IMS is phenotypically plastic, we expect changes in $\delta^{13}C$ and $\Delta^{18}O$ to result in a change in IMS (e.g., movement between points A and B, A and C, or A and D, Figure 1.1A).

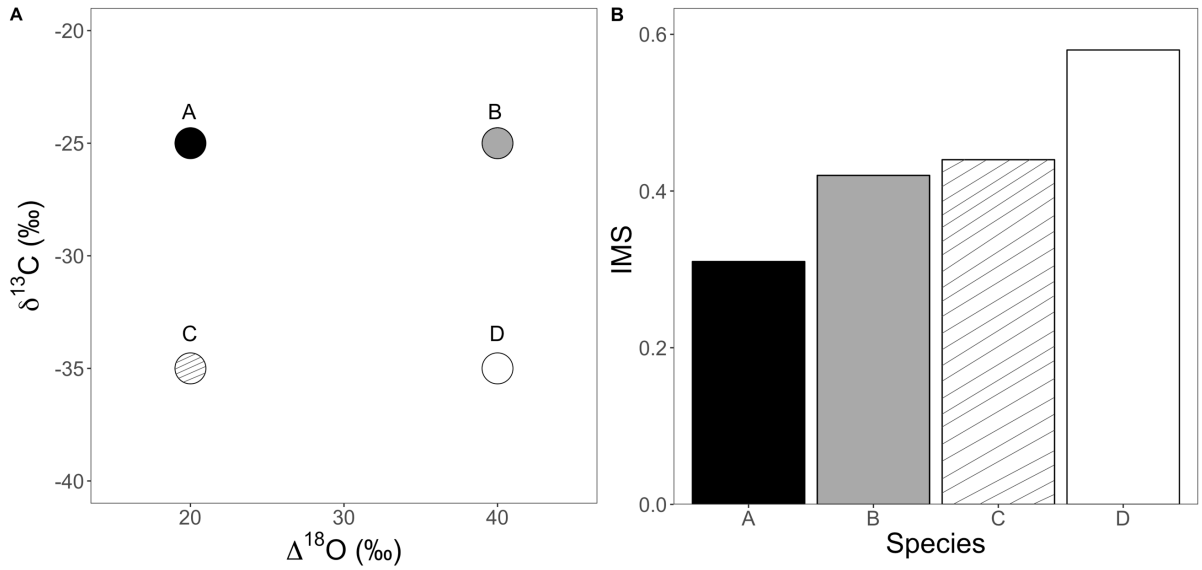

Figure 1.1: Conceptual model for variation in (A) leaf-level $\delta^{13}C$ and $\Delta^{18}O$ and (B) associated IMS values for different hypothetical plant species or individuals.

Our introduction of IMS builds on previous work that has considered $\delta^{13}C$ and $\Delta^{18}O$ separately in greenhouse (Barbour *et al.* 2004) and field settings (Ehleringer, Phillips & Comstock 1992; Sparks & Ehleringer 1997; Cernusak, Farquhar & Pate 2005). Examining the relationship between $\delta^{13}C$ and $\Delta^{18}O$ in dual isotope space has been used to differentiate photosynthetic and stomatal responses to changing environmental conditions, such as precipitation and temperature, primarily in the context of improving paleoclimate models (Offermann *et al.* 2011; Roden & Farquhar 2012). Field measurements have been used to relate variation in $\delta^{13}C$ and $\Delta^{18}O$ to variation in environmental water availability due to, for example, gradients in precipitation and topography (Moreno Gutiérrez *et al.* 2012; Flanagan & Farquhar 2014; Prieto *et al.* 2017). However, unlike previous work, we convert the relationship between $\delta^{13}C$ and $\Delta^{18}O$ to an index (IMS) that provides a single measure of the relationship between carbon set point and water availability.

Evolution of metabolic strategies

To evaluate the evolution of IMS, we combine common garden and experimental water manipulations across species spanning the range of ecological diversity within the milkweed genus *Asclepias* (Apocynaceae) (Figure 1.2). *Asclepias* includes about 140 New World, mostly herbaceous, perennial plants that display remarkable variation in morphology and habitat affiliations (Figure 1.3). Many species live in desert and arid environments of the southwestern United States. Others occupy more mesic environments, such as grasslands and forests, while still others are restricted to wetlands, such as marshes and swamps (Woodson 1954). To test for intrinsic, species-specific variation in metabolic strategies, we selected 20 taxa (19 species plus one subspecies), representing each major clade in *Asclepias* (Fishbein *et al.* 2011; 2018) that

vary in leaf morphology (e.g., leaf size and thickness; Figure 1.3), and that naturally occur in habitats that differ substantially in water availability. Specifically, we asked the following questions: (1) Does IMS differ among closely related, yet ecologically diverse species under common garden conditions? (2) Can leaf traits, physiological measures, and evolutionary history be used to predict IMS?

To evaluate whether variation in soil water availability would impact IMS of individual plants (i.e., phenotypic plasticity), we selected four of the 20 taxa to grow under experimental water treatments. These four species represented opposite ends of IMS and morphological variation within the genus; two species with the largest IMS values and small, thick leaves, and two species with the smallest IMS values and large, thin leaves. Additionally, these four species included a dryland and a wetland-specialist, and two ecologically broad species. Thus, our final question was, (3) How does a gradient of soil moisture impact IMS? We hypothesized that dryland-adapted species would have larger IMS values, indicating a more water conservative strategy (Figure 1.1B), relative to wetland-adapted species. We further hypothesized an association of higher IMS with smaller leaves, lower rates of stomatal conductance, and larger rates of carboxylation.

Methods

Plant Growth

In May 2016, seeds from 20 *Asclepias* species (Figure 1.2, wild collected or purchased from native plant suppliers), were germinated by moistening and stratifying at 4°C for at least 10 days and then at 28°C for 3 days. Seedlings were planted in Metro Mix soil (Scotts-Sierra, Marysville, OH, USA) in 500 ml plastic pots. Plants were grown for 6 weeks in a walk-in growth chamber (Conviron CMP 6050) that was maintained at 26°C (14 hour day) and 24°C (10 hour night) with an average relative humidity of 50%. Plants were monitored daily and soil water contents were maintained at field capacity. Volumetric water content (VWC) at field capacity was determined by saturating a 500 ml pot of soil with water, sealing the top with parafilm, and allowing all excess water to drain via gravity for 48 hours. At this point, the soil was at field capacity (Colman 1947) and soil volumetric water content was measured using a HydroSense II soil-water sensor (Campbell Scientific, Logan, UT). The water content of the soil at field capacity was approximately 30%.

Experimental Water Treatments

In May 2018, we selected four species based on their 2016 IMS values: *A. curassavica* (Figure 1.3A), *A. incarnata* (Figure 1.3B), *A. pumila* (Figure 1.3D) and *A. verticillata* (Figure 1.3E). These species were selected because they represent opposite ends of IMS variation that also coincide with differences in leaf morphology, and because these species are in the same clade (Figure 1.2) (Fishbein *et al.* 2011; 2018). *Asclepias curassavica* and *A. incarnata* represent the smallest IMS values and have large, thin leaves (Figure 1.3A-B). *Asclepias curassavica* is an

ecologically widespread tropical and subtropical species while *A. incarnata* is restricted to temperate wetlands. *Asclepias pumila* and *A. verticillata* represent the largest IMS values and have small, thick leaves (Figure 1.3D-E). *Asclepias pumila* occurs in temperate short-grass prairie in the Great Plains, while *A. verticillata* occurs in temperate grasslands and forest openings across the eastern and midwestern United States and southernmost Canada (Woodson 1954).

We grew individuals of *A. curassavica, A. incarnata, A. pumila* and *A. verticillata* in conditions identical to 2016 (pot size, growth medium, chamber conditions), but under three different watering regimes relative to field capacity (measured as 30% VWC, as described above): dry (one-third field capacity, approximately 10% VWC), mesic (field capacity, approximately 30% VWC), and wet (saturated, approximately 60% VWC). We measured VWC daily and watered the pots as necessary to maintain treatment VWCs.

Gas exchange and leaf traits

We measured leaf gas exchange in 2016 and in 2018 using a LI-COR LI-6400 CO_2 gas exchange analyzer (LI-COR, Lincoln, NE) on five to six replicate plants per species at 32 and 39 days old. We measured light-saturated maximum rates of photosynthesis (A_{max}) by generating light response curves on three replicate plants per species to obtain the light intensity (photosynthetically active radiation, PAR) at which photosynthesis saturated. We estimated maximum rates of carboxylation (Vc_{max}) from A/ci curves on the same three replicate plants per species used to generate light response curves. When plants were 45 days old, we recorded the total number of leaves and plant height of each individual, removed leaves, separated and washed roots to remove soil. We measured total leaf area (LA) using a LI-COR LI-3100 leaf-

area meter (LI-COR, Lincoln, NE) and weighed fresh leaf mass. We then oven-dried leaf, stem and root materials at 60°C for 48 hours. Average leaf area (leaf size, LS) was calculated by dividing LA by the total number of leaves.

Sample processing for cellulose extraction

Approximately 300 mg of ground leaf material was loaded into fiber filter bags, heat-sealed and placed in a Soxhlet apparatus to reflux a 2:1 solution of toluene:ethanol for a 24-hour period followed by a period of drying and another 24-hour period of extraction (for lipids and resins) with 95% ethanol. Bags were air-dried and boiled in water for 1 hour to extract soluble sugars and low molecular weight polysaccharides. To obtain holocellulose, the samples were soaked in a 0.7% w/v sodium chlorite/acetic acid solution that was continuously stirred on a stir plate and periodically replaced over a three-day extraction to extract lignin and other nitrogen-containing compounds. To obtain pure α-cellulose, the samples were soaked in a 17% w/v sodium hydroxide (NaOH) solution followed by an 11% w/v acetic acid solution to neutralize the pH with each step followed by extensive rinsing with distilled water. The α-cellulose was dried at 65°C for 48 hours (Leavitt & Danzer 2002).

Isotope analyses

Isotope ratios and percent element of all samples were measured using a continuous flow isotope ratio mass spectrometer (Thermo Scientific Delta V Advantage). For $\delta^{13}C$, the mass spectrometer was coupled to an elemental analyzer (Carlo Erba NC2500), and for $\delta^{18}O$ it was coupled to a Thermo Scientific TC/EA pyrolysis analyzer with a Costech Zero Blank auto sampler. Isotope ratios are expressed as δ values (per mil):

$$\delta^{13}C \text{ or } \delta^{18}O = (R_{sample}/R_{standard} - 1) \times 1000 \text{ (‰)}$$

where R_{sample} and $R_{standard}$ are the ratios of heavy to light isotope of the sample relative to the international standards for C and O, Vienna-Pee-Dee Belemnite and Vienna Standard Mean Ocean Water, respectively. $\delta^{18}O$ of irrigation (source) water was -10.1 ‰ in 2016 and -9.9 ‰ in 2018. Within run isotopic precision for quality control standards was 0.2‰ for carbon and 0.3‰ for oxygen. Mass spectrometry was performed at the Cornell University Stable Isotope Laboratory.

Phylogenetic relationships

We estimated the phylogeny of the 20 sampled species of *Asclepias* (Figure 1.2) by adding new plastid genome (plastome) sequences for *A. pumila* and *A. verticillata* to a recently published dataset of 108 samples of *Asclepias* plus four outgroup sequences (Fishbein *et al.* 2018). The *A. pumila* sample was prepared using the NEBNext Ultra II DNA Library Prep Kit for Illumina (New England BioLabs, Ipswich, MA) with a NEXTflex-HT™ Barcode (Bioo Scientific, Austin, TX) and sequenced on an Illumina NextSeq 500 at the Oklahoma State University Genomics and Proteomics Center. The *A. verticillata* sample was prepared as in (Straub *et al.* 2012). Both plastomes were assembled using Geneious 10 (Kearse *et al.* 2012);Biomatters Ltd., Auckland, New Zealand) by obtaining de novo contigs using the proprietary Geneious assembler, mapping contigs to an *A. nivea* reference (NCBI NC_022431.1), and re-mapping unassembled reads to the aligned contigs to complete the assemblies. The two copies of the inverted repeat were not distinguished in these assemblies. The phylogeny of the 114 samples was obtained following Fishbein et al. (2018). Briefly, plastome sequences were aligned using MAFFT v. 7 (Katoh, Rozewicki & Yamada 2017) and ambiguously aligned regions were

masked with the implementation of Gblocks (Castresana 2000) in Mesquite 3.5 (Maddison and Maddison 2018). The maximum likelihood phylogeny of these sequences was estimated with IQ-TREE v. 1.6.7 (Nguyen *et al.* 2015) with node support estimated by ultrafast bootstrap (Minh, Nguyen & Haeseler 2013). The maximum likelihood tree was converted to a chronogram with relative node dates using penalized likelihood optimization of rate variation among branches, implemented in treePL (Smith & O'Meara 2012). The resulting time tree was pruned to contain only the species sampled here using the drop.tip function in the ape v. 4.1 package (Paradis, Claude & Strimmer 2004) for R (R Core Team, 2016). This phylogeny contained 19 of the 20 sampled species due to a lack of sequence information for *A. fascicularis*.

Statistical analyses

We assessed relationships between IMS and leaf traits using simple linear regressions and phylogenetic independent contrasts using the pgls function of the caper package in R (Orme et al. 2018). We assessed relationships between IMS and experimental water treatments using one-way ANOVA. We estimated phylogenetic signal by calculating Pagel's λ and Blomberg's K using the phylosig function in the picante package in R (Kembel et al. 2010). We included the standard error of the mean for each variable. All analyses were performed with the full 20 species except for phylogenetic signal and independent contrasts (19 species) in R3.2.4 (R Core Team, 2016).

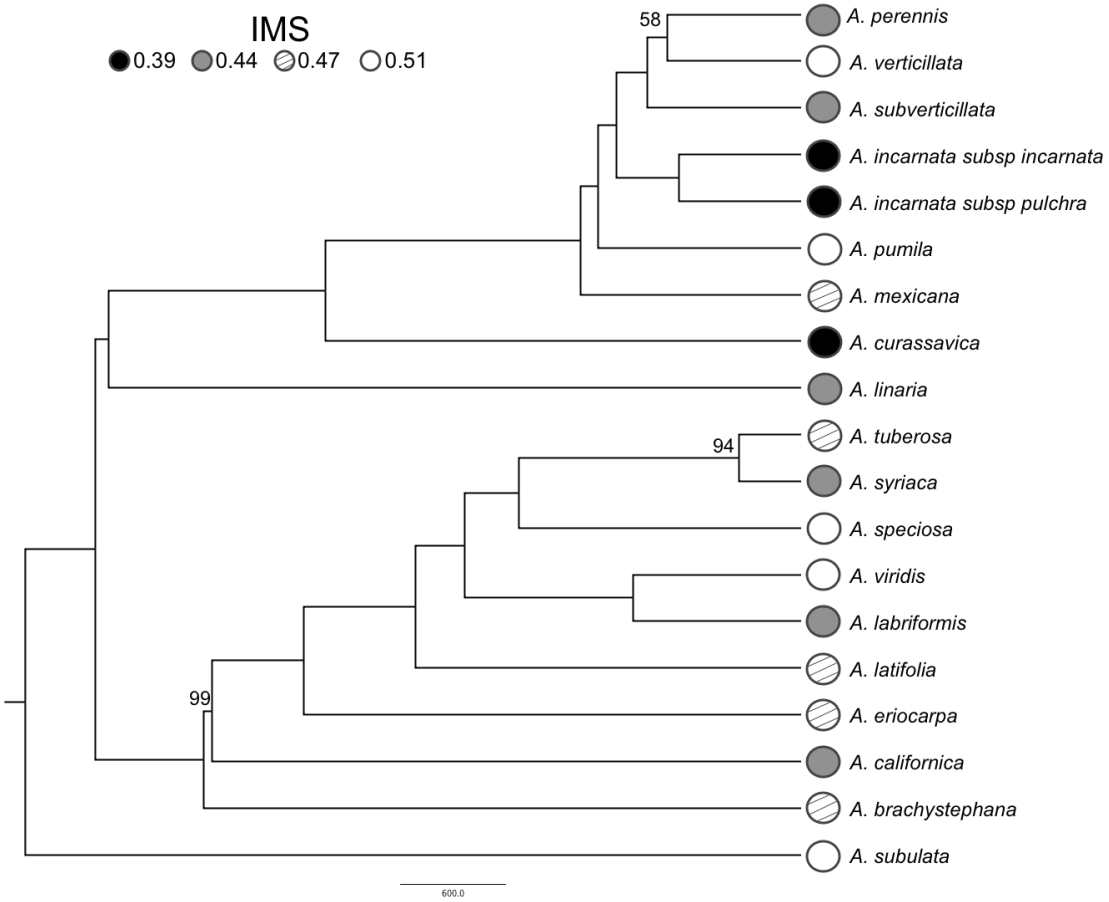

Figure 1.2: Maximum likelihood chronogram based on plastome sequences from 19 *Asclepias* taxa and the range of associated integrated metabolic strategies (IMS). Bootstrap values less than 100% are indicated at nodes. IMS colors among taxa correspond to the average IMS value of each Tukey post-hoc group, ranging from the lowest IMS values (0.39, black circles) to the largest IMS values (0.51, white circles). This phylogeny is missing *A. fascicularis* (see Methods), which would be placed in the clade containing *A. perennis* and *A. mexicana* (Fishbein et al. 2011).

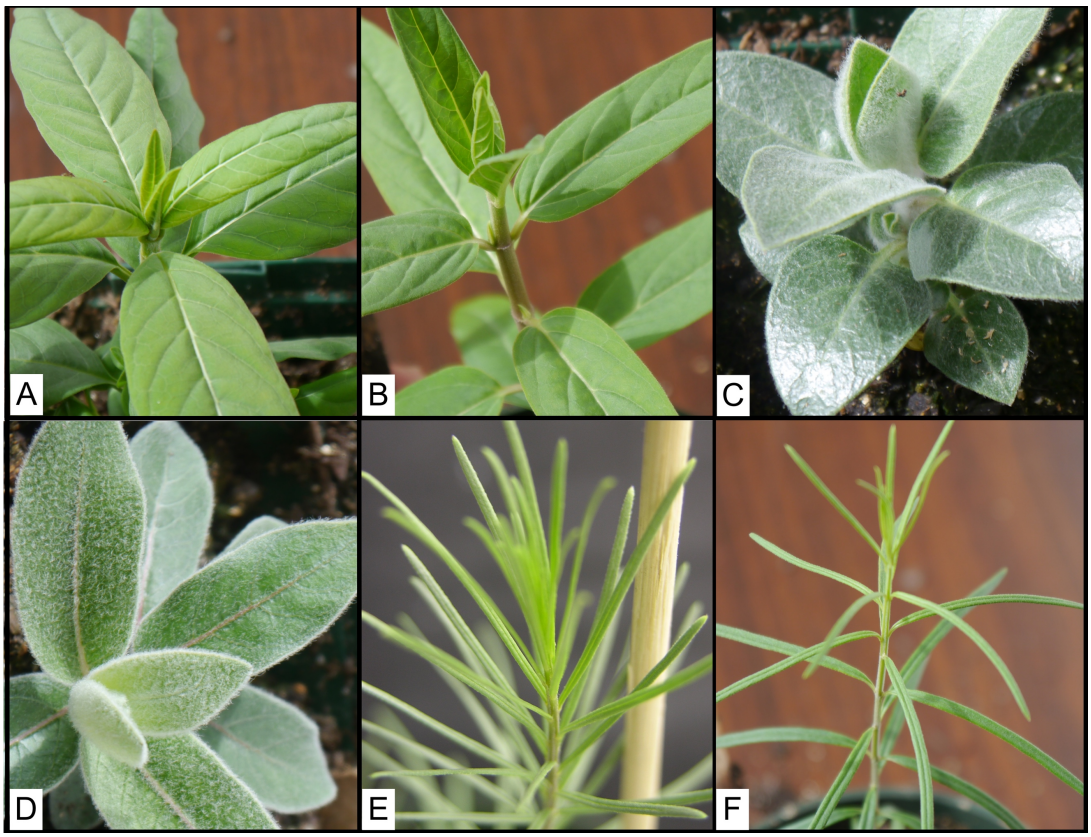

Figure 1.3: Diversity in leaf morphology among juvenile *Asclepias* species used in this study. A) *A. curassavica*; B) *A. incarnata*; C) *A. californica*; D) *A. eriocarpa*; E) *A. pumila*; F) *A. verticillata*.

Results

Metabolic diversity and evolution among Asclepias species

Species leaf cellulose varied in $\delta^{13}C$ and $\Delta^{18}O$ (Figure 1.4A), and associated integrated metabolic strategy (IMS) (Figure 1.4B). Differences among species in IMS were driven more by variation in $\delta^{13}C$, as evidenced by a stronger relationship between IMS and $\delta^{13}C$ (Figure 1.4C; $R^2 = 0.91$, $p < 0.0001$) than $\Delta^{18}O$ (Figure 1.4D; $R^2 = 0.23$, $p = 0.033$).

We predicted that IMS would be influenced by leaf traits, and found that IMS negatively correlated with leaf size and stomatal conductance (g_s) and positively correlated with leaf nitrogen and carboxylation capacity (Vc_{max}), after correcting for biases due to shared evolutionary history using phylogenetically independent contrasts (all p-values < 0.05, Figure 1.5). Together, these results suggest that IMS is mechanistically determined by anatomical and physiological traits that affect carboxylation capacity, leaf boundary layer and stomatal conductances.

IMS, $\delta^{13}C$, leaf size, and stomatal conductance showed little evidence of phylogenetic signal (λ and $K < 0.50$, $p > 0.05$), while $\Delta^{18}O$, leaf nitrogen and carboxylation capacity showed phylogenetic signal consistent with Brownian motion evolution (λ and $K > 0.50$, $p < 0.05$) (Table 1.1).

Species with the lowest IMS (shaded black, Figure 1.2, Figure 1.4) were from wetlands or mesic tropical and sub-tropical regions, and have large, thin leaves (e.g., *A. curassavica*, both subspecies of *A. incarnata*; Figure 1.3A-B). In our subsample of the genus *Asclepias,* these three taxa were found in the Incarnatae clade. Nonetheless, among the two major clades best sampled here (Incarnatae and the north temperate clade containing *A. syriaca*), there was large diversity in

IMS, with each clade containing shifts among the three highest IMS categories (white, hatched, grey in Figure 1.2). Species with mid-range IMS (grey, hatched, Figure 1.4B) were from deserts, grasslands and woodlands and have variably sized leaves generally with hairs or waxes (e.g., *A. californica, A. eriocarpa*; Figure 1.3C-D), while species with the highest IMS (white, Figure 1.4B) have small, thin leaves and are from grasslands and more arid habitats (e.g., *A. pumila*, *A. subulata*; Figure 1.3E). In other words, milkweed species from drier habitats showed relatively higher IMS than those from wetlands, indicative of higher carbon gain for a given water loss under common growth conditions. Moreover, each of the major *Asclepias* clades were well represented in this study (Incarnatae and north temperate clades) and spanned the range of IMS values and leaf morphologies, and had at least two habitat affiliations (Figure 1.2), suggesting that different metabolic strategies and their respective mechanistic underpinnings may have had multiple independent origins.

Metabolic diversity within Asclepias species in response to different water levels

We next conducted manipulations of soil water availability using four milkweed species, from opposite ends of IMS variation. Although $\delta^{13}C$ and $\Delta^{18}O$ varied within species in response to water treatments (Figure 1.6C-D, Figure A1.2), IMS did not vary among the three water treatments for *A. curassavica, A. incarnata* and *A. pumila.* However, IMS was higher under dry conditions for *A. verticillata* (Figure 1.6A). For lower IMS species *A. curassavica* and *A. incarnata*, $\delta^{13}C$ and $\Delta^{18}O$ jointly changed from wet to dry treatments in a positive direction (Figure 1.6C-D, Figure A1.2) that is consistent with the prediction that plants may alter the magnitude of carbon and water fluxes together and maintain a similar IMS in response to water limitation (Figure 1.1). In contrast, $\delta^{13}C$ and $\Delta^{18}O$ of higher IMS species *A. pumila* and *A.*

verticillata changed from wet to dry treatments in a negative direction (Figure 1.6C-D, Figure A1.2). This is consistent with the prediction that plants differentially change the magnitude of carbon and water fluxes, with consequent changes in IMS values in response to water limitation (Figure 1.1).

On average, biomass was much lower for plants grown under the driest conditions (Figure 1.6B). Similarly, $\Delta^{18}O$ was relatively larger under the driest conditions (Figure 1.6D), indicating less foliar water loss. Interestingly, $\delta^{13}C$ and was relatively larger under the driest conditions for *A. curassavica* and *A. incarnata*, but was unchanged in *A. pumila* and relatively lower in *A. verticillata* (Figure 1.6C). In other words, *A. curassavica*, *A. incarnata* and *A. pumila* responded to water limitation by reducing water loss and carbon gain in a similar stoichiometry that ultimately didn't alter their IMS. In contrast, *A. verticillata* reduced water loss in response to water limitation, but did not reduce carbon gain, allowing for greater metabolic efficiency under dry conditions.

Larger IMS values were associated with smaller leaf size and larger stomatal conductances across but not within species (Figure A1.4A-B). Larger IMS values were associated with larger amounts of leaf nitrogen and rates of carboxylation across species but smaller amounts of leaf nitrogen within species, smaller carboxylation rates within wetland-adapted species and larger carboxylation rates within dryland-adapted species (Figure A1.4C-D). See Figures A1.1 and A1.3 for additional trait means across IMS groups and within species in response to water treatments (maximum photosynthetic rates, stomatal conductance, plant height, total leaf area, leaf size, leaf nitrogen content, carboxylation capacity, root/shoot).

Table 1.1: Phylogenetic signal of isotopes and leaf traits using Pagel's λ and Blomberg's K. * $p < 0.05$, ** $p < 0.01$, *** $p < 0.0001$. Larger λ and K values indicate proportional phenotypic similarity to phylogenetic distance based on a Brownian Motion model.

Trait	**Pagel's λ**	**K**
IMS	0.06	0.45
$\delta^{13}C$	< 0.01	0.38
$\Delta^{18}O$	0.83*	0.98*
Leaf size	< 0.01	0.38
Nitrogen content (%)	0.59*	0.88*
Stomatal conductance, g_s	< 0.01	0.44
Maximum rate of carboxylation, Vc_{max}	0.50*	0.65*

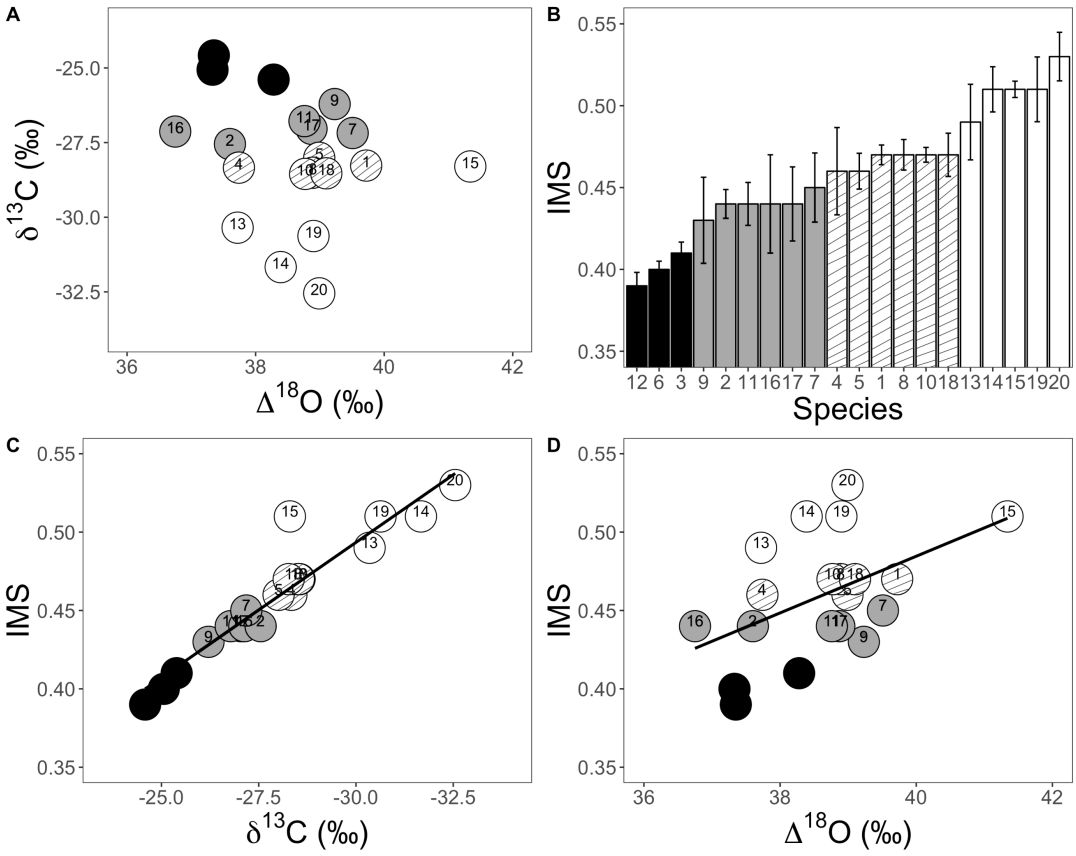

Figure 1.4: Relationships between A) $\delta^{13}C$ and $\Delta^{18}O$ of leaf cellulose ($p = 0.3$); B) integrated metabolic strategy (IMS) values, in order from lowest to highest IMS values; C) IMS values and $\delta^{13}C$ ($R^2 = 0.91$, $p < 0.0001$); and D) IMS and $\Delta^{18}O$ of leaf cellulose ($R^2 = 0.23$, $p = 0.033$) for 20 *Asclepias* taxa grown under common conditions. Larger IMS values indicate higher metabolic efficiency. Data are species means with standard error. Colors correspond to four distinct groups in mean IMS values based on Tukey post-hoc comparisons. 1 = *A. brachystephana*, 2 = *A. californica*, 3 = *A. curassavica*, 4 = *A. eriocarpa*, 5 = *A. fascicularis*, 6 = *A. incarnata* subsp. *incarnata*, 7 = *A. labriformis*, 8 = *A. latifolia*, 9 = *A. linaria*, 10 = *A. mexicana*, 11 = *A. perennis*, 12 = *A. incarnata* subsp. *pulchra*, 13 = *A. pumila*, 14 = *A. speciosa*, 15 = *A. subulata*, 16 = *A. subverticillata*, 17 = *A. syriaca*, 18 = *A. tuberosa*, 19 = *A. verticillata*, 20 = *A. viridis*.

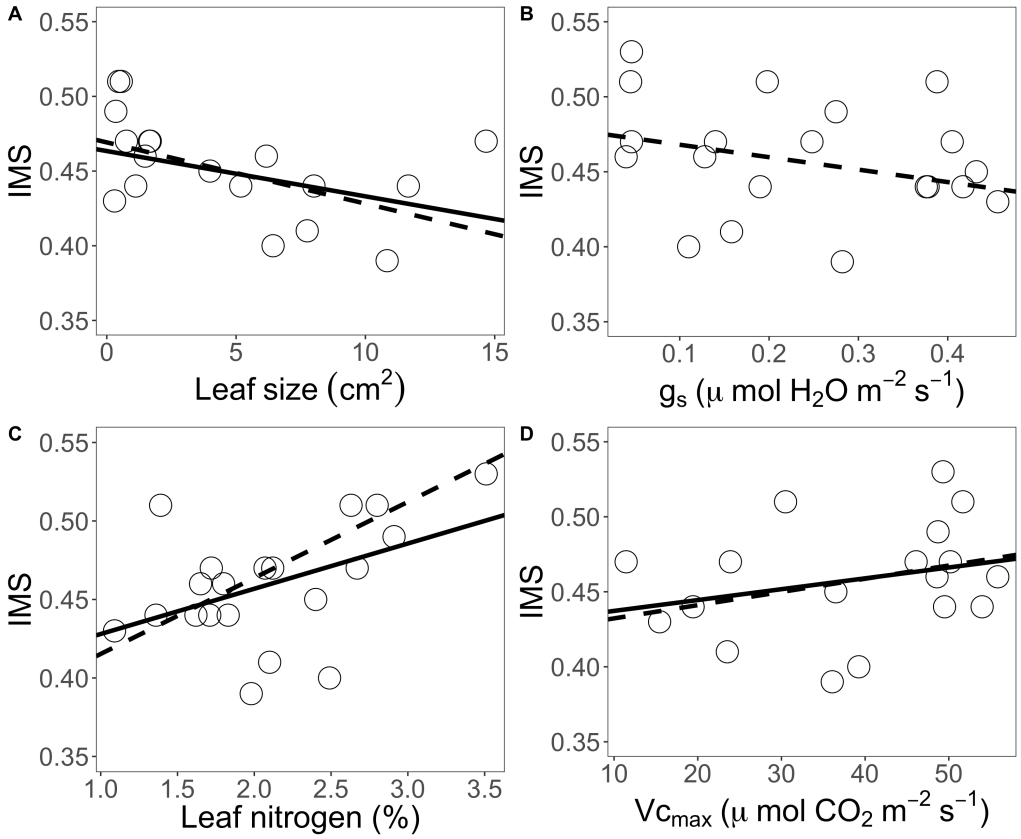

Figure 1.5: Linear relationships based on ordinary least squares regressions (OLS, solid lines) and phylogenetic independent contrasts (PIC, dashed lines) between IMS and A) leaf size (OLS $R^2 = 0.26$*, PIC $R^2 = 0.36$*); B) stomatal conductance, g_s (OLS $R^2 = 0.06$, PIC $R^2 = 0.13$*); C) nitrogen content (OLS $R^2 = 0.23$*, PIC $R^2 = 0.45$**); and D) maximum rate of carboxylation, Vc_{max} (OLS $R^2 = 0.13$*, PIC $R^2 = 0.13$*) for 20 *Asclepias* taxa grown under common conditions. Data are raw species means, * $p < 0.05$, ** $p < 0.01$, *** $p < 0.0001$.

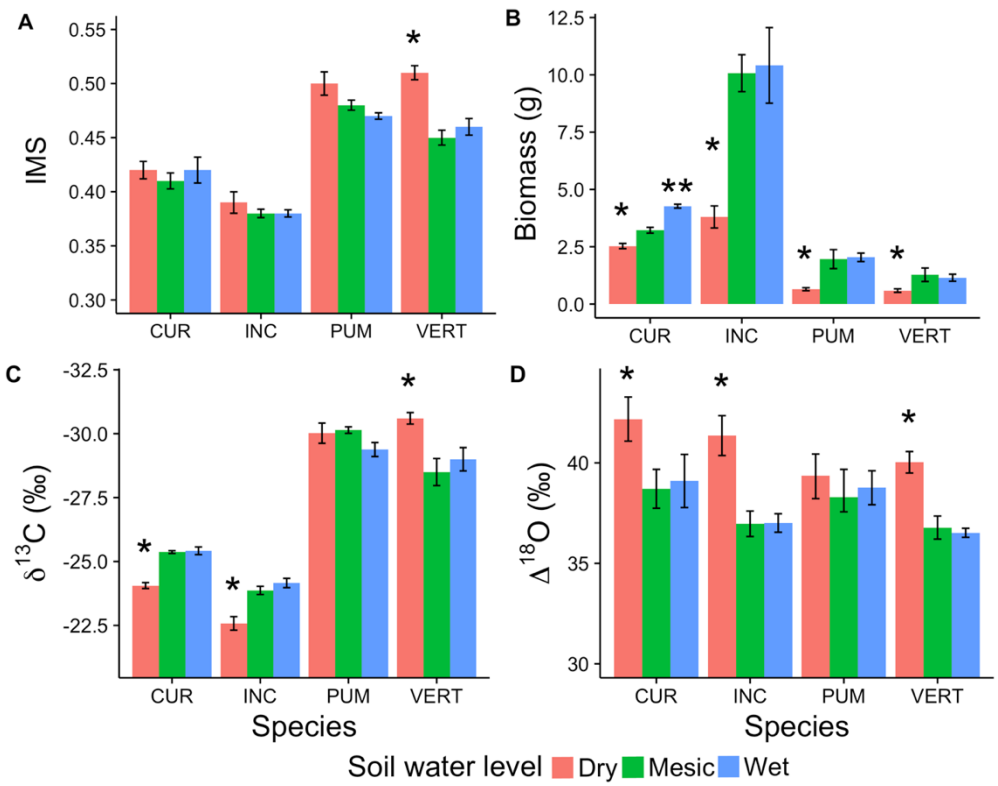

Figure 1.6: Results of one-way ANOVAs between A) IMS, B) biomass, C) $\delta^{13}C$, and D) $\Delta^{18}O$ for four *Asclepias* species grown under three different soil water treatments: dry (one-third field capacity), mesic (field capacity), and wet (twice field capacity). Data are means ± standard error (n=6). Asterisks indicate significant differences between water levels ($P < 0.05$), based on post-hoc Tukey tests.

Discussion

We asked whether closely related yet ecologically diverse milkweed species would vary in IMS when grown under controlled, common conditions. We found that IMS varied substantially among species (Figure 1.4), suggesting differential tradeoffs between carbon gain and water loss. Variation along both $\delta^{13}C$ and $\Delta^{18}O$ axes reflect fundamentally different rates of leaf-level carbon gain among species that likely result from differences in long term CO_2 supply and demand, c_i/c_a. Examining interspecific variation in $\Delta^{18}O$ allowed us to tease apart the separate effects of water loss from metabolic carbon gain that are independent of carboxylation. Moreover, relatively greater interspecific variation in $\delta^{13}C$ than $\Delta^{18}O$ (Figure 1.4) indicated a stronger effect of photosynthesis on c_i/c_a relative to stomatal conductance (Scheidegger *et al.* 2000; Grams *et al.* 2007); thus, metabolic diversity among these species may be driven more by CO_2 demand than factors affecting CO_2 supply and water loss via diffusion. However, we acknowledge that the observed variation in carboxylation is also co-controlled by resource supply, especially nitrogen and phosphorus, which were not limiting in this growth chamber study. Species-specific variation in carboxylation may not be expressed as strongly in nature under nutrient limitations.

We also found that different trait combinations resulted in similar IMS values as predicted by our conceptual model. For example, showy milkweed (*A. speciosa*) is the only broad-leaf representative in the high IMS group (Figure 1.2), and *A. speciosa* had lower $\Delta^{18}O$ and disproportionately smaller $\delta^{13}C$ than other high-IMS species. Pine-needle milkweed (*A. linaria*) had mid-range $\delta^{13}C$ and $\Delta^{18}O$, but based on its stiff, needle-like leaves we would have expected larger $\Delta^{18}O$ (more water conservative). It is unclear if the rocky habitats of *A. linaria* provide access to water pockets, or if our growth chamber conditions did not necessitate

conserving water at the leaf-level. Rush milkweed (*A. subulata*), a desert species, had by far the largest $\Delta^{18}O$, indicating that it is the most water conservative species in this study. The narrow leaves of *A. subulata* are ephemeral and photosynthesis continues primarily through its green stem, although it is unclear whether this relates to water conservation. These species demonstrate how IMS is not necessarily predicted by macroclimate and that similar metabolic efficiencies can be reached via different morphological solutions.

Variation in IMS: leaf traits, habitat affiliations and evolutionary history

Our second goal was to determine the drivers of interspecific variation in IMS, including anatomy, physiology, environment, and evolutionary history. We clearly have not measured all anatomical and physiological characters affecting $\delta^{13}C$ and $\Delta^{18}O$. However, the most influential traits are likely to be those that directly relate to enzymatic carbon fixation and gaseous diffusion rates. As such, we used leaf nitrogen content and maximum rate of carboxylation (Vc_{max}) to represent fixation, and leaf size and stomatal conductance (g_s) to represent gaseous diffusion resistances. Accordingly, IMS positively correlated with leaf nitrogen and Vc_{max} and negatively correlated with leaf size and g_s when accounting for shared evolutionary history, using phylogenetically independent contrasts (Figure 1.5). Previous work has suggested positive relationships between $\delta^{13}C$ and leaf nitrogen and negative relationships between $\Delta^{18}O$ and g_s (Sparks & Ehleringer 1997; Moreno Gutiérrez *et al.* 2012; Ellsworth, Ellsworth & Cousins 2017). Here, we consider these isotopes together in a single index, which allows us to identify potential mechanisms that underlie integrated leaf metabolism as a whole rather than the sum of its parts. Leaf nitrogen and Vc_{max} explained more of the total variation in IMS than leaf size and g_s, further supporting our interpretation that IMS among these species is defined primarily by

differences in leaf-level CO_2 demand rather than differences in CO_2 and water vapor diffusion resistances.

Previous work using gas exchange measurements have found water-use efficiency to be equally controlled by leaf nitrogen and stomatal conductance across tropical woody and herbaceous angiosperm species (Cernusak *et al.* 2007), while stomatal conductance was the primary driver across a diverse range of tropical gymnosperm and angiosperm trees and lianas (Cernusak *et al.* 2008). At least two reasons could account for differences between other studies and ours: first, we use integrated isotopic measures rather than instantaneous gas exchange, thus controlling for temporal variability in fluxes. Second, by comparing closely related species rather than across a broad taxonomic scale (e.g., gymnosperms and angiosperms), we are controlling for confounding effects that characterize such diverse plants (Edwards *et al.* 2014).

Dryland-adapted plants are generally more water-use efficient relative to those from mesic and water-logged environments (Field, Merino & Mooney 1983; Dudley 1996). Consistent with this idea, many of the species with the largest IMS values in this study are from arid habitats (e.g., *A. brachystephana*, *A. subulata*), while those with the lowest IMS values are from wetlands (e.g., *A. incarnata*, *A. perennis*) (Figure 1.2). Although there are few studies that compare $\delta^{13}C$ and $\Delta^{18}O$ across multiple species, if we convert previously presented isotopic data to IMS values, Mediterranean shrubland species occupying more xeric microhabitats also had larger IMS values relative to species restricted to more mesic microhabitats (see Table A1.1 for converted data from Moreno Gutiérrez *et al.* 2012). Larger IMS values in dryland species suggest not only less foliar water loss, but also a greater carboxylation efficiency achieved by fixing similar amounts of carbon at a lower internal CO_2 concentration (c_i) and lower stomatal conductance relative to wetland-adapted species. It is well documented that C_3 plants from arid

ecosystems, especially deserts, are able to maintain high rates of carboxylation while restricting water loss by operating at a lower c_i. Moreover, plants from arid environments often have larger leaf nitrogen content and invest proportionally more of their leaf nitrogen into photosynthesis (i.e., Rubisco enzyme). This allows for a greater drawdown of internal CO_2 (lower c_i), in order to achieve relatively higher photosynthetic rates at a given stomatal conductance than non-arid plants (Wright, Reich & Westoby 2003; Prentice *et al.* 2014). In agreement with this, milkweeds from drylands had larger total leaf nitrogen contents and maximum rates of carboxylation (Figure A1.1F-G), while photosynthetic rates did not vary (Figure A1.1A).

IMS did not show phylogenetic signal (Table 1.1), indicating that the balance between leaf-level carbon gain and water loss is not primarily defined by shared ancestry. As IMS is the end-point integration of many traits, each with potentially different rates of evolution (Ackerly 2009), it is perhaps not surprising that there is no phylogenetic signal. Interestingly, $\Delta^{18}O$, leaf nitrogen content, and carboxylation capacity (Vc_{max}) showed phylogenetic signal, while $\delta^{13}C$, leaf size, and stomatal conductance did not. A strong phylogenetic signal in $\Delta^{18}O$, but a lack of phylogenetic signal in the water-use related traits that we measured (leaf size, stomatal conductance), could arise if other traits important to water loss that we did not measure are phylogenetically conserved and contributed to phylogenetic signal in $\Delta^{18}O$. For example, stomatal pore index and stem and leaf hydraulic conductances across the Magnoliaceae showed phylogenetic signal, but not instantaneous rates of transpiration and stomatal conductance (Liu *et al.* 2015). Similarly, leaf size did not show phylogenetic signal across *Asclepias* (Agrawal *et al.* 2009a) or Ericaceae (Goud & Sparks 2018).

A lack of phylogenetic signal in $\delta^{13}C$ could be indicative of differential trait combinations among species to achieve an overall carbon metabolism that is not necessarily

phylogenetically conserved, despite conservatism in biochemical traits such as leaf nitrogen and Vc_{max}. Leaf nitrogen has been reported to have phylogenetic signal for Magnoliaceae species (Liu *et al.* 2015) but not across the Ericaceae (Goud & Sparks 2018) or closely related Asteraceae (Münzbergová & Šurinová 2015). We previously used discrete foliar traits to characterize *Asclepias* habitat affiliations, with hairy & waxy species being from drier environments than glabrous species (Agrawal *et al.* 2009b). Consistent with this study, wetland species also had larger $\delta^{13}C$ and lower nitrogen content than dryland species (Figure 1.4A, Figure A1.1F).

An additional consideration for the interpretation of our results is the limited sampling of *Asclepias* species in the current study. Mechanistic studies can be limited in the number of taxa to compare, and 20 species is quite high for these types of detailed physiological measurements. However, it is well established that phylogenetically controlled analyses are suspect to sampling bias, including *Asclepias* (Fishbein *et al.* 2018). Increased sampling may improve our understanding about the shifts in IMS among milkweed species. For example, we expect that a few other *Asclepias* species outside of the Incarnatae clade (e.g., *A. lanceolata* and *A. rubra* in the north temperate clade; Figure 1.2) will fall into the lowest IMS category (typical of wetland species), and such independent origins may help to clarify the repeated evolution of physiology-environment associations over macroevolutionary time.

Within-species IMS across an experimental soil moisture gradient

Given that instantaneous gas fluxes and leaf traits can vary by orders of magnitude with environment, it would be reasonable to expect IMS values to be similarly plastic and potentially respond in multiple directions based on growth conditions. Our results suggest that some species

may be constrained by an intrinsic strategy for balancing carbon and water loss at the leaf-level. The question is, how fixed are these strategies? One might expect plants to alter their IMS under severely dry and constantly saturated conditions relative to mesic conditions, and that dryland- and wetland-adapted species may have differential responses. Surprisingly, IMS did not change within species across an experimental soil moisture gradient, with the exception of *A. verticillata* (larger IMS values under dry conditions) (Figure 1.6A). Similar IMS values were maintained across water levels because of proportional changes in $\delta^{13}C$ and $\Delta^{18}O$ for *A. curassavica* and *A. incarnata*, and because of no change in $\delta^{13}C$ and $\Delta^{18}O$ values for *A. pumila* (Figure 1.6C-D).

Consistent IMS across levels of water availability in *A. curassavica* and *A. incarnata* demonstrates a leaf-level strategy to minimize carbon-water tradeoffs. This is in agreement with previous studies that observed changes in $\delta^{13}C$ and $\Delta^{18}O$ between years that differed in water availability, but the relative ranking among species in a community remained consistent (Garten & Taylor 1992; Moreno Gutiérrez *et al.* 2012). It is possible that species-specific carbon-water tradeoffs could buffer plants from short-term environmental fluctuations, or it may limit acclimation and resilience to more persistent environmental change. Future work that explicitly tests species mechanistic responses to long-term environmental change in general, and their IMS responses in particular, will be critical in addressing the generality of these results for other dryland plant species.

A common plastic response to water limitation is stomatal closure and reduced growth often associated with more enriched $\delta^{13}C$ and $\Delta^{18}O$ (Ellsworth *et al.* 2017) and reduced leaf area (Anyia & Herzog 2004; Edwards *et al.* 2012). Although all four species reduced growth under dry conditions (Figure 1.6B) by decreasing total leaf area and height and allocating more biomass to roots relative to leaves and stems (Figure A1.3), they largely maintained similar IMS.

This highlights that high metabolic efficiency does not have to come at the expense of slower growth (Cernusak *et al.* 2007), and that species can reduce growth via differential biomass allocation rather than reducing leaf metabolism per se. Indeed, although species had lower growth under dry conditions, they appear to have compensated by producing fewer leaves that are more efficient via up-regulating carboxylation (i.e., larger leaf nitrogen content and/or Vc_{max}). This is consistent with other studies that report lower growth in response to water limitation accompanied by increasing leaf nitrogen (Edwards *et al.* 2012) and no changes in $\delta^{13}C$ (Johnson & Bassett 1991). Moreover, *A. verticillata* had larger IMS under dry conditions, achieved by proportionally lower $\delta^{13}C$ relative to $\Delta^{18}O$. Lower $\delta^{13}C$ under water limitation is not typically expected, but has also been reported for bristlegrasses (Ellsworth *et al.* 2017). Plasticity in biomass, leaf nutrient allocation, and stomatal behavior all focus resources into water-use, either by increasing root biomass to obtain water or by conserving water via stomatal closure and reducing leaf area. This could indicate that metabolic demand for CO_2 is more fixed within a species, but that water dynamics are more plastic and drive the within-species response across different water availabilities (Gilbert, Zwieniecki & Holbrook 2011).

Evolution of plant ecophysiological strategies

Across species, those that were more metabolically efficient at the leaf-level were generally from drylands, had smaller leaves, and grew more slowly, likely conserving water at the expense of fast growth. This is consistent with predictions of leaf economic and fast-slow growth strategy theories, which predict slower growth rates under resource limitations (Wright *et al.* 2004; Reich 2014). However, within-species responses were less consistent with these predictions, as plants under water limitation did grow more slowly but were no more metabolically inefficient at the

leaf level than those under water saturated conditions (Figure 1.6). Moreover, both among and within species trait combinations were largely inconsistent with leaf economic and fast-slow growth strategy predictions, namely, that faster growing plants in our study had relatively lower leaf nitrogen, less efficient carboxylation, and no substantial differences in leaf size, structure or rates of photosynthesis relative to slower growing plants (Figures A1.1-A1.4).

Our results on the relationship between leaf economic traits and IMS highlight some of the challenges in comparing and correlating traits that cross scales and levels of plant organization (i.e., whole plant versus specific organs, area versus mass) (Lloyd *et al.* 2013). In addition, across-clade comparisons, which are a hallmark of leaf economic spectrum studies (Reich 2014; Wright *et al.* 2004; Wright *et al.* 2005), may conflate coarse-grained strategy shifts with mechanistic shifts that occur as new species are formed within a clade. Given that IMS integrates both area and mass-based traits, this is a clear advantage of applying IMS, alone or alongside other ecological strategy approaches. Although IMS is a leaf-level strategy and may be limited in its ability to predict plant growth per se, it has the distinct advantage of being an endpoint integration of multiple anatomical and physiological characters that together define a plant's strategy to balance metabolic carbon gain and water loss.

Efforts to understand and describe how general categorization of plant characteristics describe strategies for success in different environments has progressed from Grime's conceptual model (Grime 1977) to more explicitly mechanistic and predictive approaches (Chapin, Autumn & Pugnaire 1993; Wright *et al.* 2004; Reich 2014). Much of the focus has been on leaf anatomical characters and instantaneous gas exchange rates, but evidence for the generality of predicted trait combinations is decidedly mixed. This is perhaps in part because certain trait combinations that are expressed across species, presumably as a result of natural selection, may

differ from trait combinations that define plastic responses to more short-term environmental changes. Similarly, there are differential trait combinations that can arrive at a similar growth or metabolic rate. We offer the IMS framework to better understand the mechanistic basis of a plant's strategy to balance metabolic carbon gain and water loss at the leaf-level. Although not explicitly correlated with growth rates, a plant's integrated metabolic strategy appears well matched to environmental conditions. When considered alongside currently established strategy theories, and especially within a phylogenetic context, variation in IMS among and within species may shed light on currently unresolved questions relating to evolution and ecology of plant ecophysiological strategies.

Literature Cited

Ackerly, D. (2009) Conservatism and diversification of plant functional traits: Evolutionary rates versus phylogenetic signal. *Proceedings of the National Academy of Sciences of the United States of America*, **106**, 19699–19706.

Ackerly, D.D., Dudley, S.A., Sultan, S.E., Schmitt, J., Coleman, J.S., Linder, C.R., Sandquist, D.R., Geber, M.A., Evans, A.S., Dawson, T.E. & Lechowicz, M.J. (2000) The evolution of plant ecophysiological traits: Recent advances and future directions. *Bioscience*, **50**, 979–995.

Agrawal, A.A., Fishbein, M., Halitschke, R., Hastings, A.P., Rabosky, D.L. & Rasmann, S. (2009a) Evidence for adaptive radiation from a phylogenetic study of plant defenses. *Proceedings of the National Academy of Sciences of the United States of America*, **106**, 18067–18072.

Agrawal, A.A., Fishbein, M., Jetter, R., Salminen, J.P., Goldstein, J.B., Freitag, A.E. & Sparks, J.P. (2009b) Phylogenetic ecology of leaf surface traits in the milkweeds (Asclepias spp.): chemistry, ecophysiology, and insect behavior. *New Phytologist*, **183**, 848–867.

Anyia, A. (2004) Water-use efficiency, leaf area and leaf gas exchange of cowpeas under mid-season drought. *European Journal of Agronomy*, **20**, 327–339.

Anyia, A.O. & Herzog, H. (2004) Water-use efficiency, leaf area and leaf gas exchange of cowpeas under mid-season drought. *European Journal of Agronomy*, **20**, 327–339.

Barbour, M.M., Roden, J.S., Farquhar, G.D. & Ehleringer, J.R. (2004) Expressing leaf water and cellulose oxygen isotope ratios as enrichment above source water reveals evidence of a

Peclet effect. *Oecologia*, **138**, 426–435.

Caemmerer, von, S. & Farquhar, G.D. (1981) Some relationships between the biochemistry of photosynthesis and the gas exchange of leaves. *Planta*, **153**, 376–387.

Castresana, J. (2000) Selection of Conserved Blocks from Multiple Alignments for Their Use in Phylogenetic Analysis. *Molecular Biology and Evolution*, **17**, 540–552.

Cernusak, L.A., Aranda, J., Marshall, J.D. & Winter, K. (2007) Large variation in whole-plant water-use efficiency among tropical tree species. *The New phytologist*, **173**, 294–305.

Cernusak, L.A., Farquhar, G.D. & Pate, J.S. (2005) Environmental and physiological controls over oxygen and carbon isotope composition of Tasmanian blue gum, Eucalyptus globulus. *Tree Physiology*, **25**, 129–146.

Cernusak, L.A., Winter, K., Aranda, J. & Turner, B.L. (2008) Conifers, angiosperm trees, and lianas: growth, whole-plant water and nitrogen use efficiency, and stable isotope composition delta13C and delta18O of seedlings grown in a tropical environment. *Plant Physiology*, **148**, 642–659.

Chapin, F.S., III, Autumn, K. & Pugnaire, F. (1993) Evolution of Suites of Traits in Response to Environmental Stress. *The American Naturalist*, **142**, S78–S92.

Colman, E.A. (1947) A laboratory procedure for determining the field capacity of soils. *Soil Science*, **63**, 277–284.

Dìaz, S., Kattge, J., Cornelissen, J.H.C., Wright, I.J., Lavorel, S., Dray, S., Reu, B., Kleyer, M., Wirth, C., Prentice, I.C., Garnier, E., Bönisch, G., Westoby, M., Poorter, H., Reich, P.B.,

Moles, A.T., Dickie, J., Gillison, A.N., Zanne, A.E., Chave, J., Wright, S.J., Sheremet'ev, S.N., Jactel, H., Baraloto, C., Cerabolini, B., Pierce, S., Shipley, B., Kirkup, D., Casanoves, F., Joswig, J.S., Günther, A., Falczuk, V., Rüger, N., Mahecha, M.D. & Gorné, L.D. (2016) The global spectrum of plant form and function. *Nature*, **529**, 167–171.

Dudley, S.A. (1996) Differing Selection on Plant Physiological Traits in Response to Environmental Water Availability: A Test of Adaptive Hypotheses. *Evolution*, **50**, 92.

Edwards, C.E., Ewers, B.E., McClung, C.R., Lou, P. & Weinig, C. (2012) Quantitative Variation in Water-Use Efficiency across Water Regimes and Its Relationship with Circadian, Vegetative, Reproductive, and Leaf Gas-Exchange Traits. *Molecular Plant*, **5**, 653–668.

Edwards, E.J., Chatelet, D.S., Sack, L. & Donoghue, M.J. (2014) Leaf life span and the leaf economic spectrum in the context of whole plant architecture (ed W Cornwell). *Journal of Ecology*, **102**, 328–336.

Ehleringer, J.R. (1993) 11 - Carbon and Water Relations in Desert Plants: An Isotopic Perspective. *Stable Isotopes and Plant Carbon-water Relations*, Stable Isotopes and Plant Carbon-water Relations (eds J.R. Ehleringer, A.E. Hall & G.D. Farquhar), pp. 155–172. Academic Press, San Diego.

Ehleringer, J.R., Phillips, S.L. & Comstock, J.P. (1992) Seasonal variation in the carbon isotopic composition of desert plants. *Functional ecology*, **6**, 396–404.

Ellsworth, P.Z., Ellsworth, P.V. & Cousins, A.B. (2017) Relationship of leaf oxygen and carbon isotopic composition with transpiration efficiency in the C4 grasses Setaria viridis and Setaria italica. *Journal of experimental botany*, **68**, 3513–3528.

Farquhar, G.D. & Sharkey, T.D. (1982) Stomatal conductance and photosynthesis. *Annual review of plant physiology*, **33**, 317–345.

Farquhar, G.D., Cernusak, L.A. & Barnes, B. (2007) Heavy water fractionation during transpiration. *Plant Physiology*, **143**, 11–18.

Farquhar, G.D., Ehleringer, J.R. & Hubick, K.T. (1989) Carbon Isotope Discrimination and Photosynthesis. *annual review of plant physiology and plant molecular biology*, **40**, 503–537.

Field, C., Merino, J. & Mooney, H.A. (1983) Compromises between water-use efficiency and nitrogen-use efficiency in five species of California evergreens. *Oecologia*, **60**, 384–389.

Fishbein, M., Chuba, D., Ellison, C. & Mason-Gamer, R.J. (2011) Phylogenetic relationships of Asclepias (Apocynaceae) inferred from non-coding chloroplast DNA sequences. *Systematic Botany*, **36**, 1008–1023.

Fishbein, M., Straub, S.C.K., Boutte, J., Hansen, K., Cronn, R.C. & Liston, A. (2018) Evolution at the tips: Asclepiasphylogenomics and new perspectives on leaf surfaces. *American Journal of Botany*, **105**, 514–524.

Flanagan, L.B. & Farquhar, G.D. (2014) Variation in the carbon and oxygen isotope composition of plant biomass and its relationship to water-use efficiency at the leaf- and ecosystem-scales in a northern Great Plains grassland. *plant, cell and environment*, **37**, 425–438.

Garten, C.T., Jr. & Taylor, G.E., Jr. (1992) Foliar ?13C within a temperate deciduous forest: spatial, temporal, and species sources of variation. *Oecologia*, **90**, 1–7.

Gilbert, M.E., Zwieniecki, M.A. & Holbrook, N.M. (2011) Independent variation in photosynthetic capacity and stomatal conductance leads to differences in intrinsic water use efficiency in 11 soybean genotypes before and during mild drought. *Journal of experimental botany*, **62**, 2875–2887.

Givnish, T.J. & Vermeij, G.J. (1976) Sizes and Shapes of Liane Leaves. *The American Naturalist*, **110**, 743–778.

Goud, E.M. & Sparks, J.P. (2018) Leaf stable isotopes suggest shared ancestry is an important driver of functional diversity. *Oecologia*, **187**, 967–975.

Grams, T.E.E., Kozovits, A.R., Haberle, K.-H., Matyssek, R. & Dawson, T.E. (2007) Combining delta 13C and delta 18O analyses to unravel competition, CO2 and O3 effects on the physiological performance of different-aged trees. *plant, cell and environment*, **30**, 1023–1034.

Grime, J.P. (1977) Evidence for the Existence of Three Primary Strategies in Plants and Its Relevance to Ecological and Evolutionary Theory. *The American Naturalist*, **111**, 1169–1194.

Johnson, R.C. & Bassett, L.M. (1991) Carbon Isotope Discrimination and Water Use Efficiency in Four Cool-Season Grasses. *Crop Science*, **31**, 157–162.

Katoh, K., Rozewicki, J. & Yamada, K.D. (2017) MAFFT online service: multiple sequence alignment, interactive sequence choice and visualization. *Briefings in Bioinformatics*, **30**, 3059.

Kearse, M., Moir, R., Wilson, A., Stones-Havas, S., Cheung, M., Sturrock, S., Buxton, S., Cooper, A., Markowitz, S., Duran, C., Thierer, T., Ashton, B., Meintjes, P. & Drummond, A. (2012) Geneious Basic: An integrated and extendable desktop software platform for the organization and analysis of sequence data. *Bioinformatics*, **28**, 1647–1649.

Keenan, T.F., Hollinger, D.Y., Bohrer, G., Dragoni, D., Munger, J.W., Schmid, H.P. & Richardson, A.D. (2013) Increase in forest water-use efficiency as atmospheric carbon dioxide concentrations rise. *Nature*, **499**, 324–327.

Kembel, S.W., Cowan, P.D., Helmus, M.R., Cornwell, W.K., Morlon, H., Ackerly, D.D., Blomberg, S.P. & Webb, C.O. (2010) Picante: R tools for integrating phylogenies and ecology. *Bioinformatics*, **26**, 1463–1464.

Lambers, H., Chapin, F.S. & Pons, T.L. (2008) *Plant Physiological Ecology*, 2nd ed. Springer New York, New York.

Leavitt, S.W. & Danzer, S.R. (2002) Method for batch processing small wood samples to holocellulose for stable-carbon isotope analysis. *Analytical Chemistry*, **65**, 87–89.

Liu, H., Xu, Q., He, P., Santiago, L.S., Yang, K. & Ye, Q. (2015) Strong phylogenetic signals and phylogenetic niche conservatism in ecophysiological traits across divergent lineages of Magnoliaceae. *Scientific Reports*, **5**, 343.

Lloyd, J., Bloomfield, K., Domingues, T.F. & Farquhar, G.D. (2013) Photosynthetically relevant foliar traits correlating better on a mass vs an area basis: of ecophysiological relevance or just a case of mathematical imperatives and statistical quicksand? *The New phytologist*, **199**, 311–321.

Mason, C.M. & Donovan, L.A. (2015) Evolution of the leaf economics spectrum in herbs: Evidence from environmental divergences in leaf physiology across Helianthus(Asteraceae). *Evolution*, **69**, 2705–2720.

Minh, B.Q., Nguyen, M.A.T. & Haeseler, von, A. (2013) Ultrafast Approximation for Phylogenetic Bootstrap. *Molecular Biology and Evolution*, **30**, 1188–1195.

Monson, R.K. & Ehleringer, J.R. (1993) Evolutionary and Ecological Aspects of Photosynthetic Pathway Variation. *Annual Review of Ecology and Systematics*, **24**, 411–439.

Moreno Gutiérrez, C., Dawson, T.E., Nicolás, E. & Querejeta, J.I. (2012) Isotopes reveal contrasting water use strategies among coexisting plant species in a Mediterranean ecosystem. *New Phytologist*, **196**, 489–496.

Münzbergová, Z. & Šurinová, M. (2015) The importance of species phylogenetic relationships and species traits for the intensity of plant-soil feedback. *Ecosphere*, **6**, 1–16.

Nguyen, L.-T., Schmidt, H.A., Haeseler, von, A. & Minh, B.Q. (2015) IQ-TREE: a fast and effective stochastic algorithm for estimating maximum-likelihood phylogenies. - PubMed - NCBI. *Molecular Biology and Evolution*, **32**, 268–274.

O'Leary, M.H. (1988) Carbon isotopes in photosynthesis. *Bioscience*, **38**, 328–336.

Offermann, C., Ferrio, J.P., Holst, J., Grote, R., Siegwolf, R., Kayler, Z. & Gessler, A. (2011) The long way down--are carbon and oxygen isotope signals in the tree ring uncoupled from canopy physiological processes? *Tree Physiology*, **31**, 1088–1102.

Osmond, C.B., Bjorkman, O. & Anderson, D.J. (1980) Photosynthesis. *Physiological Processes*

in Plant Ecology: Toward a Synthesis with Atriplex, Physiological Processes in Plant Ecology: Toward a Synthesis with Atriplex (eds C.B. Osmond, O. Bjorkman & D.J. Anderson), pp. 291–377. Springer Berlin Heidelberg, Berlin, Heidelberg.

Paradis, E., Claude, J. & Strimmer, K. (2004) APE: Analyses of Phylogenetics and Evolution in R language. *Bioinformatics*, **20**, 289–290.

Prentice, I.C., Dong, N., Gleason, S.M., Maire, V. & Wright, I.J. (2014) Balancing the costs of carbon gain and water transport: testing a new theoretical framework for plant functional ecology. (ed J Peñuelas). *Ecology letters*, **17**, 82–91.

Prieto, I., QUEREJETA, J.I., Segrestin, J., Volaire, F. & Roumet, C. (2017) Leaf carbon and oxygen isotopes are coordinated with the leaf economics spectrum in Mediterranean rangeland species (ed R Oliveira). *Functional ecology*, **32**, 612–625.

Pugnaire, F. & Valladares, F. (1999) *Handbook of Functional Plant Ecology*. CRC Press, New York.

R Core Team (2016). R: A language and environment for statistical computing. R Foundation for Statistical Computing, Vienna, Austria. URL https://www.R-project.org/.

Reich, P.B. (2014) The world-wide "fast-slow" plant economics spectrum: a traits manifesto (ed H Cornelissen). *Journal of Ecology*, **102**, 275–301.

Roden, J.S. & Ehleringer, J.R. (2000) Hydrogen and oxygen isotope ratios of tree ring cellulose for field-grown riparian trees. *Oecologia*, **123**, 481–489.

Roden, J.S. & Farquhar, G.D. (2012) A controlled test of the dual-isotope approach for the

interpretation of stable carbon and oxygen isotope ratio variation in tree rings. *Tree Physiology*, **32**, 490–503.

Sage, R.F. (2004) The evolution of C 4photosynthesis. *The New phytologist*, **161**, 341–370.

Scheidegger, Y., Saurer, M., Bahn, M. & Siegwolf, R. (2000) Linking stable oxygen and carbon isotopes with stomatal conductance and photosynthetic capacity: a conceptual model. *Oecologia*, **125**, 350–357.

Seibt, U., Rajabi, A., Griffiths, H. & Berry, J.A. (2008) Carbon isotopes and water use efficiency: sense and sensitivity. *Oecologia*, **155**, 441–454.

Smith, S.A. & O'Meara, B.C. (2012) treePL: divergence time estimation using penalized likelihood for large phylogenies. *Bioinformatics*, **28**, 2689–2690.

Sparks, J.P. & Ehleringer, J.R. (1997) Leaf carbon isotope discrimination and nitrogen content for riparian trees along elevational transects. *Oecologia*, **109**, 362–367.

Straub, S.C.K., Parks, M., Weitemier, K., Fishbein, M., Cronn, R.C. & Liston, A. (2012) Navigating the tip of the genomic iceberg: Next-generation sequencing for plant systematics. *American Journal of Botany*, **99**, 349–364.

Wright, I.J., Reich, P.B. & Westoby, M. (2003) Least-cost input mixtures of water and nitrogen for photosynthesis. *The American Naturalist*, **161**, 98–111.

Wright, I.J., Reich, P.B., Cornelissen, J.H.C., Falster, D.S., Garnier, E., Hikosaka, K., Lamont, B.B., Lee, W., Oleksyn, J., Osada, N., Poorter, H., Villar, R., Warton, D.I. & Westoby, M. (2005) Assessing the generality of global leaf trait relationships. *The New phytologist*, **166**,

485–496.

Wright, I.J., Reich, P.B., Westoby, M., Ackerly, D.D., Baruch, Z., Bongers, F., Cavender-Bares, J., Chapin, T., Cornelissen, J.H.C., Diemer, M., Flexas, J., Garnier, E., Groom, P.K., Gulias, J., Hikosaka, K., Lamont, B.B., Lee, T., Lee, W., Lusk, C., Midgley, J.J., Navas, M.-L., Niinemets, Ü., Oleksyn, J., Osada, N., Poorter, H., Poot, P., Prior, L., Pyankov, V.I., Roumet, C., Thomas, S.C., Tjoelker, M.G., Veneklaas, E.J. & Villar, R. (2004) The worldwide leaf economics spectrum. *Nature*, **428**, 821–827.

CHAPTER TWO

Metabolic diversity: an important mechanism contributing to species diversity in ecological communities?

Abstract

Variation in metabolism may be an important mechanism underlying patterns of biodiversity, but the extent and role of metabolic diversity in plant communities is largely unknown. Plant primary metabolism is intrinsically linked to water loss during leaf gas exchange, and different strategies to balance carbon gain and water loss can arise among taxa. I compared metabolic strategies, measured by leaf carbon and oxygen stable isotopes ($\delta^{13}C$, $\Delta^{18}O$), among old-field species over two years that differed in precipitation. Species with a strategy to gain carbon at the expense of water loss generally decreased in abundance in the drier year, while water-conservative species generally increased in cover. Some species decreased water loss while maintaining high rates of carbon gain, indicating an uncoupling between carbon and water gas exchange. Metabolic diversity may have consequences for species coexistence by influencing growth and competitive outcomes that appear related to variation in climate between years.

Introduction

What maintains community-level species diversity is a fundamental question in ecology (Whittaker 1965, Sutherland et al. 2013). Differences in niches (Wright 2002; Levine & HilleRisLambers 2009), competitive ability (Tilman 1994; Hacker & Bertness 1999; Mayfield & Levine 2010), and species interactions (e.g., pollination; Gentry 1974; Fontaine *et al.* 2005), predation; Collins 1998; Olff & Ritchie 1998) are classically invoked to explain species coexistence in ecological communities. Despite a large theoretical and empirical literature describing patterns of species diversity, the physiological mechanisms underlying species differences are less understood. In particular, the role of metabolism, broadly defined as all anabolic and catabolic cellular processes, is not clear but may play a critical role in structuring patterns of diversity across scales. Given that an organism's basal or intrinsic metabolism determines energy production and expense, metabolic diversity may underlie differences in resource allocation for growth and survival. As such, variation in metabolism among co-occurring species may have important consequences for niche partitioning, competition, and other species interactions that influence community composition (Angert *et al.* 2009; Whittaker 1965).

Despite theoretical advances in how individual metabolism should scale-up to influence community processes (Brown et al. 2004, Tilman et al. 2004), studies to date have mainly focused on animal communities. Consequently, our understanding of the influence of metabolic diversity on plant community composition has been limited. In part, this is due to challenges in measuring intrinsic metabolism among plant species in ecologically meaningful ways (Brown *et al.* 2004). Photosynthetic carbon fixation is the primary metabolic process in plants; as CO_2 diffuses into leaves, water vapor simultaneously diffuses out, resulting in a tradeoff between

leaf-level carbon gain and water loss. These leaf-level fluxes are typically measured as instantaneous gas exchange rates of CO_2 and water vapor. Comparing these fluxes is complicated by the fact that leaf gas exchange varies instantaneously with light, temperature, and relative humidity, which can result in broad metabolic variation throughout a plant's life, across a growing season, and within the course of a day (Caemmerer and Farquhar 1981). To avoid problematic comparisons between instantaneous point measurements of metabolic fluctuations, comparing metabolic diversity among different species requires a measure of long-term, average gas exchange that is integrated over the lifespan of a leaf.

An emerging approach to overcome the limitations of instantaneous gas exchange measurements is to use leaf carbon and oxygen stable isotopes (Moreno Gutiérrez et al. 2012, Goud et al. 2019). In Chapter 1, I introduced the concept of *integrated metabolic strategy* (IMS) to describe carbon-water tradeoffs using the carbon and oxygen stable isotope composition of leaf cellulose (Goud *et al.* 2019). The carbon stable isotope ratio ($\delta^{13}C$) of leaves integrates the long-term supply and demand of CO_2 and is a measure of the concentration gradient between leaf internal and external CO_2 (c_i/c_a) (Farquhar *et al.* 1989). Because atmospheric water vapor can vary independently of changes in atmospheric CO_2, $\delta^{13}C$ alone cannot consistently represent the simultaneous exchange of CO_2 and water vapor. However, evaporative conditions of the leaf (*i.e.*, an approximation of the rate of water loss) can be integrated by measuring the oxygen stable isotope enrichment of leaf material above source water ($\Delta^{18}O = \delta^{18}O_{leaf} - \delta^{18}O_{source\ water}$; Farquhar *et al.* 2007; Roden & Farquhar 2012). Generally, smaller (depleted) $\delta^{13}C$ and $\Delta^{18}O$ values indicate smaller concentration gradients, with depleted $\delta^{13}C$ reflective of relatively more carbon gain and depleted $\Delta^{18}O$ reflective of relatively more water loss. When considered together, $\delta^{13}C$ and $\Delta^{18}O$ can be used to represent the endpoint integration of the various

anatomical and physiological factors that determine the carbon-water tradeoff in leaves.

The relationship between $\delta^{13}C$ and $\Delta^{18}O$ can be converted to an index (IMS value) that provides a single measure of a plant's metabolic strategy to balance leaf-level carbon gain and water loss:

$$IMS = |\delta^{13}C| / (100 - \Delta^{18}O),$$

with increasing IMS values corresponding to increases in leaf-level carbon gain per unit of evaporative water loss (Goud et al. 2019). In Chapter 1, I demonstrated that factors such as environment, leaf anatomy, physiology, and evolutionary history generally predict metabolic strategies in milkweeds (*Aslcepias* spp., Apocynaceae) (Goud *et al.* 2019). Species with overlapping IMS values were often from similar habitats and shared common traits such as leaf size, nitrogen content, and gas exchange rates. For example, species from water-limited environments, such as deserts and arid grasslands, shared a metabolic strategy to efficiently gain carbon while minimizing foliar water loss, achieved via thick leaves with high carboxylation capacity and tightly controlled stomatal conductance. Conversely, species from wetlands had considerably higher evaporative water loss relative to carbon gain, with characteristic broad, thin leaves and fast growth rates. This work shed light on the macroevolution of metabolic strategies across a diverse clade, but provided little direct insight onto how metabolism might vary among potentially distantly related species that co-occur in the same community.

Here, I test two alternative hypotheses for how physiological variation may be an underlying mechanism for plant community diversity. Under one hypothesis, within a given community, co-occurring species are likely to converge on similar metabolic strategies dictated by common adaptations to the local climate and soil conditions. Similar metabolic strategies

would be indicated by overlap in $\delta^{13}C$ and $\Delta^{18}O$ dual-isotope space and similar IMS values. In this case, species diversity would be more strongly controlled by variation in characteristics that do not directly affect leaf CO_2 and water gas exchange, such as pollination (Eisen *et al.* 2019) and defense against herbivores (Agrawal *et al.* 2012). An alternative hypothesis is that co-occurring plant species have fundamentally different metabolic strategies, which would be seen as separation in dual-isotope space and different IMS values. In this case, species and metabolic diversity may be maintained by variation in characteristics that directly affects carbon-water tradeoffs, such as light and water. For example, spatial and temporal variation in resources (e.g., wet and dry microsites) and/or differential uptake strategies (e.g., relative rooting depths) could allow for the co-occurrence of plants with distinct resource acquisition needs. To test these hypotheses, I compared metabolic strategies among 18 co-occurring plant species in a successional old field community in upstate New York. I measured leaf $\delta^{13}C$, $\Delta^{18}O$, and IMS values over two growing seasons that differed in summer precipitation, which allowed us to compare potential influences of climate on community metabolic diversity and species composition. To explore the potential role of morphology, physiology, and evolutionary history on $\delta^{13}C$ and $\Delta^{18}O$ variation, I also measured plant height, leaf nitrogen content, relative rooting depth, and phylogenetic relationships among species. Collectively, I used these measurements to test for the role of metabolic diversity on trait and species diversity within a successional old field community.

Material and methods

Study site and soil sampling

All measurements were made in an old field in Ithaca, NY, USA (42.46, -76.45). The site is a

mid-successional old field that was last tilled and mowed in 2006 (Agrawal, A.A., personal communication). Plant species composition is predominantly perennial herbaceous forbs, mostly of the Asteraceae family (e.g., *Cirsium, Solidago*), some grasses (e.g., *Phleum pratense*), and sparse shrub cover (e.g., *Rosa multiflora*). The most dominant species is *Solidago altissima* (Marks 1983). The site is approximately 400 m x 300 m (1200 m^2), with well-drained soils on top of glacial till and relatively flat terrain. The climate is moderate continental with an average annual temperature of 8^oC and a mean annual precipitation of 947 mm.

In May 2017, I established five 10 m by 10 m (100 m^2) plots spaced 5 m apart. In June 2017 and 2018, I collected soil samples (n = 3 per plot) at a depth of 30 cm using a cylindrical auger. In mid-July 2017 and 2018, I collected soil samples (n = 1 per plot) at depth intervals of 10 cm reaching a maximum depth of 70 cm. Soil samples were oven dried at 75^oC for 48 hours. Water was extracted from soils using a cryogenic vacuum distillation line (Ehleringer et al, 2000) and stored in a freezer until they were measured for $\delta^{18}O$. Soil carbon (C) and nitrogen (N) content were measured using an elemental analyzer (Thermo Finnigan Carlo Erba NC2500).

Community composition: species and phylogenetic diversity

I selected 18 focal species that were common to all plots (Figure 2.1): *Cirsium arvense* (L.) Scop., *C. vulgare* (Savi) Ten., *Erigeron philadelphicus* L., *Euthamia graminifolia* (L.) Nutt., *Solidago altissima* L., *S. juncea* Aiton., *S. rugosa* Mill., *Sonchus arvensis* L., and *Taraxacum officinale* F.H. Wigg. Additional species were from Apiaceae (*Daucus carota* L.), Asclepiadaceae (*Asclepias syriaca* L.), Caprifoliaceae (*Lonicera morrowii* A. Gray), Lythraceae (*Lythrum salicaria* L.), Malvaceae (*Malva moschata* L.), Poaceae (*Phleum pratense* L.), Rosaceae (*Geum aleppicum* Jacq., *Rosa multiflora* Thunb.), and Rubiaceae (*Galium triflorum*

Michx.). All species are perennial angiosperms; one species is a grass (*P. pratense*), two are shrubs (*L. morrowii, R. multiflora*), and the remaining species are forbs.

In mid-July 2017 and 2018, I estimated species' relative abundance by visually estimating the percent cover of each species present in each plot. To estimate evolutionary relationships among species in the community, we constructed a phylogeny using maximum likelihood analyses using the 'phangorn v2.5.3' R-package (Schliep 2010). I obtained mat*K*, *nr*ITS and rbcL gene sequence data for all 18 species from GenBank. The tree was rooted on the only monocot species in the community, *Phleum pratense*, and the final tree (Figure 2.1) was topologically congruent with recent phylogenies of the angiosperms as a whole (APG IV 2016). I assessed the level of community phylogenetic diversity using Faith's phylogenetic diversity (PD) index (Faith 1992).

Plant sampling

One replicate plant per species was collected in each plot in 2017 and in 2018 for a total of 10 replicate plants per species (n = 5 per year). For each individual plant, I recorded its height, collected fully expanded sun-exposed leaves (n = 10 per plant) and suberized tissue (stem or root material, depending on the species). Suberized tissue (stem or root material, depending on the species) was immediately placed in capped plastic vials, wrapped in Parafilm, and stored in a freezer until further analyses. Water was extracted from stem/root tissue using a cryogenic vacuum distillation line (Ehleringer et al, 2000) and stored in a freezer until they were measured for $\delta^{18}O$. Leaf tissue was oven-dried at 60^{o}C for 48 hours before being finely ground by hand with mortar and pestle. Leaf carbon (C) and nitrogen (N) content were measured using an elemental analyzer (Thermo Finnigan Carlo Erba NC2500).

Leaf cellulose extraction and isotope analyses

Leaf α-cellulose was extracted in multiple steps following the protocol of Goud et al., 2019; lipids and resins were extracted using toluene and ethanol solvents in a Soxhlet apparatus, lignin was then extracted by bleaching in acidified sodium chlorite at 70^{o}C. Hemicellulose was removed in sodium hydroxide (10%) followed by an acetic acid solution (10%) and rinsing in distilled water.

The carbon and oxygen isotope ratios ($\delta^{13}C$, $\delta^{18}O$) of bulk leaf and leaf cellulose were measured using a continuous flow isotope ratio mass spectrometer (Thermo Scientific Delta V Advantage). For $\delta^{13}C$, the mass spectrometer was coupled to an elemental analyzer (Carlo Erba NC2500) and for $\delta^{18}O$ it was coupled to a Thermo Scientific TC/EA pyrolysis analyzer with a Costech Zero Blank auto sampler. Samples were analysed for stable isotope composition at the Cornell University Stable Isotope Lab, Ithaca, NY. Isotope ratios are expressed as δ values (per mil):

$$\delta^{13}C, \delta^{18}O = (R_{sample}/R_{standard} - 1) \times 1000 \text{ (‰)},$$

where R_{sample} and $R_{standard}$ are the ratios of heavy to light isotope of the sample relative to the international standards for C and O, Vienna-Pee-Dee Belemnite and Vienna Standard Mean Ocean Water, respectively.

Statistical analyses

I assessed interspecific and interannual differences in response variables using linear mixed effects models and analysis of variance (ANOVA) with 'plot' as a random effect. Response variables were integrated metabolic strategy values (IMS), carbon isotope composition ($\delta^{13}C$),

and leaf oxygen isotope enrichment above source water ($\Delta^{18}O$) obtained from bulk leaf material and leaf cellulose. Additional response variables were species' relative abundance (% cover), plant height, plant source water oxygen isotope composition ($\delta^{18}O$), and leaf nitrogen content (% N). Independent fixed factors were species, year, and their interaction.

To assess the degree to which closely related species are more functionally similar to one another than expected by chance, I calculated phylogenetic signal using Pagel's λ and Blomberg's *K* for continuous variables ($\delta^{13}C$, $\delta^{18}O$, IMS, %N, height). Pagel's λ and Blomberg's *K* assume a Brownian motion model of trait evolution, and for both indices, a value of 1 indicates that the trait distribution scales with tree topology in accordance with Brownian motion (*i.e.*, relatives are more similar to each other than expected by random chance). Values closer to 0 indicate that the tree topology does not structure trait variation (Pagel 1999, Blomberg et al. 2003). I tested whether λ and *K* were > 0 by comparing the log-likelihood of the fitted λ and *K* values with that of λ and $K = 0$ using a log-likelihood ratio test using the 'phylosig' function in the phytools R package (Revell 2012). All analyses were performed in R5.3.2 (R Core Team 2019).

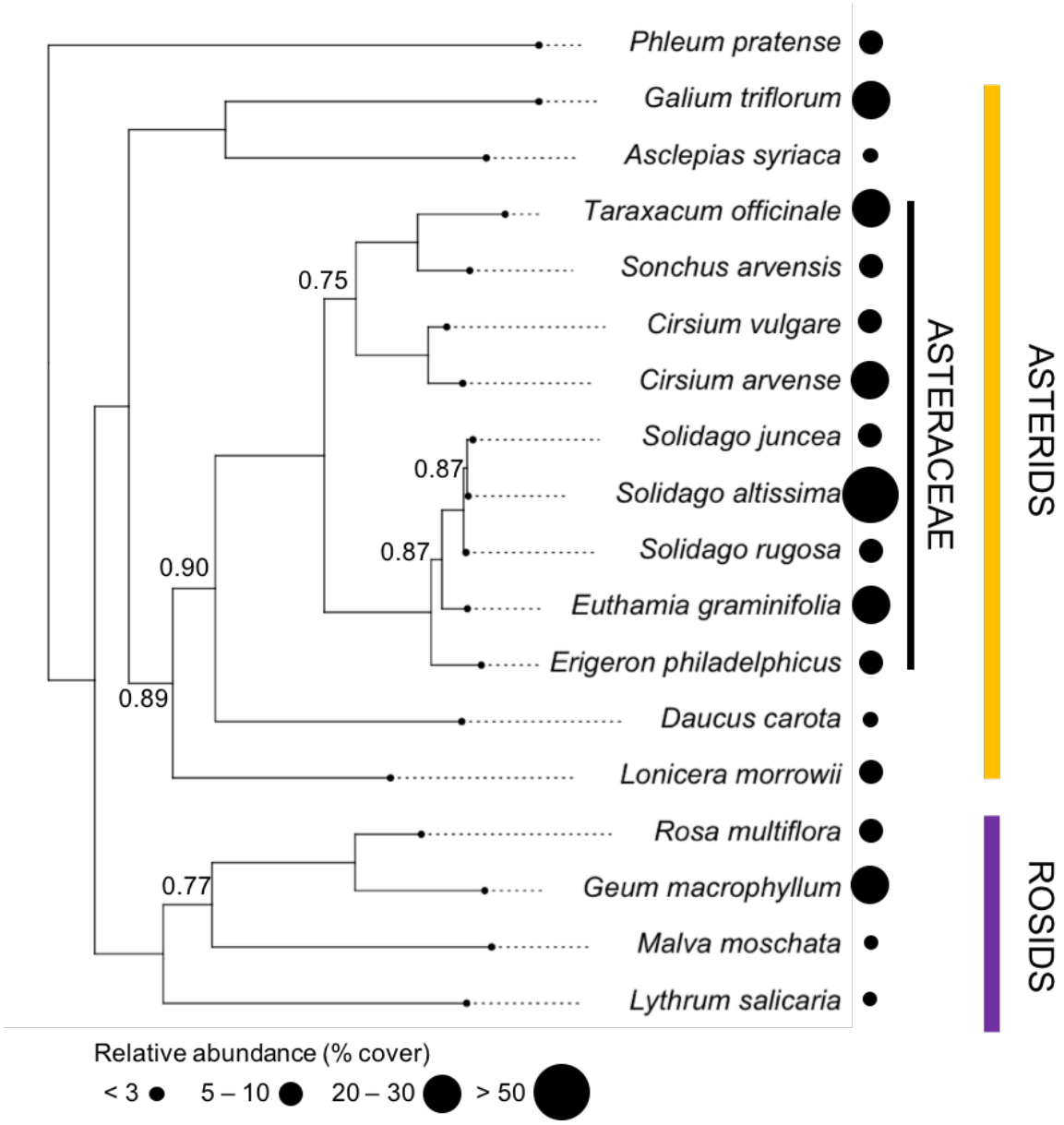

Figure 2.1: Species composition and evolutionary relationships for 18 perennial angiosperm species co-occurring in a successional old field community in Ithaca, NY. Relative abundance (% cover) for each species, indicated at the tips, is the average % cover (2017 and 2018). Phylogenetic branch supports are > 0.95 unless otherwise indicated.

Results

Site properties

Total precipitation in May was similar in 2017 and 2018, while June-July received more rain in 2017 compared to 2018. Total growing season precipitation in 2017 was 371mm, which is similar to the long-term 30 year climate normal for the region. In contrast, 2018 growing season precipitation of 251 mm is drier than normal. Average growing season air temperature was similar between years (Table 2.1). Individual plots did not differ from each other in topography, volumetric soil water content (VWC, %), soil water $\delta^{18}O$, or soil carbon to nitrogen ratios (C/N). Between years, soils were wetter in 2017 (top 60 cm, VWC 25 ± 0.1%) relative to 2018 (VWC 19 ± 0.1%), but did not differ between years in C/N (9.6 ± 0.05%; Table 2.1). Average $\delta^{18}O$ of soil water was approximately 1‰ heavier in 2017 (top 60 cm, -8 ± 2‰) relative to 2018 (top 60 cm, -9 ± 2‰). Average soil water $\delta^{18}O$ was relatively more enriched in the top 10 cm and became isotopically depleted with depth (Figure A2.1).

Plant species composition

Canada goldenrod (*S. altissima*) was the most abundant species, and accounted for approximately 50% of the total vegetative cover in both years (Figure 2.1). Rare species each accounted for < 3% cover and included common milkweed (*A. syriaca*), wild carrot (*D. carota*), purple loosestrife (*L. salicaria*), and musk mallow (*M. moschata*). Phylogenetic diversity was low, as evidenced by a Faith's PD value of 1.34, driven by the large representation of species from the Asteraceae family (Figure 2.1).

Eight species had similar cover between years ($p > 0.05$): *E. philadelphicus, E. graminifolia, G. triflorum, L. morrowii, P. pratense, S. altissima, S. rugosa,* and *T. officinale*. Five species increased in % cover between 2017 and 2018 (i.e., had larger cover in the drier year, $p < 0.01$): *A. syriaca*, *C. vulgare*, *G. macrophyllum*, *R. multiflora*, and *S. juncea*. Five species decreased in % cover between 2017 and 2018 (i.e., had larger cover in the normal year, $p < 0.01$): *C. arvense*, *D. carota, L. salicaria, M. moschata,* and *S. arvensis*.

Leaf isotope ratios, integrated metabolic strategies, and plant traits

$\delta^{13}C$, $\Delta^{18}O$, and IMS of both bulk leaf material and of leaf cellulose varied by species and year, with the exception of cellulose $\Delta^{18}O$ which did not vary between years (Table 2.2). I observed a species x year interaction, indicating differential responses among species between a normal and a dry growing season, for bulk leaf $\delta^{13}C$, $\Delta^{18}O$, and IMS, cellulose $\delta^{13}C$, leaf N, plant height, relative abundance, and plant source water $\delta^{18}O$ (Table 2.2).

Two plant characteristics displayed phylogenetic signal: plant height (Pagel's $\lambda = 0.82$, Blomberg's $K = 0.79$, $p = 0.01$) and source water $\delta^{18}O$ ($\lambda = 0.73$, $K = 0.75$, $p = 0.03$). The remaining variables showed no evidence of phylogenetic signal (all $\lambda < 0.20$, $K < 0.60$, $p > 0.5$; Table 2.3).

IMS negatively correlated with $\delta^{13}C$ (bulk $R^2 = 0.74$, cellulose $R^2 = 0.81$, both $P < 0.001$) and with $\Delta^{18}O$ (bulk $R^2 = 0.13$, cellulose $R^2 = 0.05$, both $P < 0.01$; Table A2.1). IMS did not correlate with $\delta^{18}O_{source}$, leaf N, plant height, or species % cover (all $P > 0.08$; Table A2.1). Bulk leaf $\delta^{13}C$ positively correlated with $\Delta^{18}O$ ($R^2 = 0.53$ $p < 0.0001$). This correlation was weaker for leaf cellulose ($R^2 = 0.34$, $p = 0.0002$; Table A2.1). $\delta^{13}C$ and $\Delta^{18}O$ negatively correlated with

$\delta^{18}O_{source}$ and leaf N, but had little explanatory power (all $R^2 < 0.11$, $P < 0.01$; Table A2.1). Neither $\delta^{13}C$ or $\Delta^{18}O$ correlated with plant height or species % cover ($P > 0.1$).

Leaf metabolic responses between a wet and dry growing season

Cellulose $\delta^{13}C$, $\Delta^{18}O$, and resultant IMS values did not vary substantially between years for most species (Table 2.2, Figure 2.2). Conversely, there was considerable inter-annual variation in bulk leaf $\delta^{13}C$, $\Delta^{18}O$, and IMS (Table 2.2, Figure 2.2), likely reflecting differences in peak growing season conditions. The majority of leaf cellulose is synthesized in early spring and does not undergo further isotopic fractionations throughout the growing season (Lehmann *et al.* 2017). Thus, similar climatic conditions in April and May of 2017 and 2018 are likely reflected in the isotopic signatures in leaf cellulose, despite large inter-annual differences in late-summer, which are reflected in bulk isotopic signatures.

I evaluated relationships between bulk leaf $\delta^{13}C$ and $\Delta^{18}O$ between years for each species by calculating regression coefficients via linear mixed effects models with 'plot' as a random effect. For 10 species, bulk leaf $\delta^{13}C$ and $\Delta^{18}O$ were linearly correlated ($p < 0.05$, Table 2.4, Figure 2.3A). Resultant IMS values were similar between years due to increases in both bulk leaf $\delta^{13}C$ and $\Delta^{18}O$ (Figure 2.3B), indicative of a coupled decrease in CO_2 and H_2O leaf gas exchange in the drier year. For 8 species, bulk leaf $\delta^{13}C$ and $\Delta^{18}O$ were not linearly correlated ($p > 0.5$, Table 2.4, Figure 2.3C). Resultant IMS values increased in the drier year (2018) due to an increase in $\Delta^{18}O$ while $\delta^{13}C$ remained constant, suggesting decreases in leaf evaporative water loss that are uncoupled from CO_2 exchange. We distinguished between these strategies by categorizing species into "coupled" and "uncoupled" IMS response groups. For *C. vulgare*, $\delta^{13}C$

decreased while $\Delta^{18}O$ remained the same (Figure 2.3D), indicating an increase in potential carbon gain without an accompanying increase in leaf water loss.

Leaf metabolic strategies relate to changes in species abundance between years

IMS related to the change in species relative abundance between years such that higher IMS species generally decreased in % cover in the drier year (2018) while lower IMS species increased % cover ($R^2 = 0.18$, $P = 0.047$, Figure 2.4A). Similarly, species that decreased in % cover in the drier year displayed a coupled $\delta^{13}C$-$\Delta^{18}O$ response between years while species that increased in % cover had an uncoupled $\delta^{13}C$-$\Delta^{18}O$ response ($R^2 = 0.11$, $P = 0.048$, Figure 2.4B). Moreover, the change in relative abundance between the normal and dry season was positively correlated with bulk $\delta^{13}C$ ($R^2 = 0.22$, $P = 0.046$) and bulk $\Delta^{18}O$ ($R^2 = 0.19$, $P = 0.043$, Table A2.1).

Table 2.1: Growing season climate and soil properties in 2017 and 2018 for Ithaca, New York. Data were obtained from Ithaca Tompkins Regional Airport weather station. Asterisks indicate significant differences between years. * $p < 0.05$, ** $p < 0.01$, *** $p < 0.001$.

Variable	**2017 (normal)**	**2018 (dry)**
Total precipitation, May (mm)	114	98
Total precipitation, June (mm)	94	53***
Total precipitation, July (mm)	169	100***
Total growing season precipitation (mm)	377	251***
Average air temperature, May (^{o}C)	18	23
Average air temperature, June (^{o}C)	24	24
Average air temperature, July (^{o}C)	26	28
Average growing season air temperature (^{o}C)	23	25
Soil volumetric water content (%)	25	19*
Soil water oxygen isotope composition ($\delta^{18}O$, ‰)	-8	-9
Soil carbon/nitrogen ratio (C/N)	9.6	9.1

Table 2.2: Results of a linear mixed effects model analysis of variance showing the effects of species, year, and their interaction on leaf carbon isotope composition ($\delta^{13}C$), leaf oxygen isotope enrichment above source water ($\Delta^{18}O$), integrated metabolic strategy value (IMS), relative abundance (% cover), plant height, plant source water oxygen isotope composition ($\delta^{18}O$), and leaf nitrogen content (N). Data are for 18 species co-occurring in a temperate old field in Ithaca, NY (n=10 per species).

Model Term	df	F	p
Bulk leaf $\delta^{13}C$ (‰)			
Species	17	58.4071	< 0.0001
Year	1	8.68	0.004
Species x Year	17	3.18	< 0.0001
Bulk leaf $\Delta^{18}O$ (‰)			
Species	17	16.9591	< 0.0001
Year	1	107.0147	< 0.0001
Species x Year	17	1.8534	0.027
Bulk leaf IMS			
Species	17	20.509	< 0.0001
Year	1	23.8325	< 0.0001
Species x Year	17	2.7383	0.0006
Cellulose $\delta^{13}C$ (‰)			
Species	17	55.5658	< 0.0001
Year	1	21.9437	< 0.0001
Species x Year	17	2.5041	0.002
Cellulose $\Delta^{18}O$ (‰)			
Species	17	3.2425	< 0.0001
Year	1	2.1988	0.141
Species x Year	17	0.5831	0.899
Cellulose IMS			
Species	17	21.9875	< 0.0001
Year	1	7.2172	0.008
Species x Year	17	1.0902	0.37
Leaf nitrogen (%)			
Species	17	15.0183	< 0.0001
Year	1	0.8869	0.348
Species x Year	17	2.4973	0.0018
Plant height (m)			
Species	17	12.9642	< 0.0001
Year	1	20.8424	< 0.0001
Species x Year	17	2.0815	0.011

Relative abundance (%)			
Species	17	475.5628	< 0.0001
Year	1	1.2326	0.269
Species x Year	17	2.3733	0.003
Source water $\delta^{18}O$ (‰)			
Species	17	3.4383	< 0.0001
Year	1	10.7405	0.0013
Species x Year	17	2.4973	0.0018

Table 2.3: Phylogenetic signal estimated by Pagel's λ and Blomberg's K of bulk leaf and cellulose carbon isotope composition ($\delta^{13}C$), bulk leaf and cellulose oxygen isotope enrichment above source water ($\Delta^{18}O$), bulk leaf and cellulose integrated metabolic strategy value (IMS), plant height, plant source water oxygen isotope composition ($\delta^{18}O$), leaf nitrogen content (% N), and relative abundance (% cover). Data are species means for two years ± standard error (n=10 per species).

Variable	**Pagel's λ**	**Blomberg's K**	***P***
Bulk leaf $\delta^{13}C$ (‰)	0.01	0.06	0.78
Bulk leaf $\Delta^{18}O$ (‰)	0.01	0.23	0.73
Bulk leaf IMS	0.14	0.08	0.86
Cellulose $\delta^{13}C$ (‰)	0.01	0.08	0.61
Cellulose $\Delta^{18}O$ (‰)	0.01	0.61	0.39
Cellulose IMS	0.05	0.16	0.38
Leaf nitrogen (%)	0.01	0.09	0.94
Plant height (m)	0.82	0.79	0.01
Relative abundance (%)	0.01	0.26	0.19
Source water $\delta^{18}O$ (‰)	0.73	0.75	0.03

Table 2.4: The extent to which species display coupled or uncoupled gas exchange responses between years: slopes and standard errors for the relationships between leaf carbon isotope ($\delta^{13}C$) and oxygen enrichment above source water ($\Delta^{18}O$), obtained from linear mixed effects models.

Species	**Slope**	**SE**	**df**	***P***
1. Asclepias syriaca	-0.095	0.166	140	0.567
2. Cirsium arvense	0.096	0.087	141	0.141
3. Cirsium vulgare	0.188	0.369	142	0.378
4. Daucus carota	0.418	0.157	141	0.003
5. Erigeron philadelphicus	0.527	0.182	141	0.003
6. Euthamia graminifolia	0.029	0.084	141	0.184
7. Galium triflorum	0.336	0.084	142	0.003
8. Geum macrophyllum	0.327	0.118	141	0.018
9. Lonicera morrowii	0.718	0.129	142	< 0.0001
10. Lythrum salicaria	0.425	0.142	141	0.011
11. Malva moschata	0.081	0.105	141	0.102
12. Phleum pratense	0.934	0.269	142	0.001
13. Rosa multiflora	0.032	0.134	140	0.455
14. Solidago altissima	0.723	0.159	141	0.000
15. Solidago juncea	0.272	0.087	141	0.022
16. Solidago rugosa	0.234	0.123	141	0.068
17. Sonchus arvensis	0.242	0.076	140	0.013
18. Taraxacum officinale	-0.066	0.096	143	0.282

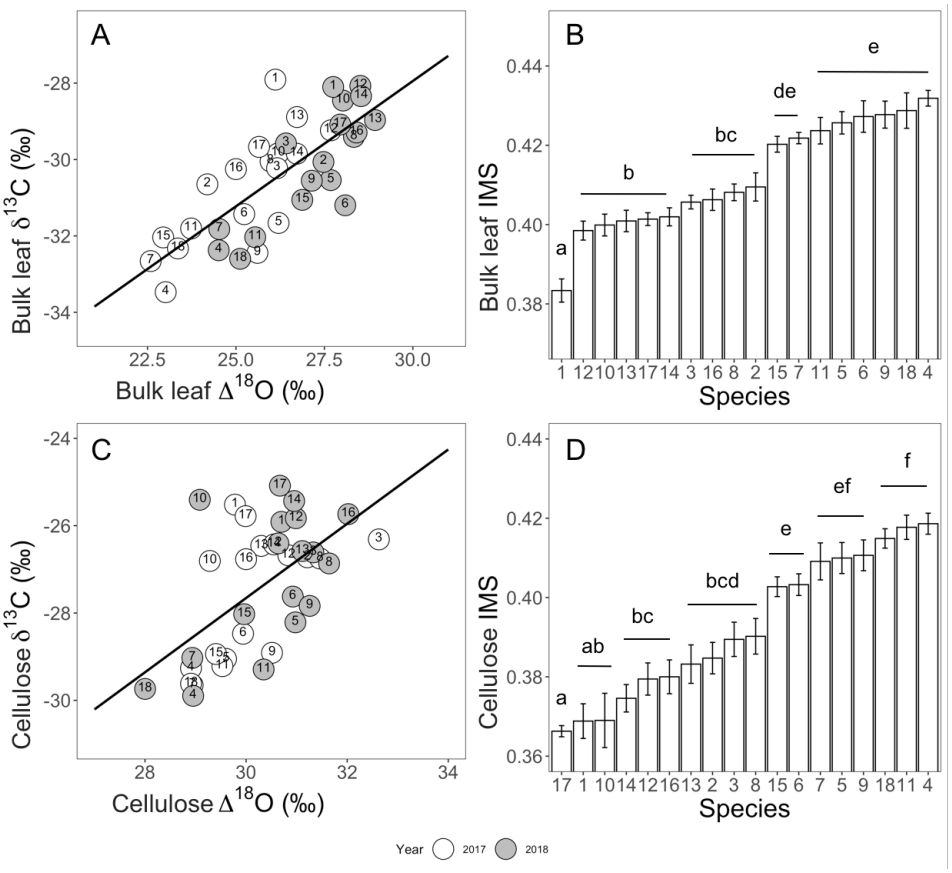

Figure 2.2: Relationships over a normal (open circles, 2017) and a dry (grey circles, 2018) growing season between (A) $\delta^{13}C$ and $\Delta^{18}O$ of bulk leaf material ($R^2 = 0.53$, $P < 0.0001$); (B) average IMS values calculated from bulk leaf material, (C) $\delta^{13}C$ and $\Delta^{18}O$ of leaf cellulose ($R^2 = 0.34$, $P = 0.0002$); and (D) average integrated metabolic strategy (IMS) values calculated from leaf cellulose. Data are species means ± standard error (n=5 per species, per year) for 18 co-occurring old field species: 1 = *A. syriaca*, 2 = *C. arvense*, 3 = *C. vulgare*, 4 = *D. carota*, 5 = *E. philadelphicus*, 6 = *E. graminifolia*, 7 = *G. triflorum*, 8 = *G. macrophyllum*, 9 = *L. morrowii*, 10 = *L. salicaria*, 11 = *M. moschata*, 12 = *P. pratense*, 13 = *R. multiflora*, 14 = *S. altissima*, 15 = *S. arvensis*, 16 = *S. juncea*, 17 = *S. rugosa*, 18 = *T. officinale*. Species that share the same letters in (B) and (D) are statistically indistinguishable based on ANOVA Tukey post-hoc tests. Species full names are in Figure 2.1.

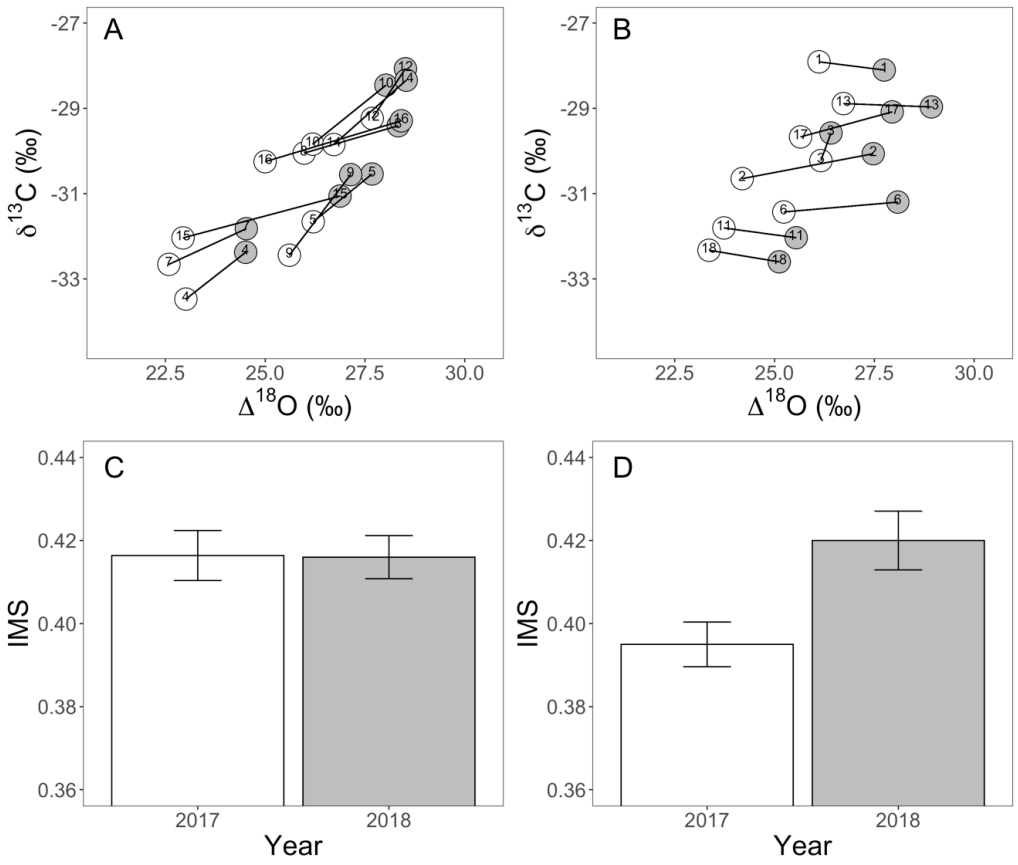

Figure 2.3: Species responses in (A-B) bulk leaf $\delta^{13}C$ and $\Delta^{18}O$; (C-D) IMS between average growing season conditions (2017) and a dry growing season (2018) for (A) species with a coupled gas exchange response (linear correlation), and (B) species with an uncoupled gas exchange response (no correlation). Average IMS across all species with a (C) coupled and (D) uncoupled response are shown for each year. Data are species means ± standard error (n=5 per species, per year) for 18 co-occurring old field species: 1 = *A. syriaca*, 2 = *C. arvense*, 3 = *C. vulgare*, 4 = *D. carota*, 5 = *E. philadelphicus*, 6 = *E. graminifolia*, 7 = *G. triflorum*, 8 = *G. macrophyllum*, 9 = *L. morrowii*, 10 = *L. salicaria*, 11 = *M. moschata*, 12 = *P. pratense*, 13 = *R. multiflora*, 14 = *S. altissima*, 15 = *S. arvensis*, 16 = *S. juncea*, 17 = *S. rugosa*, 18 = *T. officinale*. Species full names are in Figure 2.1.

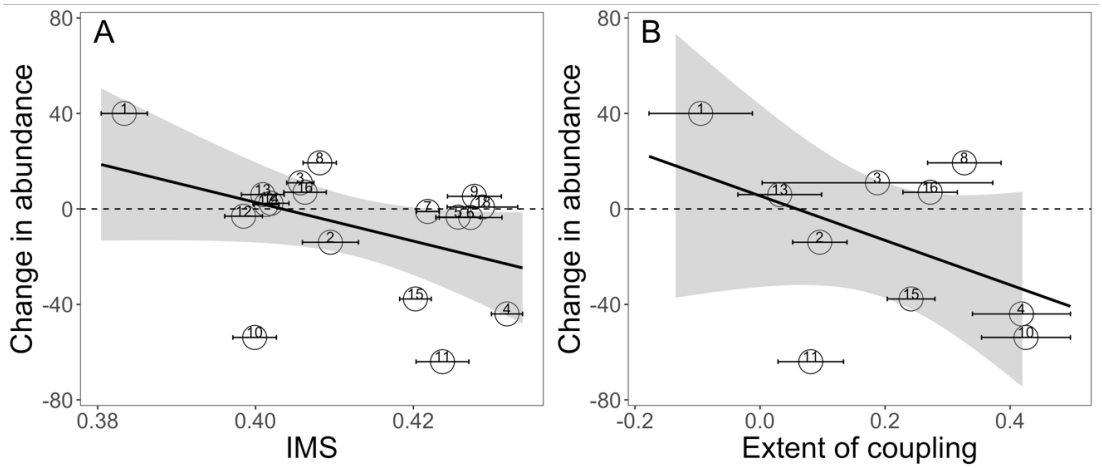

Figure 2.4: Relationships between the change in species relative abundance (% cover) in a drier year (2018) and (A) average integrated metabolic strategy (IMS) values between years ($R^2 = 0.18$, $P = 0.047$); (B) the extent to which a species has coupled or uncoupled gas exchange (i.e., the slope of the $\delta^{13}C$-$\Delta^{18}O$ correlation between years; $R^2 = 0.11$, $P = 0.048$). Data are species means ± standard error (both years combined, n=5 per species, per year) of bulk leaf material for 18 co-occurring old field species: 1 = *A. syriaca*, 2 = *C. arvense*, 3 = *C. vulgare*, 4 = *D. carota*, 5 = *E. philadelphicus*, 6 = *E. graminifolia*, 7 = *G. triflorum*, 8 = *G. macrophyllum*, 9 = *L. morrowii*, 10 = *L. salicaria*, 11 = *M. moschata*, 12 = *P. pratense*, 13 = *R. multiflora*, 14 = *S. altissima*, 15 = *S. arvensis*, 16 = *S. juncea*, 17 = *S. rugosa*, 18 = *T. officinale*. Species full names are in Figure 2.1. Correlations for leaf cellulose data and for additional variables are in Table A2.1.

Discussion

Does intrinsic metabolism vary among species within a single community? Although a seemingly simple question, there are few data that demonstrate the role of metabolic diversity in structuring plant communities. Differences in intrinsic metabolism, measured as the tradeoff between photosynthetic carbon gain and foliar water loss, can arise from variation in the local environment (e.g., resource availability, climate), leaf traits, and/or evolutionary history. Nevertheless, within a single community, I expected co-occurring plant species to largely overlap in their metabolic strategies. Surprisingly, I observed considerable variation in $\delta^{13}C$, $\Delta^{18}O$, and integrated metabolic strategy (IMS) values among 18 old field species despite a relatively invariable environment in terms of topography and soil moisture. Moreover, metabolic diversity among species was associated with changes in relative abundance between years that differed in water availability, suggesting that metabolic diversity may be contributing to species composition within this community.

Variation in metabolic strategies among species

The 18 species could be broadly classified along a spectrum of carbon-acquisitive to water-conservative metabolic strategies (Figure 2.2). Consistent with my previous work on diverse milkweeds in Chapter 1 (Goud *et al.* 2019), species with lower IMS had a lower carbon-gain potential per rate of foliar water loss (i.e., relatively more enriched in $\delta^{13}C$ across a given range of $\Delta^{18}O$). Species with higher IMS prioritized carbon gain, though not necessarily at the expense of water loss, and were relatively more depleted in $\delta^{13}C$ and had a higher leaf N content, indicative of greater photosynthetic investment. In contrast to milkweeds, high-IMS species in this study were not more water-conservative than low-IMS species (Figure 2.2A,C). Rather,

species had largely overlapping $\Delta^{18}O$ values, with many high-IMS species having more depleted $\Delta^{18}O$, suggestive of higher rates of evaporative water loss (Figure 2.2A,C). Thus, higher IMS for these species is more suggestive of a higher metabolic efficiency achieved from greater carboxylation capacity during carbon fixation at similar levels of foliar water loss, rather than lower rates of evaporative water loss per se. Low-IMS species with relatively high rates of water loss without an accompanying increase in carbon gain (e.g., *Lythrum salicaria*) suggest biochemical limitations to gas exchange, rather than resistances to diffusion. This could be driven by a lower metabolic demand for carbon from sink tissues, or carboxylation occurring at a higher CO_2 partial pressure (c_i) inside the leaf (Schultz et al. 1996, Šantrůček et al. 2014).

Similar to milkweeds, species with a more efficient metabolic strategy (larger IMS, depleted $\delta^{13}C$) generally had smaller, narrow, and/or dissected leaves (e.g., *D. carota, E. graminifolia*) while less efficient (lower IMS, enriched $\delta^{13}C$) generally had broader leaves (e.g., *G. macrophyllum, S. rugosa)*. In addition, leaf-level metabolism ($\delta^{13}C$, $\Delta^{18}O$, IMS) did not show evidence of phylogenetic signal (Table 2.4). Thus, at this level of sampling, there does not appear to be any influence of evolutionary history on metabolic diversity in this community, despite species being more phylogenetically similar than expected by change (Figure 2.1). This result contrasts with a common assumption in plant ecology that phylogenetic relationships predict variation in functional traits (Cavender-Bares et al. 2009). In this successional plant community, it's possible that traits shared among closely related species, such as height and relative rooting depth (Table 2.4), allow for initial colonization while divergence in other traits, such as leaf-level metabolism, promote differentiation and long-term co-occurrence (Cavender-Bares et al. 2009, Mo et al. 2013).

Metabolic responses between growing seasons

In this study, I observed considerable intra-specific variation in bulk leaf $\delta^{13}C$ and $\Delta^{18}O$ between years, but leaf cellulose data do not appear to capture the same magnitude of physiological responses between different growing seasons (Figure 2.2). One challenge with using cellulose lies in the timing of cellulose biosynthesis. Cellulose is produced early in leaf development and is biologically and isotopically inert once synthesized (Lehmann *et al.* 2017), making it an ideal compound for interspecific comparisons (Moreno Gutiérrez *et al.* 2012). However, due to its inert nature, isotopic ratios in cellulose reflect physiology mainly during early growth and development and appears less effective at capturing physiological responses to inter-annual differences in soil moisture that are evident in peak-summer.

Changes in bulk leaf tissue $\delta^{13}C$ and $\Delta^{18}O$ followed two general responses between years. For ten species, $\delta^{13}C$ and $\Delta^{18}O$ co-varied, indicative of a coupling between CO_2 and water gas exchange (Figure 2.3A). For these species, proportional changes in $\delta^{13}C$ and $\Delta^{18}O$ between the wet and dry season resulted in no net change in IMS (Figure 2.3C). Maintaining a similar balance between leaf-level carbon gain and water loss suggests a fixed IMS that does not appear to be phenotypically plastic. This is consistent with our conceptual model for IMS, which predicts that plants with fixed IMS may differentially adjust anatomy and/or physiology in response to changing resource availability, but $\delta^{13}C$ and $\Delta^{18}O$ will vary proportionally (Goud *et al.* 2019). It's likely that in response to lower soil water availability during the 2018 growing season, these species closed stomata to conserve water, while simultaneously limiting CO_2 diffusion and carboxylation.

For the remaining eight species, $\delta^{13}C$ and $\Delta^{18}O$ varied independently, reflecting an

uncoupling of leaf gas exchange (Figure 2.3B). In these species, disproportionate changes in $\delta^{13}C$ and $\Delta^{18}O$ resulted in a net increase in IMS in the dry season (Figure 2.3D). This is consistent with predictions for plants whose IMS is phenotypically plastic in response to a driving force (e.g., water availability). Seven of the species with this 'uncoupled' response maintained similar $\delta^{13}C$ values between years, but increased $\Delta^{18}O$ in the dry season, while one species (*C. vulgare*) decreased $\delta^{13}C$ and maintained similar $\Delta^{18}O$ in the dry season. This uncoupling of evaporative water loss and carbon gain likely results from more efficient carboxylation via increased Rubisco content and/or activity, consistent with prior observations that milkweed species with plastic IMS increased carboxylation efficiency in response to decreased soil water availability (Goud *et al.* 2019). What determines whether a species will display a coupled or uncoupled response is not clear. Future studies that explicitly seek to identify anatomical, physiological, and genetic bases of phenotypic plasticity in metabolic strategies will be essential to better understand the role of metabolism in species responses to variable resources.

Metabolic strategies relate to changes in species' abundance

Species that increased abundance in the drier year generally had lower IMS, were more enriched in $\delta^{13}C$ and $\Delta^{18}O$, and were uncoupled, while species that decreased abundance had the opposite suite of characteristics (Figure 2.3). Changes in vegetative cover could result from whole-plant changes in biomass and/or changes in density. Our consideration of metabolic strategies is an explicitly leaf-level parameter, and we acknowledge that leaf metabolism does not always scale up to whole-plant biomass (Cernusak et al. 2006, Goud et al. 2019). Nevertheless, increasing cover for low-IMS species under dry conditions could indicate a competitive advantage when

water availability is limiting, potentially compensating for a competitive disadvantage in wet seasons due to their lower potential for leaf-level carbon gain. Similarly, uncoupled species responded to lower water availability in the dry year by adjusting leaf gas exchange to be more water-conservative at the same level of carbon gain, or to increase carbon gain at the same water-loss potential, with both responses resulting in a similar or increased cover, possibly via increased growth and/or density in the dry year. Alternatively, species with coupled responses appear to maintain their leaf-level metabolism when water resources are more limiting, but grow smaller and/or have less individuals as a consequence. This decrease in cover may be advantageous to conserve below-ground resources during unfavorable growing seasons, postponing growth until future seasons with better conditions. Together, these different responses in relative abundance suggest that metabolic diversity may have consequences for growth and competitive outcomes that appear related to variation in climate between years.

Metabolic strategies and maintenance of species diversity

Large differences in metabolic strategy could indicate a consistent competitive advantage of some plants over others. All else being equal, plants with a more efficient strategy (*i.e.*, more carbon gain relative to water loss) are likely to out-compete those with a less efficient strategy. If so, then how is the observed metabolic diversity maintained in this community? Variation in resources that most strongly drive carbon and water exchange are likely to be important, such as light, soil nutrients, and water availability. Although there were no obvious differences in microsite in this community, variation in water availability with depth through the soil profile and/or temporal variation in water resources may serve to reduce competition and minimize niche overlap (Chesson 2000; Silvertown *et al.* 2015).

I used $\delta^{18}O$ of extracted source water ($\delta^{18}O_{source}$) to estimate belowground water partitioning and identify where in the soil profile species are accessing water (Ehleringer et al. 1991, Silvertown et al. 2014). Two species in this community, *C. vulgare* and *G. triflorum*, had $\delta^{18}O_{source}$ values that were more depleted and enriched, respectively, relative to the other species. Depleted $\delta^{18}O_{source}$ values indicate that *C. vulgare* is accessing deeper sources of water in the soil profile that may be more stable (i.e., groundwater). Similarly, *G. triflorum* appears to use surface waters from more recent, but less temporally stable precipitation events.

Temporal variation in water availability also appears to be influencing physiological diversity in this community. Two species differed in phenology relative to the others; *T. officinale* and *G. triflorum* comprise the ground layer (< 0.4 m) and were the first to leaf-out, flower, and set seed in the spring, effectively completing most of their reproductive life cycles by the time the remaining 16 species – which largely overlapped in phenology – began flowering. Both *T. officinale* and *G. triflorum* were of the most depleted in $\delta^{13}C$ and $\Delta^{18}O$, indicating a strategy to maximize carbon gain at the expense of water loss, presumably because water resources were high and inter-specific competition was minimal during their periods of active growth in the spring. In addition, variation in $\delta^{13}C$, $\Delta^{18}O$, and relative abundance were clearly coincident with inter-annual variation in precipitation such that some water-conservative species increased in abundance in the drier year while some less water-conservative species decreased abundance in the drier year. Differential responses between years could indicate that inter-annual variation in rainfall might be an important mechanism structuring functional diversity in this community (Chesson 2000). Long-term data or experimental water manipulations in the field would be required to more thoroughly test this hypothesis.

Future directions

In this first application of applying IMS to community ecology, I found that variation in IMS was a strong indicator of metabolic diversity among co-occurring old field species. Moreover, IMS values related to changes in abundance between years that differed in growing season precipitation, suggesting differential species responses to temporal variation in water availability. These data have implications for the consideration of species- and community-level functional responses to changes in climate. At the same time, I also encountered challenges to applying IMS in the field. IMS reliably indicates the relative ranking among species in leaf-level metabolic efficiency in terms of the carbon to water balance. However, IMS values alone were not sufficient to classify species as carbon-acquisitive or water-conservative per se, because IMS is sensitive to the *ratio* between $\delta^{13}C$ and $\Delta^{18}O$, rather than their individual magnitude. Consequently, different magnitudes of $\delta^{13}C$ and $\Delta^{18}O$ result in similar IMS when the ratio between them is maintained. For example, *C. vulgare* is enriched in $\delta^{13}C$ and $\Delta^{18}O$ relative to *E. philadelphicus*, yet obtains similar IMS because the ratio of carbon to water exchange is similar. Likewise, within-species plasticity in $\delta^{13}C$ and $\Delta^{18}O$ was large between years for some species, but IMS only changed if $\delta^{13}C$ and $\Delta^{18}O$ varied disproportionally. As such, we advocate for examining variation in IMS alongside variation in $\delta^{13}C$ and $\Delta^{18}O$ values independently in order to better understand the interplay between diversity and plasticity in leaf metabolism. Assessing IMS, $\delta^{13}C$ and $\Delta^{18}O$ in other systems could reveal a previously under-appreciated role of metabolism for species distributions and community diversity.

Literature Cited

Agrawal, A. A., A. P. Hastings, M. T. J. Johnson, J. L. Maron, and J. P. Salminen. 2012. Insect Herbivores Drive Real-Time Ecological and Evolutionary Change in Plant Populations. Science 338:113–116.

Angert, A.L., Huxman, T.E., Chesson, P., and Venable, D.L. Functional tradeoffs determine species coexistence via the storage effect. 2009. Proceedings of the National Academy of Sciences of the United States of America 106(28):11641–11645.

APG IV. 2016. An update of the Angiosperm Phylogeny Group classification for the orders and families of flowering plants: APG IV. Botanical Journal of the Linnean Society 181:1–20.

Barbour, M. M., J. S. Roden, G. D. Farquhar, and J. R. Ehleringer. 2004. Expressing leaf water and cellulose oxygen isotope ratios as enrichment above source water reveals evidence of a Peclet effect. Oecologia 138:426–435.

Blomberg, S. P., T. Garland, and A. R. Ives. 2003. Testing for phylogenetic signal in comparative data: behavioral traits are more labile. Evolution 57:717–745.

Brown, J. H., J. F. Gillooly, A. P. Allen, Van M Savage, and G. B. West. 2004. Toward a metabolic theory of ecology. Ecology 85:1771–1789.

Caemmerer, von, S., and G. D. Farquhar. 1981. Some relationships between the biochemistry of photosynthesis and the gas exchange of leaves. Planta 153:376–387.

Cavender-Bares, J., K. H. Kozak, P. V. A. Fine, and S. W. Kembel. 2009. The merging of community ecology and phylogenetic biology. Ecology letters 12:693–715.

Cernusak, L. A., J. Aranda, J. D. Marshall, and K. Winter. 2006. Large variation in whole-plant water-use efficiency among tropical tree species. New Phytologist 173:294–305.

Ehleringer, J. R., S. L. Phillips, W. S. F. Schuster, and D. R. Sandquist. 1991. Differential utilization of summer rains by desert plants. Oecologia 88:430–434.

Eisen, K. E., D. R. Campbell, E. Richards, and M. A. Geber. 2019. Differences in Flowering Phenology Are Likely Not the Product of Competition for Pollination in Clarkia Communities. International Journal of Plant Sciences 180:974–986.

Faith, D. P. 1992. Conservation evaluation and phylogenetic diversity. Biological Conservation 61:1–10.

Goud, E. M., J. P. Sparks, M. Fishbein, and A. A. Agrawal. 2019. Integrated metabolic strategy: A framework for predicting the evolution of carbon-water tradeoffs within plant clades. Journal of Ecology 107:1633–1644.

Lehmann, M. M., B. Gamarra, A. Kahmen, R. T. W. Siegwolf, and M. Saurer. 2017. Oxygen isotope fractionations across individual leaf carbohydrates in grass and tree species. Plant, Cell and Environment 40:1658–1670.

Mo, X.-X., L.-L. Shi, Y.-J. Zhang, H. Zhu, and J. W. F. Slik. 2013. Change in Phylogenetic Community Structure during Succession of Traditionally Managed Tropical Rainforest in Southwest China. PLoS ONE 8:e71464.

Moreno Gutiérrez, C., T. E. Dawson, E. Nicolás, and J. I. Querejeta. 2012. Isotopes reveal contrasting water use strategies among coexisting plant species in a Mediterranean

ecosystem. New Phytologist 196:489–496.

Pagel, M. 1999. Inferring the historical patterns of biological evolution. Nature 401:877–884.

R Core Team. 2019. R: A language and environment for statistical computing. R Foundation for Statistical Computing. Vienna, Austria.

Revell, L. J. 2012. phytools: an R package for phylogenetic comparative biology (and other things). Methods in Ecology and Evolution 3:217–223.

Schliep, K. P. 2010. phangorn: phylogenetic analysis in R. Bioinformatics 27:592–593.

Schultz, H. R., W. Kiefer, and W. Gruppe. 1996. Photosynthetic duration, carboxylation efficiency and stomatal limitation of sun and shade leaves of different ages in field-grown grapevine (Vitis vinifera L.). Vitis 35:169–176.

Silvertown, J., Y. Araya, and D. Gowing. 2014. Hydrological niches in terrestrial plant communities: a review. Journal of Ecology 103:93–108.

Sutherland, W. J., R. P. Freckleton, H. C. J. Godfray, S. R. Beissinger, T. Benton, D. D. Cameron, Y. Carmel, D. A. Coomes, T. Coulson, M. C. Emmerson, R. S. Hails, G. C. Hays, D. J. Hodgson, M. J. Hutchings, D. Johnson, J. P. G. Jones, M. J. Keeling, H. Kokko, W. E. Kunin, X. Lambin, O. T. Lewis, Y. Malhi, N. Mieszkowska, E. J. M. Gulland, K. Norris, A. B. Phillimore, D. W. Purves, J. M. Reid, D. C. Reuman, K. THOMPSON, J. M. J. Travis, L. A. Turnbull, D. A. Wardle, and T. Wiegand. 2013. Identification of 100 fundamental ecological questions. Journal of Ecology 101:58–67.

Šantrůček, J., M. Vráblová, M. Šimková, M. Hronková, M. Drtinová, J. Květoň, D. Vrábl, J.

Kubásek, J. Macková, D. Wiesnerová, J. Neuwithová, and L. Schreiber. 2014. Stomatal and pavement cell density linked to leaf internal CO2 concentration. Annals of Botany 114:191–202.

Tilman, D., J. HilleRisLambers, S. Harpole, R. Dybzinski, J. Fargione, C. Clark, and C. Lehman. 2004. Does metabolic theory apply to community ecology? It's a matter of scale. Ecology 85:1797–1799.

Whittaker, R. H. 1965. Dominance and Diversity in Land Plant Communities: Numerical relations of species express the importance of competition in community function and evolution. Science 147:250–260.

CHAPTER THREE

Is variation in inter-annual precipitation a mechanism for maintaining plant metabolic diversity?

Abstract

In order for diverse species to coexist in ecological communities, they must vary in ways that reduce competition, such as variation in anatomical and physiological characteristics. Here, I asked whether inter-annual variation in growing season precipitation could provide sufficient variation in water availability to allow plant species with different intrinsic metabolism to co-occur. I hypothesized that species would differentially respond to soil water availability, and that species with a metabolic strategy to conserve water at the expense of carbon gain would grow better in dry conditions relative to species with a metabolic strategy to gain carbon at the expense of foliar water loss. I measured above-ground biomass and leaf-level metabolism using carbon and oxygen isotope ratios for seven Asteraceae species across five experimental water treatments. Species differentially responded to variation in growing season water availability and, importantly, how they responded could be explained by differences in metabolism. Water-conservative species grew best in the dry treatments and had their minimal growth in wet treatments. Carbon-acquisitive species displayed the opposite pattern, with maximal growth in wet treatments and steep declines in dry treatments. Metabolic differences among co-occurring species may help explain temporal variation in growth, and could provide an underlying physiological mechanism for long-term dynamics that promote biodiversity.

Introduction

How is it that different species are able to live together in ecological communities? This fundamental question is at the heart of ecology, and although it has been investigated for centuries, it remains a current topic of active research (Levine and HilleRisLambers 2009, Silvertown et al. 2014). We have long-known that for communities to house a diversity of species, co-occurring species need to be substantially different from one another, which can be seen in differences in niches and relative fitness (HilleRisLambers et al. 2012). But what are the underlying mechanisms that define a species niche or relative fitness? Much work has been done to understand the role of anatomy and morphology, but diversity may also be maintained by variation in species' intrinsic metabolism (Angert at al. 2009; Whittaker 1965).

In plants, primary metabolism involves the conversion of carbon dioxide (CO_2) during photosynthesis to produce energy. However, CO_2 uptake by leaves causes the simultaneous loss of water through leaf stomata (Farquhar and Sharkey 1982), resulting in a fundamental tradeoff between leaf-level carbon gain and water loss that may influence a plant's productivity and competitive success in a given environment. For example, some plants may be able to rapidly gain carbon but lose substantial amounts of water in the process. Others may have a more conservative strategy, minimizing water loss at the expense of carbon gain (Monson et al. 1993, Goud et al. 2019). A plant's ability to balance carbon gain and water loss is largely dictated by characteristics that affect the exchange rates of both CO_2 and water vapor. Because CO_2 enters and water vapor exits through stomatal pores, stoma are often focused on as an intersection point of carbon gain and water loss (Potvin and Werner 1983, Schultz et al. 1996, Liu et al. 2015). While stomatal behavior is a primary dynamic in this exchange, leaf boundary layer conditions, resistances within the leaf to diffusion, and enzymatic activity driving CO_2 consumption within

the leaf also make significant contributions and are likely coordinated as a plant metabolic strategy to manage these two fluxes.

In Chapter 1, I introduced the concept of 'integrated metabolic strategy' as a way to represent leaf carbon-water tradeoffs that are integrated over the lifespan of a leaf (Goud et al. 2019). The integrated metabolic strategy (IMS) approach leverages the relationship between leaf carbon and oxygen stable isotope ratios. The carbon stable isotope ratio ($\delta^{13}C$) of leaves integrates the long-term supply and demand of CO_2, and is a reliable representation of leaf-level carbon metabolism (Farquhar et al. 1989). The oxygen isotope enrichment of leaf material above source water ($\Delta^{18}O = \delta^{18}O_{leaf} - \delta^{18}O_{source}$) integrates the evaporative conditions of the leaf and can represent the magnitude of foliar water loss (Farquhar et al. 2007, Roden and Farquhar 2012). Generally, smaller (depleted) $\delta^{13}C$ and $\Delta^{18}O$ values indicate a smaller concentration gradient of CO_2 and water vapor between the inside and outside of the leaf, indicating relatively more carbon gain and water loss, respectively. Therefore, the combination of these two isotope values describe a plant's leaf-level strategy to balance carbon gain and water loss over the lifetime of the leaf.

One can identify and compare metabolic strategies by examining a plant's position in a $\delta^{13}C$-$\Delta^{18}O$ biplot. Leaves that are enriched (more positive) in $\delta^{13}C$ and $\Delta^{18}O$ display a strategy to minimize foliar water loss, which also limits CO_2 diffusion and potential carbon gain. Conversely, leaves with more depleted (more negative) $\delta^{13}C$ and $\Delta^{18}O$ reflect a strategy to maximize carbon gain without limiting foliar water loss. Plants that cluster together on a biplot are interpreted as having similar metabolic strategies, while separation in dual isotope space indicates intrinsic metabolic differences. Moreover, metabolic strategies can be converted to a

single IMS value by calculating the adjusted ratio between $\delta^{13}C$ and $\Delta^{18}O$:

$$IMS = |\delta^{13}C| / (100 - \Delta^{18}O).$$

Increasing IMS values generally correspond to increases in leaf-level carbon gain per unit of evaporative water loss (Goud et al. 2019).

In Chapter 2, I demonstrated variation in metabolic strategies among 18 co-occurring plant species in a successional old field community, indicating fundamental differences in how these species balance the tradeoff between leaf-level carbon gain and water loss. Large differences in metabolic strategy may indicate a competitive advantage of some species over others. All else being equal, plants with a more productive strategy (*i.e.*, more carbon gain) should out-compete those with a less productive strategy when water resources are high, but may face considerable risk when water resources are low. In order for diverse strategies to persist in the same community, co-occurring species would need to effectively partition water resources in ways that limit competitive exclusion (Silvertown et al. 1999).

In Chapter 2, I found that differences in metabolic strategies among species were associated with changes in their relative abundance between growing seasons that differed in summer precipitation. Specifically, species with a strategy to minimize water loss at the expense of carbon gain (a.k.a., 'water-conservative') increased in vegetative cover in the dry season while those with a strategy to maximize carbon gain at the expense of water loss (a.k.a, 'carbon-acquisitive') suffered decreases in cover. Moreover, I found that gas exchange was coupled (i.e., $\delta^{13}C$ and $\Delta^{18}O$ co-varied) for some species, but was uncoupled (i.e., $\delta^{13}C$ and $\Delta^{18}O$ varied independently) for other species. Those species with a coupled metabolic response between years generally decreased in vegetative cover in the drier year while those with an uncoupled response

increased in cover. Together, these results suggest that metabolic diversity may have consequences for growth and/or competitive outcomes that are related to variation in climate between years.

My next natural question was whether interannual variation in rain, and thus soil water availability, plays a role in maintaining metabolic diversity in this community. Variation in rainfall from one growing season to the next might favor the growth and competitive success of different plant species in different years, which could serve to maintain the presence of potentially less productive water-conservative species. To test this hypothesis, I performed a field experiment to manipulate soil water availability in order to address the following questions: Do co-occurring plant species with different metabolic strategies have differential performance based on hydrologic year? If so, what are the morphological and physiological mechanisms underlying differential growth responses? I expected species to differentially respond to soil water availability. Specifically, I hypothesized that species with a metabolic strategy to conserve water at the expense of carbon gain would grow better in dry conditions relative to species with a metabolic strategy to gain carbon at the expense of foliar water loss.

Methods

Study site and experimental setup

The study was conducted in a 1200 m^2 mid-successional old field in Ithaca, NY, USA (42.46, -76.45) that was abandoned from agriculture in 2006 (Agrawal, A.A., personal communication). Plant community composition is dominated by perennial herbaceous forbs in the Asteraceae family (e.g., *Cirsium, Solidago*), with some grasses (e.g., *Phleum*), and sparse shrub cover (e.g., *Rosa, Lonicera*) (Marks 1983). The climate is moderate continental with an average annual temperature of 8^{o}C and a mean annual precipitation of 947 mm. Average growing season (May - August) temperature and precipitation are 18^{o}C and 372 mm, respectively (Ithaca Airport weather station).

In April, 2018, I established a manipulative experiment in a randomized block design at the site by constructing three 4.3 m by 11 m GrowSpan round cold frames from galvanized steel (FarmTek, Dyersville, IL) to serve as rainout shelters. The shelters were spaced approximately 8 m apart, with five 3 m by 2 m plots within each shelter. The perimeter of each plot was trenched to 2 feet deep and lined with polyethylene plastic to limit the movement of roots and water between plots. Treatments were maintained by excluding all natural rainfall by covering the top of each shelter with clear polyethylene greenhouse plastic (FarmTek, Dyersville, IL), and then re-watering the plots with a predetermined amount of water. Each plot was individually watered on a weekly basis via a drip irrigation system consisting of polyethylene tubes arranged in a rectangular grid containing pressure-compensating button drip emitters to provide even water distribution across the plot (DIG Corp, Vista, CA). Water was supplied to each grid through a pressure regulator attached to a storage tank filled with local water. The shelters were covered and treatments were initiated on May 25, 2018, and continued until August 24, 2018. The shelter

sides remained open to maximize air movement and minimize temperature and relative humidity artifacts.

Each plot was randomly assigned to one of five experimental water treatments corresponding to monthly average rain amounts spanning the driest to the wettest growing season on record from the last 30 years:

(1) the driest year on record, 26 mm of rain per month (104 mm total);

(2) a typical dry year, 60 mm of rain per month (240 mm total);

(3) the 30 year average, 93 mm of rain per month (372 mm total);

(4) a typical wet year, 141 mm of rain per month (564 mm total);

(5) the wettest year on record, 188 mm of rain per month (752 mm total).

In each plot, I measured soil water content (%) on a weekly basis using a portable HydroSense II soil-water sensor (Campbell Scientific, Logan, UT). I took monthly soil cores at 30 cm depth and subdivided the cores into three 10 cm depths. For each 10 cm depth, I measured volumetric soil water content (%), and extracted soil water for $\delta^{18}O$ using a cryogenic vacuum distillation line (Ehleringer et al, 2000). Soil samples were oven dried at 75^{o}C for 48 hours.

Plant sampling

I selected seven focal plant species from the Asteraceae family that were represented in each treatment and covered a general range of morphological and physiological diversity of the community as a whole: *Cirsium arvense* (L.) Scop., *Euthamia graminifolia* (L.) Nutt., *Solidago altissima* L., *S. juncea* Aiton., *S. rugosa* Mill., *Symphyotrichum novae-angliae* (L.) G.L. Nesom, and *Taraxacum officinale* F.H. Wigg.

Nine replicate plants per species were collected in each treatment. For each individual plant, I recorded its height and the total number of leaves. All the leaves were removed, and suberized tissue (stem or root material, depending on the species) was collected and immediately placed in capped plastic vials after collection, wrapped in Parafilm, and stored in a freezer until further analyses. Water was extracted from stem/root tissue using a cryogenic vacuum distillation line (Ehleringer et al, 2000) and stored in a freezer until they were measured for $\delta^{18}O$. Fresh leaf mass was weighed and total leaf area (LA) was measured using a LI-COR LI-3100 leaf-area meter (LI-COR, Lincoln, NE). Total above-ground biomass (leaves and stems) were oven-dried at $60^{o}C$ for 48 hours and weighed. Leaf carbon (C) and nitrogen (N) content were measured using an elemental analyzer (Thermo Finnigan Carlo Erba NC2500).

Isotope analyses

Carbon and oxygen isotope ratios ($\delta^{13}C$, $\delta^{18}O$) were measured using a continuous flow isotope ratio mass spectrometer (Thermo Scientific Delta V Advantage). For $\delta^{13}C$, the mass spectrometer was coupled to an elemental analyzer (Carlo Erba NC2500) and for $\delta^{18}O$ it was coupled to a Thermo Scientific TC/EA pyrolysis analyzer with a Costech Zero Blank auto sampler. Samples were analysed for stable isotope composition at the Cornell University Stable Isotope Lab,

Ithaca, NY. Isotope ratios are expressed as δ values (per mil):

$\delta^{13}C$, $\delta^{18}O = (R_{sample}/R_{standard} - 1) \times 1000$ (‰),

where R_{sample} and $R_{standard}$ are the ratios of heavy to light isotope of the sample relative to the international standards for C and O, Vienna-Pee-Dee Belemnite and Vienna Standard Mean Ocean Water, respectively.

Statistical analyses

Aboveground biomass was standardized in order to account for interspecific differences in initial plant size: for each individual species, biomass measurements were divided by the species' mean biomass across all treatments, resulting in standardized values ranging between 0.5 - 1.5, with a value of 1.0 for the species mean.

Integrated metabolic strategy (IMS) values were calculated by the following ratio:

$IMS = |\delta^{13}C| / (100 - \Delta^{18}O)$ (Goud et al. 2019).

Treatment and species differences among variables were assessed using linear mixed effects models and analysis of variance (ANOVA) to account for potential variation among the three precipitation-exclusion shelters. Each shelter was defined as a block and used as a random effect. Independent fixed factors were species, water treatments, and their interaction. Response variables included standardized total aboveground biomass, leaf carbon isotope composition ($\delta^{13}C$), leaf oxygen isotope enrichment above source water ($\Delta^{18}O$), integrated metabolic strategy values (IMS), total leaf area (LA, cm^2), plant height (m), plant source water oxygen isotope composition ($\delta^{18}O$), and leaf nitrogen content (% N).

Linear relationships between continuous variables (i.e.., biomass, $\delta^{13}C$, $\Delta^{18}O$, IMS, LA, height, N, source water $\delta^{18}O$) were assessed using simple and multiple linear regressions. The slope of the linear correlation obtained from mixed effects models for each species was used as a measure of the extent of covariation between $\delta^{13}C$ and $\Delta^{18}O$. The term 'coupled' refers to species for which $\delta^{13}C$ and $\Delta^{18}O$ covary, and 'uncoupled' refers to species for which either $\delta^{13}C$ or $\Delta^{18}O$ varied independently from the other. All correlation statistics were calculated using linear mixed effects models with block as a random effect using the 'lmer' function in the lme4 R package (Bates et al. 2015). All analyses were performed in R5.3.2 (R Core Team 2019).

Results

Soil moisture content immediately before treatment initiation was approximately 30% in all plots. Coincident with warming air temperatures, soil moisture declined in all plots throughout the course of the growing season. The five water treatments were consistently maintained throughout the season, with growing season average moisture contents of 12%, 16%, 21.5%, 25.5%, and 30% from driest (treatment 1) to wettest (treatment 5).

As metrics of plant performance, I measured aboveground biomass (g) as well as leaf physiological and morphological traits: leaf $\delta^{13}C$, $\Delta^{18}O$, IMS values, LA, plant height, leaf N content, and plant source water $\delta^{18}O$ (estimate of relative rooting depth). Biomass and all of the measured traits varied by species ($p < 0.0001$; Table 3.1) and by treatment, with the exception of IMS and LA that did not vary by treatment ($p = 0.28$, all others $p < 0.02$; Table 3.1). I observed a species x treatment interaction for biomass, $\delta^{13}C$, LA, plant height, and source water $\delta^{18}O$ (all $p < 0.02$), indicating differential species responses to the water treatments.

Variation in integrated metabolic strategies across species

Species varied in their metabolic strategies, as indicated by their position on a $\delta^{13}C$-$\Delta^{18}O$ biplot (Figure 3.1A) and in their average IMS values (Figure 3.1B). Species with relatively enriched $\delta^{13}C$ and $\Delta^{18}O$ included the three *Solidago* species *S. altissima, S. juncea* and *S. rugosa*. *Taraxacum officinale* had the most depleted $\delta^{13}C$ and $\Delta^{18}O$; the remaining species, *C. arvense, E. graminifolia*, and *S. novae-angliae* had intermediate $\delta^{13}C$ and $\Delta^{18}O$ values falling in between *T. officinale* and the *Solidago* species.

Inter-specific differences in IMS were dictated by whether $\delta^{13}C$ values were above or below the overall regression line across all species and treatments ($R^2 = 0.73$, $p < 0.0001$; slope = 0.65; Figure 3.1). The most metabolically efficient species (i.e., highest IMS), *T. officinale*, had $\delta^{13}C$ values below the regression line, resulting in relatively more depleted $\delta^{13}C$ values at a given $\Delta^{18}O$. In contrast, the two species with the lowest IMS values, *C. arvense* and *S. altissima* (Figure 3.1B) had $\delta^{13}C$ values above the regression line, resulting in relatively more enriched $\delta^{13}C$ values at a given $\Delta^{18}O$ relative to other species. Mid-range IMS species *E. graminifolia, S. rugosa,* and *S. novae-angliae* had $\delta^{13}C$ and $\Delta^{18}O$ values that fell on the line. Interestingly, *S. juncea* was relatively more enriched in $\delta^{13}C$ and $\Delta^{18}O$ overall, but its $\delta^{13}C$ values fell below the regression line in treatments 1-3 (dry to average soil moisture), resulting in mid-range IMS (Figure 3.1).

Four species displayed a 'coupled' gas exchange response across water treatments, indicated by a positive correlation between $\delta^{13}C$ and $\Delta^{18}O$ ($p < 0.05$; Figure 3.1A). The correlation slopes for *E. graminifolia* (0.63) and *S. rugosa* (0.70) were indistinguishable from the overall across-species slope of 0.73. *Solidago altissima* and *S. juncea* had slopes that were larger (0.84) and smaller (0.52), respectively, compared to the overall slope. The remaining three species, *C. arvense*, *S. novae-angliae*, and *T. officinale* displayed an 'uncoupled' gas exchange response across water treatments, indicated by $\delta^{13}C$ and $\Delta^{18}O$ not being correlated ($p > 0.2$; Figure 3.1A). For these uncoupled species, $\Delta^{18}O$ decreased from dry to wet treatments while $\delta^{13}C$ remained similar across treatments.

Changes in biomass and leaf metabolism in response to variation in water availability

Species differentially responded to the water treatments in their aboveground biomass (Figure 3.2A; Figure A3.5). *Cirsium arvense, E. graminifolia,* and *S. altissima* had the smallest biomass in dry treatments and largest biomass in wet treatments ($p < 0.01$). In contrast, *S. juncea* and *S. rugosa* had the largest biomass in dry treatments and smallest in wet treatments ($p < 0.01$). Two species, *S. nova-angliae* and *T. officinale*, maintained similar biomass across treatments ($p > 0.5$).

All species, except for uncoupled species *C. arvense, S. nova-angliae* and *T. officinalis*, were more enriched in $\delta^{13}C$ and $\Delta^{18}O$ in the dry treatments and became more depleted in the wet treatments (Figure 3.2 C, D), indicating relatively more carbon gain potential and evaporative water loss in wet treatments relative to dry. Across treatments, *S. altissima, S. juncea* and *S. rugosa* remained the most enriched and *T. officinale* remained the most depleted in $\delta^{13}C$ and $\Delta^{18}O$.

Morphological and physiological drivers of biomass responses

Across all species and treatments, biomass positively correlated with LA ($t = 7.0$, $p < 0.0001$) and plant height ($t = 12.6$, $p < 0.0001$; Table 3.2). Biomass negatively correlated with leaf $\delta^{13}C$ ($t = -2.4$, $p = 0.02$), $\Delta^{18}O$ ($t = -2.2$, $p = 0.03$), and source water $\delta^{18}O$ ($t = -2.6$, $p = 0.01$). Biomass was not correlated with leaf N content ($t = 1.6$, $p = 0.10$). Across all species, changes in biomass between dry and wet treatments was not directly related to species' average IMS values ($t = -0.42$, $p = 0.69$; Figure 3.3A) or the extent of coupling between $\delta^{13}C$ and $\Delta^{18}O$ ($t=0.22$, $p = 0.83$, Figure 3.3B).

Within-species growth responses were not all driven by the same traits. Larger biomass in *C. arvense* was related to increases in plant height (Figure A3.2) and decreases in leaf $\Delta^{18}O$ (Figure 3.2D). For *E. graminifolia* and *S. rugosa*, increasing biomass was related to increases in LA (Figure A3.1) and plant height (Figure A3.2). Larger biomass in *S. altissima* and *S. juncea*, was related to larger LA (Figure A3.1), increases in plant height (Figure A3.2), and increasing IMS (Figure 3.2C). Variation in *S. nova-angliae* biomass was related to changes in leaf $\Delta^{18}O$ (Figure 3.2D), LA (Figure A3.1) and plant height (Figure A3.2). Biomass did not vary substantially enough in *T. officinale* to correlate with any measured variables.

Table 3.1: Results of a linear mixed effects model analysis of variance showing the effects of species, water treatments, and their interaction on standardized total aboveground biomass, leaf carbon isotope composition ($\delta^{13}C$), leaf oxygen isotope enrichment above source water ($\Delta^{18}O$), integrated metabolic strategy value (IMS), total leaf area, plant height, plant source water oxygen isotope composition ($\delta^{18}O$), and leaf nitrogen content. Data are for seven Asteraceae species co-occurring in a temperate old field in Ithaca, NY (n=45 per species).

Model Term	**df**	**F**	**p**
Aboveground biomass (g)			
Species	6	44.5519	< 0.0001
Treatment	4	3.0667	0.0173
Species x Treatment	24	1.952	0.0064
Leaf $\delta^{13}C$ (‰)			
Species	6	77.0341	< 0.0001
Treatment	4	28.642	< 0.0001
Species x Treatment	24	2.0287	0.0057
Leaf $\Delta^{18}O$ (‰)			
Species	6	25.7046	< 0.0001
Treatment	4	12.9207	< 0.0001
Species x Treatment	24	0.5493	0.9560
Integrated metabolic strategy			
Species	6	12.961	< 0.0001
Treatment	4	1.2853	0.2784
Species x Treatment	24	1.0581	0.3985
Leaf area (cm^2)			

Species	6	52.8347	< 0.0001
Treatment	4	1.2681	0.2834
Species x Treatment	24	2.0935	0.0029
Plant height (m)			
Species	6	127.8102	< 0.0001
Treatment	4	3.7018	0.0060
Species x Treatment	24	1.8508	0.0111
Source water $\delta^{18}O$ (‰)			
Species	6	32.5222	< 0.0001
Treatment	4	46.8281	0.0004
Species x Treatment	24	4.5115	< 0.0001
Leaf nitrogen (%)			
Species	6	33.9784	< 0.0001
Treatment	4	3.2169	0.0150
Species x Treatment	24	1.0826	0.3731

Table 3.2: Multiple linear regression model showing effects of leaf carbon isotope composition ($\delta^{13}C$), leaf oxygen isotope enrichment above source water ($\Delta^{18}O$), total leaf area, plant height, plant source water oxygen isotope composition ($\delta^{18}O$), and leaf nitrogen content on variation in aboveground biomass. Data are for seven Asteraceae species co-occurring in a temperate old field in Ithaca, NY (n=45 per species). Total model $R^2 = 0.782$, $p < 0.0001$.

Variable	Estimate	Standard error	t	p
Leaf $\delta^{13}C$ (‰)	-0.14337	0.0594	-2.414	0.0171
Leaf $\Delta^{18}O$ (‰)	-0.12201	0.05571	-2.19	0.0302
Leaf area (cm^2)	0.37499	0.05358	6.998	< 0.0001
Height (m)	0.7365	0.05843	12.605	< 0.0001
Leaf nitrogen (%)	0.0681	0.04152	1.64	0.1032
Source water $\delta^{18}O$ (‰)	-0.11276	0.04359	-2.587	0.0107
Intercept	-0.02609	0.04356	-0.599	0.5502

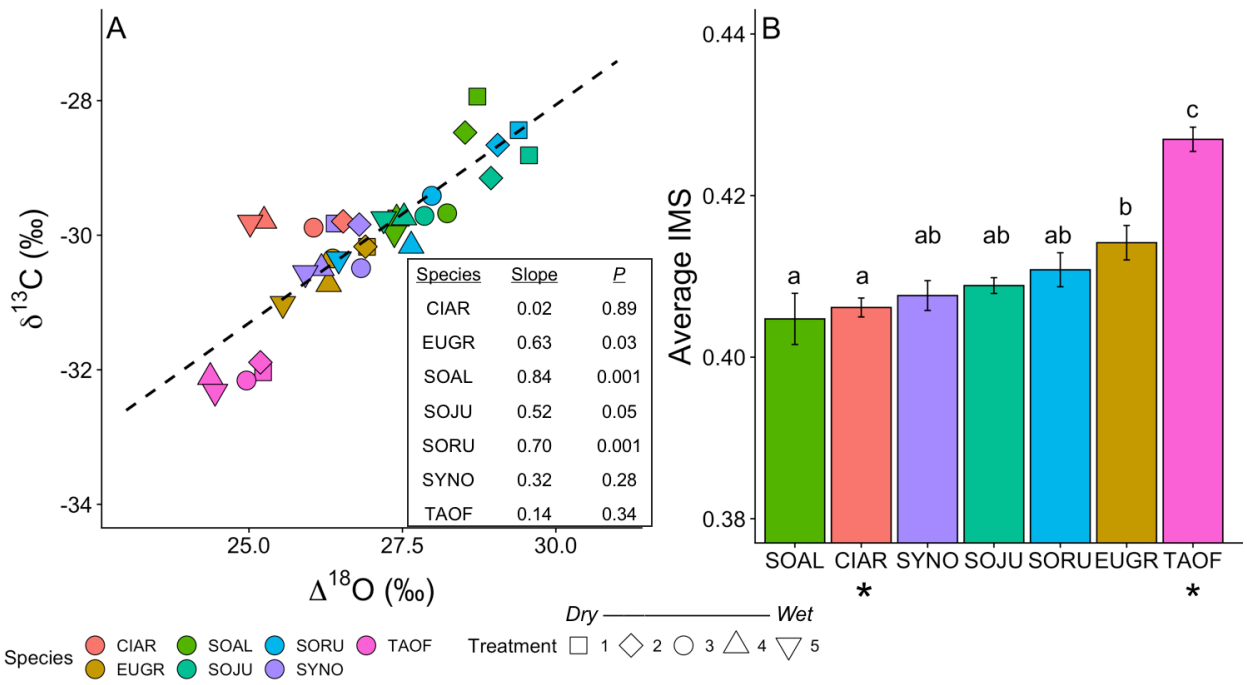

Figure 3.1: Variation within and among seven co-occurring Asteraceae species in (A) leaf carbon isotope composition (δ13C) and leaf oxygen isotope enrichment above source water (Δ18O). δ13C and Δ18O were positively correlated across all species and water treatments (R2 = 0.73, p < 0.0001, slope = 0.65). Linear regression slopes and significance (within-species values reported in the inset) were calculated from linear mixed effects models with 'block' as a random effect. (B) Inter-specific variation in integrated metabolic strategy (IMS) values. Data are species means across five experimental water treatments ± standard error (n = 45 per species). Species that share the same letter are statistically indistinguishable, based on Tukey post-hoc tests. Species abbreviations are the first two letters of the genus and species epithet given in Materials and Methods. Asterisks indicate non-native species.

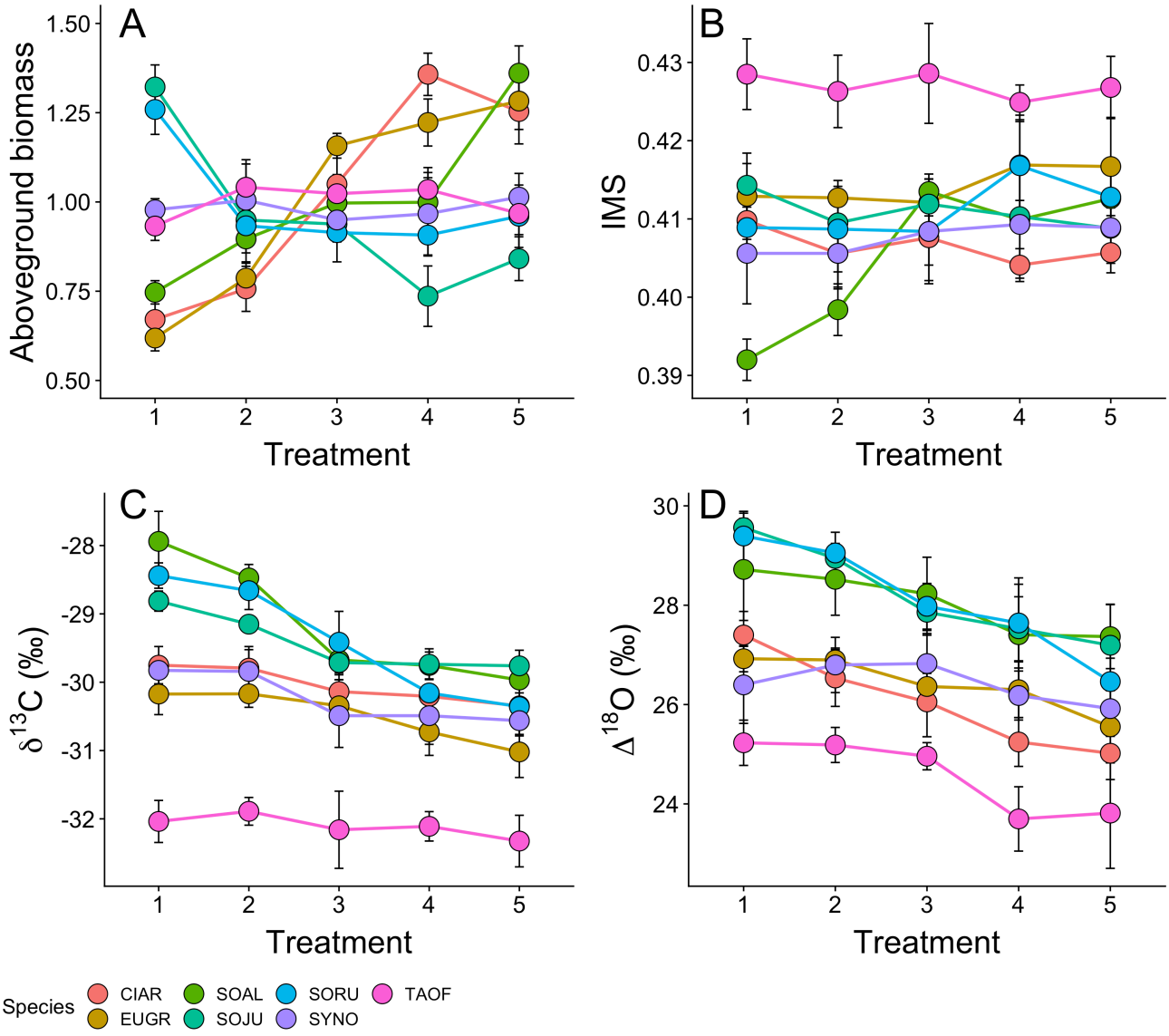

Figure 3.2: Observed changes in (A) aboveground biomass (g, standardized), (B) integrated metabolic strategy (IMS) values, (C) leaf carbon isotope composition ($\delta^{13}C$) and (D) leaf oxygen isotope enrichment above source water ($\Delta^{18}O$) across five experimental water treatments that span a gradient from the driest ('treatment 1') to the wettest ('treatment 5') year on record from the last 30 years in Ithaca, NY. Data are species means ± standard error for seven co-occurring Asteraceae species (n = 9 per species, per treatment). Species abbreviations are the first two letters of the genus and species epithet given in *Materials and Methods*.

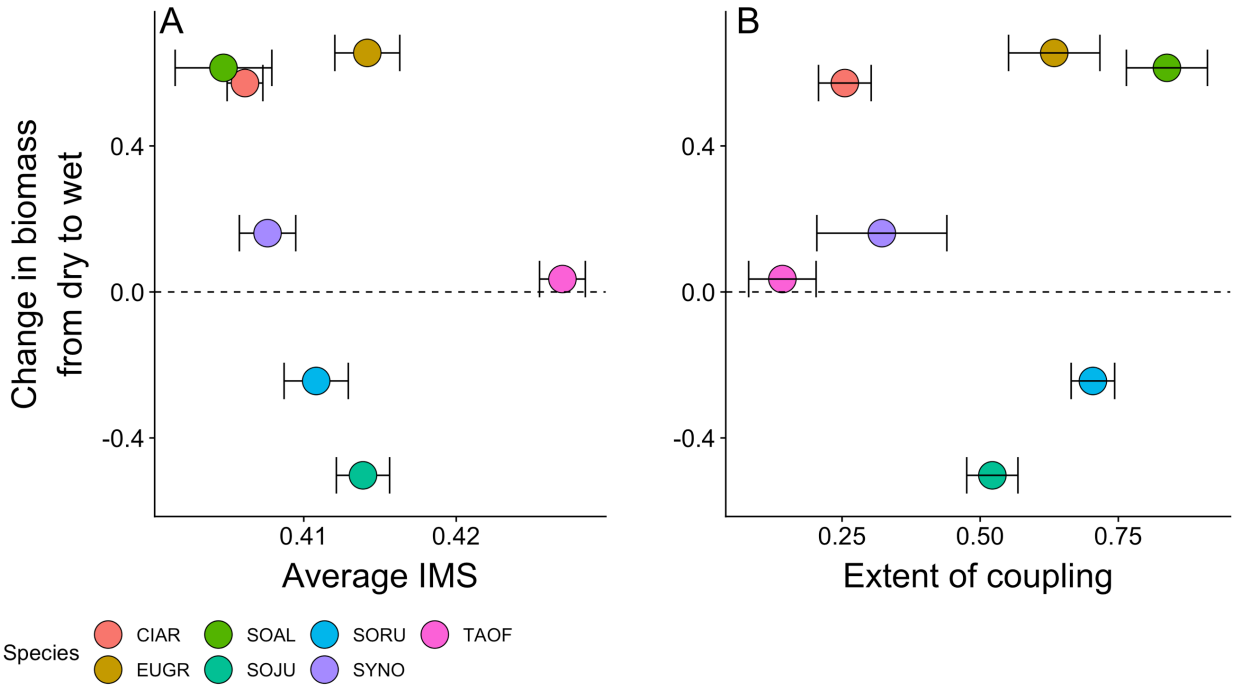

Figure 3.3: The change in biomass between the driest and wettest treatments in relation to (A) average integrated metabolic strategy (IMS) values across all treatments (t=-0.42, p = 0.69), and (B) the extent of coupling between carbon and water leaf gas exchange, measured as the linear regression slope between leaf carbon isotope composition ($\delta^{13}C$) and leaf oxygen isotope enrichment above source water ($\Delta^{18}O$) (t = 0.22, p = 0.83). Linear regression slopes were calculated from linear mixed effects models with 'block' as a random effect. Data are species means across five experimental water treatments ± standard error (n = 45 per species).

Discussion

In order for diverse species to coexist in ecological communities, limiting resources must vary in ways that allows species to capitalize on different aspects of those resources in space and/or time. Observing species-specific responses to environmental variation may seem ubiquitous, yet, the underlying mechanisms responsible for differential responses are largely unknown. Here, I tested the hypothesis that species differential responses to inter-annual variation in growing season precipitation is associated with differences in metabolism. In support of this, species differentially responded to variation in growing season water availability and, importantly, how they responded could be explained by differences in metabolism, as measured by carbon and oxygen stable isotopes. Indeed, water-conservative species grew best in the dry treatments and had their minimal growth in wet treatments. Carbon-acquisitive species displayed the opposite pattern, with maximal growth in wet treatments and steep declines in dry treatments. The most metabolically efficient species, *T. officinale*, maintained similar growth and high leaf-level carboxylation across all water levels. Metabolic differences among co-occurring species may help explain temporal variation in growth, and could provide an underlying physiological mechanism for long-term dynamics that promote biodiversity.

Species metabolic strategies: inter and intraspecific variation

Here, I examine species' $\delta^{13}C$ and $\Delta^{18}O$ across an experimental rainfall gradient from the driest to the wettest growing seasons relative to the 30-year average for the region. This extensive range in water availability allowed me to assess each species' average metabolism in the field, as well as their range of phenotypic plasticity in response to variation in water availability. Examining species on a $\delta^{13}C$ and $\Delta^{18}O$ biplot (Figure 3.1A) shows that these seven species fall

along a continuous spectrum of metabolic strategies from isotopically depleted carbon-acquisitive to isotopically enriched water-conservative. Variation in overall metabolic efficiency among species, indicated by average integrated metabolic strategy (IMS) values across all treatments, was driven primarily by differences in carbon gain potential (i.e., relatively enriched or depleted $\delta^{13}C$ values) at a given rate of water loss (i.e., similar range of $\Delta^{18}O$ values). For example, across all water treatments *C. arvense*, *E. graminifolia*, and *S. novae-angliae* had overlapping $\Delta^{18}O$ values but *C. arvense* had leaves that were consistently more enriched in $\delta^{13}C$ (Figure 3.1A), resulting in a lower metabolic efficiency (lower overall IMS) than *E. graminifolia* and *S. novae-angliae* (Figure 3.1B). Similarly, *S. altissima* was less metabolically efficient than congeners *S. juncea* and *S. rugosa* (Figure 3.1B) due to leaves with relatively enriched $\delta^{13}C$ values in the dry treatments at similar rates of water loss (Figure 3.1A). The species with the highest metabolic efficiency, *T. officinale*, had overlapping $\Delta^{18}O$ with *C. arvense* and *E. graminifolia*, but was far more depleted in $\delta^{13}C$ (Figure 3.1A).

Species varied not only in their relative position in dual-isotope space, indicating differences in intrinsic metabolic efficiency, but also in the direction and magnitude of $\delta^{13}C$ and $\Delta^{18}O$ plasticity across experimental water treatments. The degree of plasticity across water availabilities, measured as the extent to which $\delta^{13}C$ and $\Delta^{18}O$ are coupled (i.e., covary), revealed differential physiological responses among species. As predicted by the Goud et al. (2019) conceptual model (Figure 1.1), species with a coupled gas exchange response may change the magnitude of carbon gain and water loss, but maintain similar ratios between the two fluxes, resulting in negligible changes in IMS in response to a driving force (in this case, variation in water availability). In contrast, an uncoupled response should result in increasing IMS in

conditions where either $\delta^{13}C$ decreases across constant $\Delta^{18}O$, or where $\Delta^{18}O$ enriches across constant $\delta^{13}C$. In this study, four species had strongly coupled $\delta^{13}C$ and $\Delta^{18}O$, suggesting tight stomatal regulation that co-limits the diffusion of CO_2 and water vapor. One species, *C. arvense*, was strongly decoupled, with broad increases in $\Delta^{18}O$ in dry treatments while $\delta^{13}C$ remained constant (Figure 3.1A; Figure 3.2C-D), resulting in higher IMS (Figure 3.2B) and thus more metabolically efficient leaves in the dry treatments. Similarly, *T. officinale* increased $\Delta^{18}O$ in the dry treatments while $\delta^{13}C$ remained constant, while *S. novae-angliae* had slight increases in $\delta^{13}C$ across constant $\Delta^{18}O$ (Figure 3.1A; Figure 3.2C-D). The ability to increase $\Delta^{18}O$ while keeping $\delta^{13}C$ constant is indicative of stomatal closure that limits the evaporative loss of water from leaves, while compensating for decreased CO_2 diffusion by increasing carboxylation rates. Increasing carboxylation can be achieved by increased enzymatic activity and/or amount of the carbon-fixing enzyme Rubisco. Indeed, I observed increases in total leaf nitrogen content and maximum rates of carboxylation in milkweed species that had uncoupled $\delta^{13}C$ and $\Delta^{18}O$ in response to experimental water limitation (Goud et al. 2019). In a similar fashion, species that maintain $\Delta^{18}O$ and vary $\delta^{13}C$ are likely keeping stomata open and not changing foliar water loss, but adjust carbon consumption by increasing Rubisco activity and/or amount (Schultz et al. 1996).

Differential growth responses to water availability

Across all species and treatments, variation in biomass was largely driven by changes in total leaf area and height, irrespective of changes in leaf-level physiology. This is consistent with other studies that found variation in growth rate among herbaceous perennials to primarily be the result of changes in biomass allocation at the whole-plant level, rather than individual leaf traits

(Lambers and Poorter 1992, Poorter et al. 2011).

Carbon-acquisitive species (relatively depleted in $\delta^{13}C$ and $\Delta^{18}O$) *C. arvense* and *E. graminifolia* strongly increased growth with increasing water availability, and displayed the largest declines in biomass in the dry treatments relative to the other species (Figure 3.2A). *Cirsium arvense* is a wide-spread non-native invasive that invades a broad range of habitats (R G Wilson 1979, Tiley 2010). It is known to grow best in mesic conditions, and is intolerant of soils that are too dry (R G Wilson 1979) or too wet (Bakker 1960). Consistent with this, *C. arvense* displayed maximal growth in average and wet conditions, but reduced biomass in the dry and wettest treatments (Figure 3.2A). *Euthamia graminifolia* is known to occupy wetter soils and have a large niche breadth relative to other Asteraceae in old fields and grasslands (Werner and Platt 1976). Consistent with this, *E. graminifolia* displayed maximal biomass in the wettest treatment (Figure 3.2A).

Other carbon-acquisitive species *S. novae-angliae* and *T. officinale* maintained similar biomass across treatments (Figure 3.2A). *Symphyotrichum novae-angliae* is known to be widely adapted to a range of soils, from wet, organic to dry, sandy soils (Gleason and Cronquist 1991, Chmielewski and Semple 2003), and has the ability to maintain high growth in dry and water-logged soils alike (Shrestha et al. 2018). Consistent with this, *S. novae-angliae* appeared unresponsive to variation in water availability not only in its growth, but in leaf-level physiology ($\delta^{13}C$, $\Delta^{18}O$, IMS) and whole-plant morphology (LA, height). However, it does appear that *S. novae-angliae* can adjust its rooting behavior to access deeper, more potentially stable sources of water in the dry treatments, as seen by depleted source water $\delta^{18}O$ values (Figure A3.4). It's possible that *S. novae-angliae* is able to maintain growth under water deficits by accessing more

stable sources of water and bypassing water limitations.

In contrast, the lack of growth response across water treatments in *T. officinale* is likely due to its unique life history relative to the other study species. Although *T. officinale* retains its aboveground biomass into the late summer, it is functionally active in the spring, producing flowers and setting seed by late May when water and light are readily available, and before the other species have fully grown (Gleason and Cronquist 1991). Thus, the relatively efficient and productive metabolic strategy of *T. officinale* that is maintained across treatments appears linked to an early-spring life history strategy that serves to avoid water deficits and inter-specific competition.

The three goldenrods, *S. altissima, S. juncea*, and *S. rugosa*, were the most enriched in $\delta^{13}C$ and $\Delta^{18}O$ across all treatments (Figure 3.1A, 3.2C-D). Both *S. juncea* and *S. rugosa* are known to be dry-site specific (Potvin and Werner 1983, Gleason and Cronquist 1991, Griffiths and Orians 2003) and displayed maximum biomass in the driest treatment, and lowest in the wet treatments (Figure 3.2A). Maximizing biomass under dry conditions could indicate that these species have distinct hydrological niches than their neighbors, defined by temporal variation in water availability across seasons. In support of this, *S. rugosa* is more typically found in dry, open habitats, especially on sandy soils (Gleason and Cronquist 1991, Griffiths and Orians 2003), and consistently grows better in drier soils even in the absence of competitors (Griffiths and Orians 2003). This suggests that *S. rugosa* is adapted to more dry, aerated conditions and is physiologically less tolerant of wetter soils. In contrast, although these results and others have observed *S. juncea* to grow better on dry soils (Potvin and Werner 1983, Gleason and Cronquist 1991), in the absence of competition *S. juncea* actually grows better in wetter soils and can grow larger than neighboring species such as *S. altissima* (Potvin and Werner 1983). This suggests that

competitive exclusion constrains *S. juncea*'s growth when water is abundant, while potential competitive release allows it to increase in dry soils when its competitors suffer reduced growth.

The most dominant species in this community, *S. altissima*, was also relatively enriched in $\delta^{13}C$ and $\Delta^{18}O$ when averaged across all treatments. Although its leaf metabolism is indicative of a water-conservative strategy, it had the smallest and largest growth in the driest and wettest treatments, respectively, which is more indicative of a carbon-acquisitive strategy. Interestingly, *S. altissima* maintained similar growth across all three average conditions (treatments 2, 3 and 4). *Solidago altissima* is reported to be relatively intolerant of dry soils, and to occur across a range of mesic to wet soils (Potvin and Werner 1983, Walck et al. 1999, Nolf et al. 2014). Examining changes in $\delta^{13}C$ and $\Delta^{18}O$ across treatments shows that *S. altissima* becomes very enriched in the driest treatment and very depleted in the wettest, suggesting strong stomatal responses to moisture availability. In support of this, Nolf et al. (2014) observed high levels of phenotypic plasticity in *S. altissima* hydraulic traits, including tight stomatal regulation and rapid stomatal closure in response to moisture deficits. Together, these results suggest that producing relatively inefficient yet water-conservative leaves allows *S. altissima* to tolerate a range of soil moisture conditions, while rapidly producing new leaves and increasing stem elongation when water is less limiting. I observed a similar response in milkweeds that had the least efficient leaves (enriched $\delta^{13}C$ but depleted $\Delta^{18}O$) but could rapidly produce additional leaves and grow taller in response to water availability (Goud et al. 2019).

Relating growth responses to metabolic diversity

In Chapter 2, I observed a relationship between the change in abundance and a species' average IMS such that species with higher IMS tended to be in higher abundance in an average year

relative to a dry year (e.g., *D. carota, M. moschata*), or maintained similar vegetative cover between years (e.g., *G. triflorum, T. officinale*), suggesting that relatively higher-IMS species were more sensitive to dry conditions than lower-IMS species. Consistent with this, Asteraceae species with the highest IMS increased biomass in the experimentally wet treatments (*E. graminifolia*) or maintained similar growth across treatments (*T. officinale*; Figure 3.3A). However, species with the lowest IMS (*C. arvense, S. altissima*) also grew best in the wet treatments, while species that decreased in the wet treatments (*S. juncea, S. rugosa*) had mid-range IMS (Figure 3.3A). It's possible that variation in vegetative cover does not track changes in aboveground biomass within a growing season, as cover can vary with changes in plant density that are independent of individual plant size. Alternatively, a lower-IMS value may not be exclusively indicative of a water-conservative strategy, but may be reflective of a lower metabolic demand for carbon at the leaf-level (i.e., intrinsically slower metabolism). Given that similar IMS values can be achieved via diverse morphological solutions, the IMS-growth relationship may not be generalizable across all taxa. This is consistent with the notion that leaf-level metabolism does not necessarily scale up to whole-plant growth; rather, variation in growth is driven more by whole-plant allocation patterns among leaf, root, and stem biomass (Lambers and Poorter 1992, Poorter et al. 2011). Nevertheless, considering IMS in concert with $\delta^{13}C$ and $\Delta^{18}O$ effectively identifies the relative ranking and extent of physiological plasticity, giving valuable insights into metabolic diversity among taxa.

In Chapter 2, I also observed a relationship between the change in abundance and the extent to which a species showed coupled gas exchange. Species that were coupled tended to increase or maintain cover in the average year relative to the dry, suggesting that some coupled species are more sensitive to water limitation. Uncoupled species either decreased or maintained

similar cover between years, suggesting a possible advantage for uncoupled species under drier conditions. When I expanded the range of water availabilities from two conditions to five, many species that were uncoupled across two seasons were coupled across all five due to strong differences in the driest and wettest conditions (e.g., *E. graminifolia, S. rugosa*; Figure 3.1A), which were not represented in Chapter 2. Thus, defining a species as 'coupled' or 'uncoupled' may require examining changes in $\delta^{13}C$ and $\Delta^{18}O$ across a wide range of possible water availabilities for some species. At the same time, species that are uncoupled across the average range of climate variation and only display the coupled response across more extreme conditions may be reflective of species that are better-adapted and perhaps more competitive across the range of conditions they would typically experience for the majority of their life. Moreover, the relationship between gas exchange coupling and growth/vegetative cover is not necessarily linear across all taxa. It appears likely that coupled species rely on stomatal control to co-limit the loss of water and gain of CO_2 under water limitation, and then quickly open stomata and increase photosynthesis when water is no longer limiting.

Variation in inter-annual precipitation and plant metabolic diversity

Examining differential species responses to precipitation in light of their metabolic strategies has implications for biodiversity outcomes in a changing climate. There is increasing evidence that rainfall patterns are already being altered due to global climate changes. Although we don't typically consider temperate mesic soils as water-limited, this work shows that the magnitude of rain between years can impose water limitations on plants, resulting in significant changes in biomass that may alter competitive hierarchies among species. It appears that across-season variation serves to shift the competitive balance among species with different metabolic strategies, favoring those that are better able to tolerate unfavorable conditions, and can quickly

capitalize on available resources that would otherwise have been used by their competitors. Other studies using precipitation-exclusion experiments in mid-western continental grasslands have also documented species-specific responses to variation in inter-annual rainfall. Similar to this study, some species respond positively to increasing water availability, others show little response, and others show positive responses to drier treatments (Fay et al. 2002; Fay et al. 2008). Moreover, individual species responses scale up to affect ecosystem function, such as primary productivity, resilience to drought, and ecosystem carbon balance (Fay et al. 2008; Hoover et al. 2014). If the frequency of water-limited years persistently decreases in this region, as predicted by climate models (Easterling et al. 2017), there may be significant ecological consequences. For example, sustained reductions in growth of species that are favored in dry years may limit their establishment and growth, potentially favoring invasive species and ultimately shifting species distributions and community composition.

Literature Cited

Angert, A.L., Huxman, T.E., Chesson, P., and Venable, D.L. Functional tradeoffs determine species coexistence via the storage effect. 2009. Proceedings of the National Academy of Sciences of the United States of America 106(28):11641–11645.

Bakker, D. 1960. A comparative life-history study of Cirsium arvense (L.) Scop. and Tussilago farfara L., the most troublesome weeds in the newly reclaimed polders of the former Zuiderzee. Pages 205–222 *in* J. L. Harper, editor. The Biology of Weeds. Biology of Weeds, Symp. Brit. ecol. Soc., Oxford.

Bates, D., M. Mächler, B. Bolker, and S. Walker. 2015. Fitting Linear Mixed-Effects Models using lme4. Journal of Statistical Software 67:1–48.

Chmielewski, J. G., and J. C. Semple. 2003. The biology of Canadian weeds. 125. Symphyotrichum ericoides (L.) Nesom (Aster ericoides L.) and S. novae-angliae (L.) Nesom (A. novae-angliae L.). Canadian Journal of Plant Science 83:1017–1037.

Easterling, D.R., K.E. Kunkel, J.R. Arnold, T. Knutson, A.N. LeGrande, L.R. Leung, R.S. Vose, D.E. Wal- iser, and M.F. Wehner. 2017: Precipitation change in the United States. In: Climate Science Special Report: Fourth National Climate Assessment, Volume I [Wuebbles, D.J., D.W. Fahey, K.A. Hibbard, D.J. Dokken, B.C. Stewart, and T.K. Maycock (eds.)]. U.S. Global Change Research Program, Washington, DC, USA, pp. 207-230.

Farquhar, G. D., and T. D. Sharkey. 1982. Stomatal Conductance and Photosynthesis. Annual review of plant physiology 33:317–345.

Farquhar, G. D., J. R. Ehleringer, and K. T. Hubick. 1989. Carbon Isotope Discrimination and

Photosynthesis. annual review of plant physiology and plant molecular biology 40:503–537.

Farquhar, G. D., L. A. Cernusak, and B. Barnes. 2007. Heavy Water Fractionation during Transpiration. Plant Physiology 143:11–18.

Fay, P. A., D. M. Kaufman, J. B. Nippert, J. D. Carlisle, and C. W. Harper. 2008. Changes in grassland ecosystem function due to extreme rainfall events: implications for responses to climate change. Global Change Biology 14:1600–1608.

Fay, P. A., J. D. Carlisle, B. T. Danner, M. S. Lett, J. K. McCarron, C. Stewart, A. K. Knapp, J. M. Blair, and S. L. Collins. 2002. Altered Rainfall Patterns, Gas Exchange, and Growth in Grasses and Forbs. International Journal of Plant Sciences 163:549–557.

Gleason, H. A., and A. Cronquist. 1991. Manual of Vascular Plants of Northeastern United States and Adjacent Canada. New York Botanical Garden.

Goud, E. M., J. P. Sparks, M. Fishbein, and A. A. Agrawal. 2019. Integrated metabolic strategy: A framework for predicting the evolution of carbon-water tradeoffs within plant clades. Journal of Ecology 107:1633–1644.

Griffiths, M. E., and C. M. Orians. 2003. Responses of common and successional heathland species to manipulated salt spray and water availability. American Journal of Botany 90:1720–1728.

HilleRisLambers, J., P. B. Adler, W. S. Harpole, J. M. Levine, and M. M. Mayfield. 2012. Rethinking Community Assembly through the Lens of Coexistence Theory. Annual Review of Ecology, Evolution, and Systematics 43:227–248.

Hoover, D. L., A. K. Knapp, and M. D. Smith. 2014. Resistance and resilience of a grassland ecosystem to climate extremes. Ecology 95:2646–2656.

Lambers, H., and H. Poorter. 1992. Inherent Variation in Growth Rate Between Higher Plants: A Search for Physiological Causes and Ecological Consequences. Pages 187–261 *in* Advances in Ecological Research Volume 23. Elsevier.

Levine, J. M., and J. HilleRisLambers. 2009. The importance of niches for the maintenance of species diversity. Nature 461:254–257.

Liu, H., Q. Xu, P. He, L. S. Santiago, K. Yang, and Q. Ye. 2015. Strong phylogenetic signals and phylogenetic niche conservatism in ecophysiological traits across divergent lineages of Magnoliaceae. Scientific Reports 5:343.

Marks, P. L. 1983. On the origin of the field plants of the northeastern United States. The American Naturalist.

Monson, R. K., Ehleringer, J. R., and J. R. Ehleringer. 1993. Evolutionary and Ecological Aspects of Photosynthetic Pathway Variation. Annual Review of Ecology and Systematics 24:411–439.

Nolf, M., K. Pagitz, and S. Mayr. 2014. Physiological acclimation to drought stress in Solidago canadensis. Physiologia Plantarum 150:529–539.

Poorter, H., K. J. Niklas, P. B. Reich, J. Oleksyn, P. Poot, and L. Mommer. 2011. Biomass allocation to leaves, stems and roots: meta-analyses of interspecific variation and environmental control. New Phytologist 193:30–50.

Potvin, M. A., and P. A. Werner. 1983. Water Use Physiologies of Co-Occurring Goldenrods (Solidago juncea and S. canadensis): Implications for Natural Distributions. Oecologia 56:148–152.

R Core Team. 2019. R: A language and environment for statistical computing. R Foundation for Statistical Computing. Vienna, Austria.

R G Wilson, J. 1979. Germination and Seedling Development of Canada Thistle (Cirsium arvense). Weed Science 27:146–151.

Roden, J. S., and G. D. Farquhar. 2012. A controlled test of the dual-isotope approach for the interpretation of stable carbon and oxygen isotope ratio variation in tree rings. Tree Physiology 32:490–503.

Schultz, H. R., W. Kiefer, and W. Gruppe. 1996. Photosynthetic duration, carboxylation efficiency and stomatal limitation of sun and shade leaves of different ages in field-grown grapevine (Vitis vinifera L.). Vitis 35:169–176.

Shrestha, P., S. E. Hurley, and B. C. Wemple. 2018. Effects of different soil media, vegetation, and hydrologic treatments on nutrient and sediment removal in roadside bioretention systems. Ecological Engineering 112:116–131.

Silvertown, J., Silvertown, J., M. E. Dodd, M. E. Dodd, D. Gowing, D. J. G. Gowing, J. O. Mountford, and J. O. Mountford. 1999. Hydrologically defined niches reveal a basis for species richness in plant communities. Nature 400:61–63.

Silvertown, J., Y. Araya, and D. Gowing. 2014. Hydrological niches in terrestrial plant

communities: a review. Journal of Ecology 103:93–108.

Tiley, G. E. D. 2010. Biological Flora of the British Isles: Cirsium arvense (L.) Scop. Journal of Ecology 98:938–983.

Walck, J. L., J. M. Baskin, and C. C. Baskin. 1999. Relative competitive abilities and growth characteristics of a narrowly endemic and a geographically widespread Solidago species (Asteraceae). American Journal of Botany 86:820–828.

Werner, P. A., and W. J. Platt. 1976. Ecological Relationships of Co-Occurring Goldenrods (Solidago: Compositae). The American Naturalist 110:959–971.

Whittaker, R. H. 1965. Dominance and Diversity in Land Plant Communities: Numerical relations of species express the importance of competition in community function and evolution. Science 147:250–260.

CHAPTER FOUR

Leaf stable isotopes suggest shared ancestry is an important driver of functional diversity[2]

Abstract

Plant physiological strategies of carbon (C) and nitrogen (N) uptake and metabolism are often regarded as outcomes of environmental selection. This is likely true, but the role of evolutionary history may also be important in shaping patterns of functional diversity. Here, we used leaf C and N stable isotope ratios ($\delta^{13}C$, $\delta^{15}N$) as integrators of physiological processes to assess the relative roles of phylogenetic history and environment in a diverse group of Ericaceae species native to North America. We found strong phylogenetic signal in both leaf $\delta^{13}C$ and $\delta^{15}N$, suggesting that close relatives have similar physiological strategies. The signal of phylogeny was generally stronger than that of the local environment. However, within some specialized environments (*e.g.*, wetlands, sandy soils), we found environmental effects and/or niche conservatism. Phylogenetic signal in $\delta^{13}C$ appears to be most closely related to the constraints on metabolic demand and supply of C, and $\delta^{15}N$ appears to be most strongly related to mycorrhizal associations within the family.

[2] Goud, E.M. and Sparks, J.P. (2018) Leaf stable isotopes suggest shared ancestry is an important driver of functional diversity. *Oecologia* 187(4): 967-975.

Introduction

Determining the mechanisms that shape the diversity of physiological and morphological features of organisms is a central question in ecology. However, in any given environment, it is challenging to partition the factors that may generate the observed adaptations. The physical environment directly drives adaptation through selection, but an underappreciated mechanism is the constraint put on an organism by its phylogenetic position. Ecologically important characters have traditionally been regarded as labile and physiological changes were assumed to be important responses to environmental variation. However, recent phylogenetic studies have revealed that many lineages of closely related species have maintained ecological and phenotypic similarities through evolutionary time (Wiens et al. 2010). Rather than selection alone driving the relationship between environment and physiology, shared ancestry may play an important role in maintaining groupings of traits important for success in a given environment.

Examining the relative influence of shared ancestry and environment on physiology is nothing new; this has been explored several times in plants by tracing the phylogenetic signal of anatomical characters (Savage and Cavender Bares 2012; Yang et al. 2014). Previous studies have focused on ecologically relevant characters or 'functional traits' that hopefully represent more direct measures of physiological processes. Examples include leaf nitrogen (N) content as a proxy for photosynthetic rate, and leaf lifespan, size and leaf mass per area (or its inverse, specific leaf area) as proxies for rates of resource acquisition and conservation (Wright et al. 2004; Osnas et al. 2013). One challenge with this approach is that trait-environment relationships and phylogenetic signal are often inconsistent among taxonomic groups and environments (Kerkhoff et al. 2006; Yang et al. 2014; Flores et al. 2014; Forrestel et al. 2015; Bhaskar et al. 2016), making interpretation and generalization difficult. One potential reason for these

inconsistencies is that traits may correlate with multiple processes that have contrasting relationships with the environment and/or different rates of evolution. Because physiological responses often involve suites of inter-related traits, single traits like leaf N content or specific leaf area may only describe a part of a physiological process or even function differently across species. Instead of looking at individual functional traits, the alternative approach we use in this work is to use a plant measurement that potentially integrates a physiological process. Stable isotope ratios of leaf C and N are good candidates because they integrate physiological processes and often vary in relation to known ecological variables.

Leaf carbon isotope ($\delta^{13}C$) values are directly related to the integrated strategy a plant uses for C acquisition. $\delta^{13}C$ reflects the long term balance of leaf internal (c_i) to external (c_a) carbon dioxide (CO_2) concentrations, which is dependent upon the resistances to CO_2 entry into the leaf and the rate of CO_2 consumption during photosynthesis (Farquhar et al. 1982). Any factor that increases the difference between c_i and c_a leads to $\delta^{13}C$ enrichment, such as photosynthetic capacity and investment in photosynthetic machinery, the size of the boundary layer of still air around the leaf, the length of the diffusion pathway between the stoma and the site of carboxylation within the chloroplast, and stomatal conductance. Morphological characteristics that increase the size of the leaf boundary layer include increasing leaf size, and surface characters such as hair, waxes and trichomes (Ehleringer et al. 1976; Evans and Loreto 2000). Stomatal conductance and behavior (*i.e.*, how often and for how long the stomata are open relative to closed) are sensitive to changes in temperature and water availability, which would also be reflected in the $\delta^{13}C$ value (Ehleringer et al. 1992).

Leaf nitrogen isotope ratios ($\delta^{15}N$) integrate variation in plant metabolism, differences in ecosystem N cycling and mutualist associations that facilitate biotic N-uptake such as

mycorrhizal fungi and N-fixing bacteria (Hobbie *et al.*, 1999). Plant metabolic processes that fractionate ^{15}N include different pathways of N assimilation (Yoneyama et al. 1991) and internal recycling of N in the plant (Kolb and Evans 2002). Leaf $\delta^{15}N$ values are also affected by changes to the baseline value of $\delta^{15}N$ present in the soil solution that is available for plant uptake. Any factor that changes the rate of soil nutrient turnover (*e.g.*, temperature, water availability) via mineralization, nitrification or denitrification can potentially change the baseline $\delta^{15}N$ of the soil solution and consequently in the leaves (Amundson et al. 2003). Additionally, leaf $\delta^{15}N$ values can vary substantially among species with belowground mutualist associations because different microorganisms access different soil N-pools which consequently affects ^{15}N fractionation (Hobbie et al. 1999; Hobbie and Colpaert 2004; Hobbie and Hobbie 2006). Although not as clearly associated to a single physiological process as $\delta^{13}C$, $\delta^{15}N$ can also integrate physiological interactions with the environment.

Determining phylogenetic signal in leaf $\delta^{13}C$ and $\delta^{15}N$ can shed light on the relative strength of shared ancestry and environment in structuring functional diversity. While $\delta^{13}C$ and $\delta^{15}N$ can vary among closely related species, they have not been evaluated from a phylogenetic perspective because it is generally thought that variation in stable isotope values are predominantly driven by environmental factors, not evolutionary history. However, if metabolic rates are phylogenetically constrained based on similar groupings of physiological traits (Liu et al. 2015), then there may be phylogenetic signal in leaf $\delta^{13}C$ and $\delta^{15}N$. Moreover, if mutualist associations that are important for resource uptake, such as mycorrhizal fungi, are phylogenetically conserved, then the physiology that depends on these mutualisms would also have phylogenetic signal.

The heath family (Ericaceae) is a diverse and geographically widespread plant group that has radiated into a variety of environments, including arctic and alpine tundra, wetlands, boreal and hardwood forests, scrublands and chaparral. 212 species from 46 genera are native to North America and display extensive variation in anatomy, physiology and ecology (Tucker 2009). Phylogenetic and ecological diversity within Ericaceae makes this plant family an excellent study system for investigating leaf $\delta^{13}C$ and $\delta^{15}N$ within a phylogenetic context. Foliar $\delta^{13}C$ and $\delta^{15}N$ values are expected to vary among Ericaceae taxa based on ecological differences such as climate (*e.g.*, temperature, precipitation), latitude and elevation (Friend et al. 1989). Most Ericaceae are evergreen shrubs (e.g., *Rhododendron*, *Vaccinium*), but deciduous shrubs and trees, herbaceous perennials, and parasitic species that lack chlorophyll are also common in North America (Tucker 2009). As such, $\delta^{13}C$ values could also vary with plant growth form (*e.g.*, trees, shrubs, herbs), leaf persistence (*e.g.*, evergreen, deciduous), and metabolism (*e.g.*, fast versus slow growth rates). Moreover, Ericaceae species are often associated with acidic and nutrient poor soils, and their success is largely attributed to mutualisms with three unique types of mycorrhizal fungi: arbutoid, ericoid and monotropoid mycorrhizae (Lallemand *et al.*, 2016). These mycorrhizal types each fractionate N in different ways, which would result in different foliar $\delta^{15}N$ values among host plants (Zimmer et al. 2007).

The objectives of this study were to (1) determine the extent of phylogenetic signal in leaf $\delta^{13}C$ and $\delta^{15}N$ and (2) to assess how phylogeny and environmental conditions relate to $\delta^{13}C$ and $\delta^{15}N$ variation. If shared ancestry is an important driver of physiological diversity, then leaf $\delta^{13}C$ and $\delta^{15}N$ values will have phylogenetic signal and similarity in $\delta^{13}C$ and $\delta^{15}N$ values among species will correlate more strongly with phylogeny than environment. To test these predictions, we compared relationships between $\delta^{13}C$ and $\delta^{15}N$, phylogeny and environment and evaluated

the strength of phylogenetic signal from a molecular phylogeny of 57 Ericaceae species native to North America. We then examined factors that could potentially contribute to phylogenetic signal in leaf stable isotopes, including different mycorrhizal types and other leaf traits important to C and N acquisition and metabolism.

Materials and methods

To determine the phylogenetic relationships among species, we constructed a phylogeny using maximum likelihood analyses in PAUP (Swofford 2002) using sequence data for all Ericaceae species native to North America that had available mat*K*, *nr*ITS and rbcL gene regions from GenBank (107 species total). The tree was rooted on two outgroups: *Enkianthus chinensis* and *E. campanulatus* and the final tree was topologically congruent with published phylogenies of the Ericaceae as a whole (Kron et al. 2002). The tree was then pruned to 57 species from 12 genera that represent the range of phylogenetic, environmental and physiological diversity of the group.

To generate trait data, we collected leaves of the 57 Ericaceae species represented on the pruned phylogeny from herbarium specimens at the Liberty Hyde Bailey Hortorium (Cornell University) in August, 2015. The 57 species were geographically widespread across North America (Figure 1). Leaf material (5 – 50 leaves, depending on leaf size) was sampled from four vouchers per species from a range of habitats and geographic locations. Each leaf was assessed for leaf longevity (deciduous, evergreen), leaf surface characteristics (glabrous, hairy), leaf size, percent element (%C, %N), C:N, and isotopic ratio ($\delta^{13}C$, $\delta^{15}N$). Isotope ratios and percent element of all samples were measured using a continuous flow isotope ratio mass spectrometer (Thermo Finnigan Environmental Delta V) coupled to an elemental analyzer (Thermo Finnigan Carlo Erba NC2500). Isotope ratios are expressed as δ values (per mil):

$\delta^{15}N$ or $\delta^{13}C = (R_{sample}/R_{standard} - 1) \times 1000$ (‰)

where R_{sample} and $R_{standard}$ are the ratios of heavy to light isotope of the sample relative to the international standards for C and N, Vienna-Pee-Dee Belemnite and atmospheric N_2, respectively. To account for atmospheric CO_2 source changes in $\delta^{13}C$ over the sampling time period (1895-2015), we adjusted leaf $\delta^{13}C$ values accordingly. Atmospheric CO_2-$\delta^{13}C$ isotope values from 1890-1970 were taken from Zachos et al. (2007) and values from 1970 to 2015 were obtained online from the Scripps CO_2 Program (http://scrippsco2.ucsd.edu, Mauna Loa Observatory, Hawaii). Using -8‰ as a baseline, we calculated the difference between the baseline and atmospheric CO_2-$\delta^{13}C$ during the collection year for each herbarium specimen.

We classified each species by mycorrhizal type using information from published floras and primary literature. Each species is reported to identify with one of three mycorrhizal types: arbutoid, ericoid or monotropoid mycorrhizae (Lallemand *et al.*, 2016). Arbutoid and monotropoid mycorrhizal fungi are similar to ectomycorrhizal fungi (Smith and Read 2008a), while ericoid mycorrhizal fungi are similar to arbuscular/endomycorrhizal fungi (Smith and Read 2008b).

We used vapor pressure deficit (VPD) as a general description of a plant's average environment in terms of temperature and water availability. VPD determines the difference between the amount of moisture in the air and the amount of moisture that the air can hold, which in turn drives water loss from plant leaves. This difference is temperature-dependent, as warmer air can hold more water than colder air. Thus, variation in VPD affects stomatal behavior and leaf gas exchange (Oren et al. 1999), and potentially C isotope discrimination (Bowling et al. 2002). Given that leaf $\delta^{15}N$ values vary with mean annual precipitation and temperature (Amundson et al. 2003), VPD also, at least indirectly, influences leaf $\delta^{15}N$ values (Craine et al.

2015). We calculated the average July VPD for each origin environment, as indicated from specimen voucher labels. We generated this dataset using long-term (1974 – 2012) July average air temperature and dew point values obtained from weather stations closest to the collection locations (National Weather Service, www.weather.gov).

In addition to the average climate environment represented by VPD, we also independently examined species within five specialized environments where either soil type (e.g., sand) or water inundation (e.g., wetlands) was likely to uncouple physiology from the local VPD environment. Using habitat descriptions from herbarium voucher labels in combination with ecological information from published floras, we identified species in our dataset that occupy peatlands, riparian zones, rock barrens, sandy soils, and swamps. Peatlands are acidic, nutrient poor wetlands common in arctic, boreal and temperate regions. Swamps and riparian zones are distributed throughout North America, and many of the species in our dataset were from swamps and riparian zones in the southern United States. Rock barrens are nutrient poor environments characterized by open rock overlain by patches of shallow organic soil and are restricted to artic and alpine tundra, particularly in coastal regions of eastern Canada. Ericaceae in sandy soils are from California chaparral, sand scrub of the southeastern US, and pine barrens of the Atlantic coast and northern Rocky Mountains (Tucker 2009).

To assess the degree to which closely related species are more similar to one another than expected by chance, we calculated phylogenetic signal using Pagel's λ for continuous ($\delta^{15}N$, $\delta^{13}C$, %C, %N, C:N, leaf size, VPD) and categorical variables (longevity, surface characteristics, mycorrhizal type, specialized environments). Pagel's λ is a branch scaling parameter, where $\lambda = 1$ indicates that the trait distribution scales with tree topology in accordance with Brownian motion. $\lambda = 0$ indicates that the tree topology does not structure trait variation (Pagel 1999;

Münkemüller et al. 2012). We tested whether λ was > 0 by comparing the log-likelihood of the fitted λ with that of λ = 0 using a log-likelihood ratio test using the 'phylosig' function in the phytools R package (Revell 2012). Variables with λ > 0.5 (at α = 0.05) have phylogenetic signal (*i.e.*, relatives are more similar to each other than expected by random chance) (Pagel 1999; Münkemüller et al. 2012).

To compare isotopic, phylogenetic, and environmental (VPD) similarity among species, we calculated the absolute difference in isotope values and VPD and the phylogenetic distance among all pair-wise species comparisons. Absolute differences were converted into similarities by subtracting absolute differences from one (S = 1 - D). We evaluated relationships between phylogenetic, isotopic and environmental (VPD) similarity using linear regression. All analyses were performed in R3.2.4 (R Core Team 2019)

Results

Phylogenetic signal was observed in $\delta^{15}N$ and $\delta^{13}C$, %C, leaf longevity (deciduous, evergreen), hairy leaves and mycorrhizal type, but not in %N, C:N, VPD, leaf size, or glabrous leaves (Table 4.1). Similarity in $\delta^{15}N$ and $\delta^{13}C$ increased with phylogenetic similarity and explained 32% and 20% of the total variation in these traits, respectively ($P < 0.0001$, Figure 4.1a, b). Similarity in $\delta^{13}C$ and $\delta^{15}N$ was also related to similarity in VPD, but these relationships explained less than 1% of the total variation ($P < 0.02$, Fig. 1c, d).

Species within each specialized environment were isotopically similar to other species from that environment (Table 4.2). Species from rock barrens and sandy soils tended to be more closely related to each other ($\lambda = 0.77$ and 0.88, respectively) while species from peatlands, riparian zones and swamps were more distantly related ($\lambda = 0.38$, <0.01 and <0.01, respectively).

$\delta^{13}C$ and $\delta^{15}N$ varied in relation to the type of mycorrhizal association (Figure 4.2). Individuals with Monotropoid mycorrhizae displayed the most enriched $\delta^{13}C$ and $\delta^{15}N$ values, followed by Arbutoid and Ericoid.

Table 4.1: Phylogenetic signal using Pagel's λ of 10 leaf characteristics, average July vapor pressure deficits and mycorrhizal type (Arbutoid, Ericoid, Monotropoid) for 57 Ericaceae species (n = 225). Phylogenetic signal is significant at Pagel's $\lambda > 0.5$ ($\alpha = 0.05$), indicating variables that are more similar among close relatives than expected by chance.

Variable	Pagel's λ
$\delta^{13}C$	**0.80**
$\delta^{15}N$	**0.92**
%C	**0.75**
%N	< 0.01
C:N ratio	< 0.01
Leaf size	< 0.01
Leaf longevity	**0.95**
Hairy leaves	**0.70**
Glabrous leaves	< 0.01
Mycorrhizal type	**0.95**
Vapor pressure deficit	< 0.01

Table 4.2: Phylogenetic signal and isotopic similarity among Ericaceae plants from specialized environments. Pagel's $\lambda > 0.5$ indicates phylogenetic signal. Isotopic similarity ranges from 0 to 1, with 1 being completely similar and 0 being completely different. The number of individuals from each environment is indicated in parentheses.

Environment	**Pagel's λ**	**$\delta^{13}C$ Similarity**	**$\delta^{15}N$ Similarity**
Peatlands *(n = 26)*	< 0.01	0.76	0.78
Riparian *(n = 26)*	0.38	0.74	0.70
Rock barrens *(n = 51)*	**0.77**	0.74	0.75
Sandy soils *(n = 40)*	**0.88**	0.75	0.75
Swamps *(n = 15)*	< 0.01	0.79	0.62

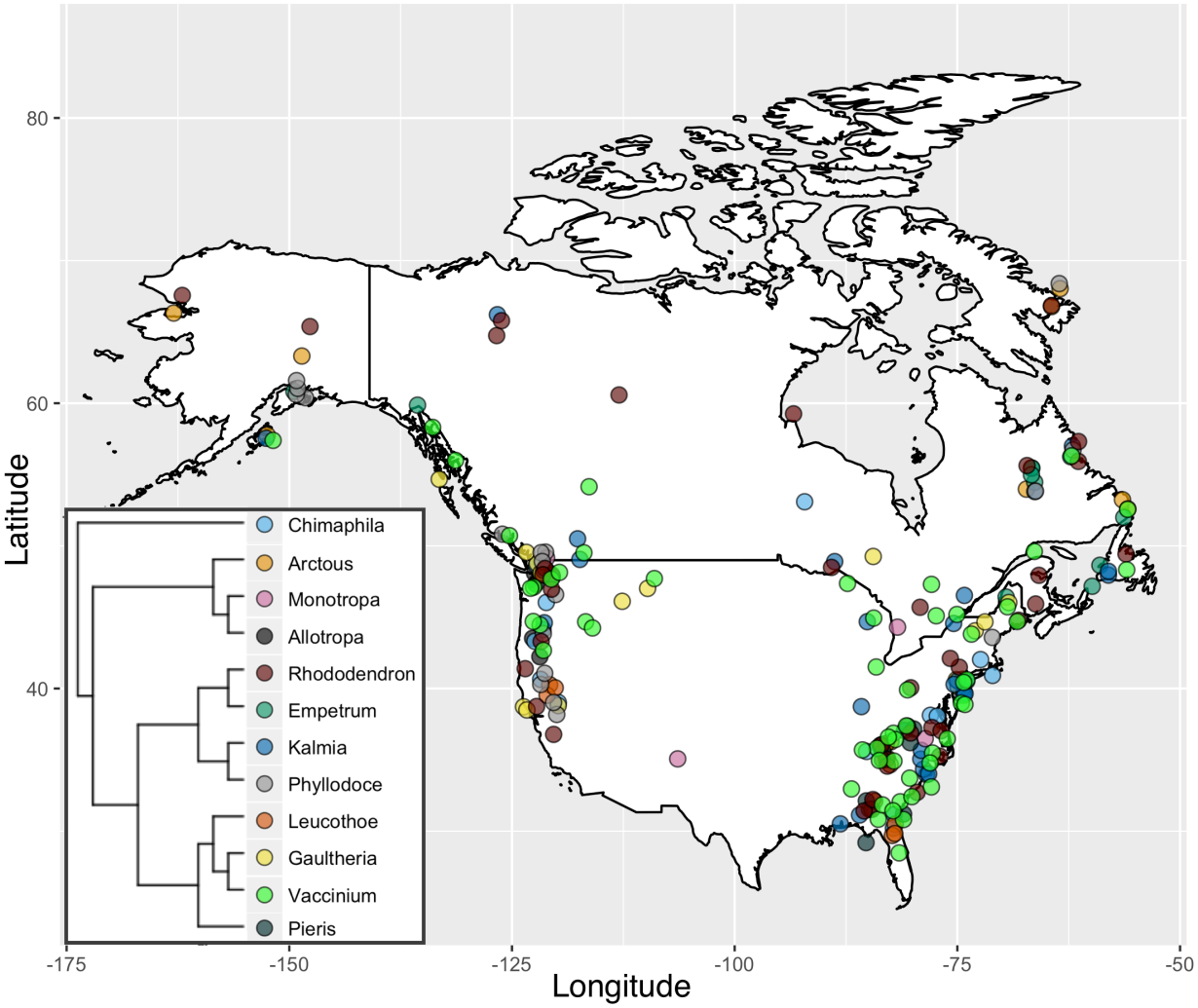

Figure 4.1 Geographic locations of herbarium specimen collection sites across North America for 57 Ericaceae species (n=225). The legend shows phylogenetic relationships among the 12 genera represented in this study. The phylogeny was constructed by maximum likelihood analyses using sequence data from mat*K*, *nr*ITS and rbcL gene regions from GenBank. This figure is available in color in the online version.

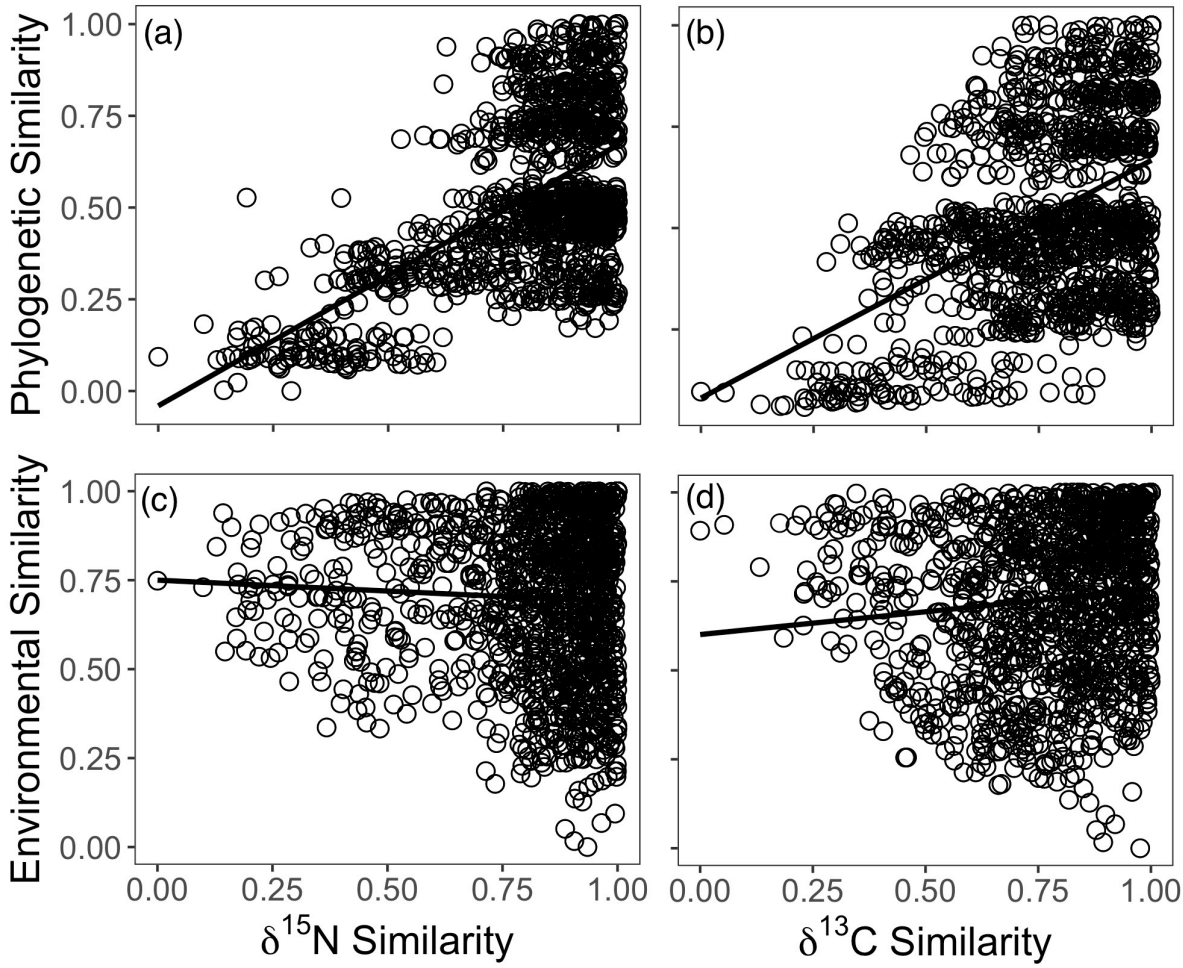

Figure 4.2 Relationships between (a) phylogenetic similarity and similarity in leaf $\delta^{15}N$ (r^2=0.32, $P < 0.0001$), (b) phylogenetic similarity and similarity in leaf $\delta^{13}C$ (r^2=0.20, $P < 0.0001$), (c) environmental similarity and similarity in leaf $\delta^{15}N$ (r^2=0.002, $P = 0.02$), and (d) environmental similarity and similarity in leaf $\delta^{13}C$ (r^2=0.01, $P < 0.0001$) for 57 Ericaceae species (n = 225). Phylogenetic similarity is derived from species pair-wise comparisons of phylogenetic branch lengths. Environmental similarity is derived from species pair-wise comparisons of average July vapor pressure deficits. Similarities range from 0 to 1, with 1 being completely similar and 0 being completely different.

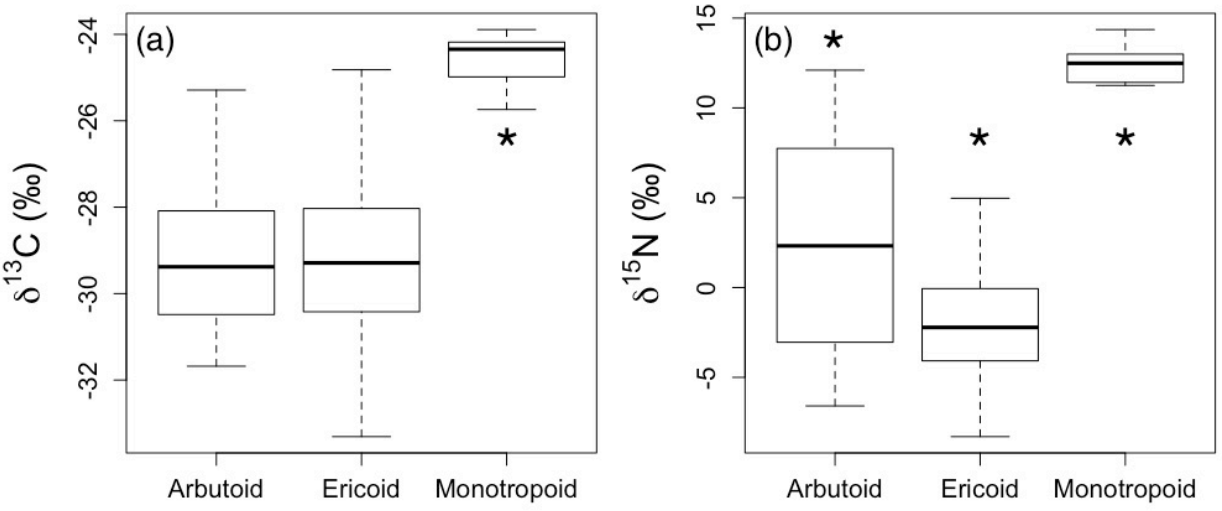

Figure 4.3 Results of a one-way analysis of variance between leaf (a) $\delta^{13}C$ and (b) $\delta^{15}N$ and three mycorrhizal associations (Arbutoid, Ericoid, Monotropoid) for 57 Ericaceae species (n = 225). Asterisks indicate significant differences among mycorrhizal types ($P < 0.0001$).

Discussion

We present evidence that physiological strategies related to C and N acquisition in the North American Ericaceae are strongly influenced by evolutionary history. As integrators of physiological processes, we suggest that isotope ratios may be a more robust predictor relative to commonly measured anatomical leaf characteristics. In support of this hypothesis, leaf $\delta^{13}C$ and $\delta^{15}N$ values exhibited strong phylogenetic signal (Table 4.1), suggesting that close relatives have similar physiological strategies with respect to C and N acquisition and metabolism.

Observing strong phylogenetic signal in isotope ratios does not necessarily preclude a strong relationship between isotope ratios and environment. To this end, we examined the relationship between foliar $\delta^{13}C$ and $\delta^{15}N$ over a range of environmental vapor pressure deficits. Representing a plant's average environment with vapor pressure deficits is a coarse measure of environment, but it is one that has long been shown to drive global patterns of plant diversity (Hutchinson 1918; Sexton et al. 2009). If species living in similar environments have comparable physiology, then similarity in $\delta^{13}C$ and potentially in $\delta^{15}N$ should correlate with similarity in vapor pressure deficits. However, the relationships we observed between $\delta^{13}C$, $\delta^{15}N$ and vapor pressure deficits explained very little variation (Figure 4.2c, d), suggesting that species with similar physiology do not necessarily occupy similar average environments. Surprisingly, the signal of phylogeny on physiological variation among species was much stronger than that of the average environment (Figure 4.2a, b). This combination of strong phylogenetic signal and a weak relationship with environment suggests that closely related species have similar physiological strategies across different environments.

While a coarse-scale environmental variable, VPD, explained a very small amount of variation in physiology, finer-scale microsite conditions could explain a larger portion of the

variation in these traits and processes. For example, a set of species could be pre-adapted to certain conditions and track favorable microclimates across different vapor pressure deficit environments. In this case, close relatives maintain some common suite of characteristics that together contribute to variation and phylogenetic signal in foliar $\delta^{13}C$ and $\delta^{15}N$. To explore this possibility, we independently examined several environments where, because of soil type or constant soil water availability, physiological patterns were less likely to be tightly coupled to the vapor pressure deficit environment. Peatlands, riparian zones, rock barrens, sandy soils and swamps are geographically widespread across North America and Ericaceae species within these environments all had similar $\delta^{13}C$ and $\delta^{15}N$ values relative to each other (Table 4.2), providing some evidence that similar physiological strategies in these species have arisen in response to strong environmental selection. However, the degree of phylogenetic relatedness was not constant across these specialized environments (Table 4.2). Individuals from rock barrens and sandy soils were more closely related than expected by chance (Pagel's $\lambda > 0.75$; Table 4.2). Rock barrens and sandy soils are water-limited environments and may represent examples of 'phylogenetic niche conservatism', whereby species maintain the phenotypes and environmental requirements of their most recent common ancestor (Wiens et al. 2010). In contrast to rock barrens and sandy soils, individuals from peatlands, riparian zones and swamps were physiologically similar but more distantly related than expected by chance (Pagel's $\lambda < 0.5$; Table 4.2); this suggests that plants from these wet habitats are potentially converging onto similar strategies regardless of their phylogenic history.

These patterns diverge from other studies that report phylogenetic similarity among wetland species (Savage and Cavender Bares 2012) and phylogenetic divergence (species less related) among species from drier environments (Savage and Cavender Bares 2012; Jara Arancio

et al. 2014). A possible explanation is that the direction of environmental shift is influencing phylogenetic and phenotypic patterns. Rather than the environmental conditions per se (*i.e.*, arid versus mesic) driving convergence or divergence, the degree of deviation from ancestral conditions may be more important (Klak et al. 2004; Kraft et al. 2007). For example, shifting into a new environment that shares features in common with the ancestral state may not require substantial adjustments or adaptations. However, a new environment that is considerably different from the ancestral state in climate or soil conditions may require novel adaptations and phenotypic divergence over time. The ancestral Ericaceae environment was likely arid and water-limited, so a shift into other water-limited environments, such as rock barrens, may not have required novel adaptations. On the other hand, key innovations for tolerance to water-logged soils may have been necessary to successfully radiate into wetlands. Convergent adaptations may have arisen independently in multiple taxa, resulting in a pattern of phylogenetic diversity and phenotypic similarity in wetlands.

Given that $\delta^{13}C$ integrates multiple aspects of C acquisition in plants, our observation of phylogenetic signal might be driven by similar groupings of traits defined by phylogenetic history. We examined the strength of phylogenetic signal for traits that impact the balance of leaf external and internal CO_2 concentrations (c_i/c_a) and C gain through their effects on CO_2 diffusive resistance or carboxylation. Leaf hair, leaf longevity and leaf C content (%) all had phylogenetic signal (Pagel's $\lambda > 0.5$; Table 4.1) and therefore may be contributing to phylogenetic signal in $\delta^{13}C$. The presence of leaf hair affects the size of the leaf boundary layer and contributes to CO_2 diffusive resistance (Ehleringer et al. 1976; Ehleringer and Mooney 1978; Meinzer and Goldstein 1985), while leaf longevity and C content relate to structural investment and stomatal control (Evans and Loreto 2000). We might also expect leaf size and N content to have an impact on C

gain and potentially contribute to phylogenetic signal because of their effect on photosynthetic efficiency and carboxylation capacity (Wright et al. 2004), but these traits did not have phylogenetic signal (Pagel's $\lambda < 0.01$; Table 4.1). Despite these limitations, integrative measures such as $\delta^{13}C$ appear to have more power than individual anatomical traits in this context because they are integrating multiple factors that influence C gain, including characters that are not often measured.

Much of the variation and phylogenetic signal in leaf $\delta^{15}N$ appears to be related to belowground mutualisms with different mycorrhizal fungi. Mycorrhizal fungi influence the leaf $\delta^{15}N$ values of their host plant both in the amount of N that they supply to the plant and in the isotopic composition of the N itself. The three mycorrhizal types that associate with Ericaceae species are more host specific than typical arbuscular and ectomycorrhizal fungi (Smith and Read 1997; Lallemand et al. 2016). Species with monotropoid mycorrhizae are 'mycoheterotrophic', meaning they are parasitic, do not photosynthesize (*e.g., Monotropa, Allotropa*) and are completely dependent on mycorrhizal fungi for both C and N (Smith and Read 2008a). Mycoheterotrophic species were considerably more enriched in $\delta^{13}C$ and $\delta^{15}N$ values (Figure 3). Strong enrichment in leaf $\delta^{13}C$ and $\delta^{15}N$ in mycoheterotrophic plants relative to other autotrophs is attributed to their dependence on isotopically enriched C and N sources that have been metabolized by mycorrhizal fungi (Tedersoo et al. 2006; Zimmer et al. 2007). Similarly, plants with arbutoid mycorrhizae can be either autotrophic (obtaining C from photosynthesis) or 'mixotrophic', meaning that they photosynthesize but also rely heavily on isotopically enriched C from mycorrhizal fungi sources (*e.g., Pyrola, Chimaphila*). While ericoid and arbutoid mycorrhizae deliver isotopically depleted N from the soil to their host plant, arbutoid mycorrhizae can also exchange isotopically enriched N that is internal to the fungi

rather than from the soil (Tedersoo et al. 2006). Consistent with this, species with arbutoid mycorrhizae in our study were relatively enriched in $\delta^{15}N$, although $\delta^{13}C$ values did not differ between arbutoid and ericoid mycorrhizal types (Figure 4.3). The large spread in $\delta^{15}N$ values for arbutoid mycorrhizae is likely driven by opposing values from those species that use enriched fungal N and other species that use depleted soil N, yet both are classified as associating with arbutoid mycorrhizae (Zimmer et al. 2007).

These large mycorrhizal effects are operating across ecosystems with differential baselines in soil ^{15}N. Variation in the baseline ^{15}N present in the soil solution is influenced in part by climate (*e.g.*, annual precipitation and temperature) and local conditions (*e.g.*, water availability) such that cold and/or wet sites are generally more depleted in $\delta^{15}N$ relative to warm and/or dry sites. These ecosystem differences would be reflected in the $\delta^{15}N$ of plant leaves (Hobbie et al. 2000; Kahmen et al. 2008; Craine et al. 2009; Craine et al. 2015). The baseline soil ^{15}N, and consequently leaf $\delta^{15}N$, are also influenced by soil N turnover rates, which can depend on rates of root N uptake, leaf N turnover and litter decomposition. Phylogenetic signal in leaf $\delta^{15}N$ may, therefore, be related to groupings of traits associated with root N uptake and leaf N turnover. The effects of root N uptake rates in Ericaceae are likely to be predominantly reflected in the mycorrhizal effects discussed above. Leaf traits related to leaf N turnover include leaf longevity and C:N. Evergreen leaves and leaves with large C content and/or large C:N generally have slower rates of nutrient turnover and can be relatively depleted in $\delta^{15}N$ values compared to deciduous leaves and leaves with less C content (Amundson et al. 2003). We found phylogenetic signal in leaf longevity and C content but not in C:N. Although leaf longevity and C content may contribute to $\delta^{15}N$ phylogenetic signal, their influence is smaller than the primary mycorrhizal effects

This is the first study to assess patterns of leaf C and N stable isotopes from a phylogenetic perspective. We found significant phylogenetic signal in leaf $\delta^{13}C$ and $\delta^{15}N$, which shows that shared ancestry is an important driver of functional diversity in the North American Ericaceae. Moreover, we demonstrated that the signal of phylogeny is stronger than that of the average, coarse-scale environment, although environmental selection and phylogenetic niche conservatism may be important at finer spatial scales. We recommend the use of stable isotopes in future studies to better represent physiology. Defining and measuring the physical environment in a more consistent way across systems will aid in identifying the underlying mechanisms that structure functional diversity.

Literature Cited

Amundson R, Austin AT, Schuur EAG, et al (2003) Global patterns of the isotopic composition of soil and plant nitrogen. Global Biogeochem Cycles. doi: 10.1029/2002GB001903

Bhaskar R, Porder S, Balvanera P, Edwards EJ (2016) Ecological and evolutionary variation in community nitrogen use traits during tropical dry forest secondary succession. Ecology 97:1194–1206. doi: 10.1890/15-1162.1

Bowling DR, McDowell NG, Bond BJ, et al (2002) 13C content of ecosystem respiration is linked to precipitation and vapor pressure deficit. Oecologia 131:113–124. doi: 10.1007/s00442-001-0851-y

Craine JM, Elmore AJ, Aidar MPM, et al (2009) Global patterns of foliar nitrogen isotopes and their relationships with climate, mycorrhizal fungi, foliar nutrient concentrations, and nitrogen availability. New Phytologist 183:980–992. doi: 10.1111/j.1469-8137.2009.02917.x

Craine JM, Elmore AJ, Wang L, et al (2015) Convergence of soil nitrogen isotopes across global climate gradients. Nature Publishing Group 5:889. doi: 10.1038/srep08280

Ehleringer J, Bjorkman O, Mooney HA (1976) Leaf Pubescence: Effects on Absorptance and Photosynthesis in a Desert Shrub. Science 192:376–377. doi: 10.1126/science.192.4237.376

Ehleringer JR, Mooney HA (1978) Leaf hairs: Effects on physiological activity and adaptive value to a desert shrub. Oecologia 37:183–200. doi: 10.1007/BF00344990

Ehleringer JR, Phillips SL, Comstock JP (1992) Seasonal Variation in the Carbon Isotopic Composition of Desert Plants. Funct Ecol 6:396. doi: 10.2307/2389277

Evans JR, Loreto F (2000) Acquisition and Diffusion of CO2 in Higher Plant Leaves. In: Photosynthesis. Springer Netherlands, Dordrecht, pp 321–351

Farquhar GD, O'Leary MHO, Berry JA (1982) On the relationship between carbon isotope discrimination and the intercellular carbon dioxide concentration in leaves. Aust J Plant Physio 9:121–137. doi: 10.1071/pp9820121

Flores O, Garnier E, Wright IJ, et al (2014) An evolutionary perspective on leaf economics: phylogenetics of leaf mass per area in vascular plants. Ecol Evol 4:2799–2811. doi: 10.1002/ece3.1087

Forrestel EJ, Ackerly DD, Emery NC (2015) The joint evolution of traits and habitat: ontogenetic shifts in leaf morphology and wetland specialization in Lasthenia. New Phytologist 208:949–959. doi: 10.1111/nph.13478

Friend AD, Woodward FI, Switsur VR (1989) Field Measurements of Photosynthesis, Stomatal Conductance, Leaf Nitrogen and δ 13 C Along Altitudinal Gradients in Scotland. Funct Ecol 3:117. doi: 10.2307/2389682

Hobbie EA, Colpaert JV (2004) Nitrogen availability and mycorrhizal colonization influence water use efficiency and carbon isotope patterns in Pinus sylvestris. New Phytologist 164:515–525. doi: 10.1111/j.1469-8137.2004.01187.x

Hobbie EA, Macko SA, Shugart HH (1999) Insights into nitrogen and carbon dynamics of ectomycorrhizal and saprotrophic fungi from isotopic evidence. Oecologia 118:353–360. doi: 10.1007/s004420050736

Hobbie EA, Macko SA, Williams M (2000) Correlations between foliar δ15N and nitrogen concentrations may indicate plant-mycorrhizal interactions. Oecologia 122:273–283. doi: 10.1007/PL00008856

Hobbie JE, Hobbie EA (2006) 15N in symbiotic fungi and plants estimates in nitrogen and carbon flux rates in arctic tundra. Ecology 87:816–822. doi: 10.1890/0012-9658(2006)87[816:NISFAP]2.0.CO;2

Hutchinson AH (1918) Limiting Factors in Relation to Specific Ranges of Tolerance of Forest Trees. Botanical Gazette 66:465–493. doi: 10.2307/2469415?ref=search-gateway:8da8808daa51d10418940208b207d17a

Jara Arancio P, Arroyo MTK, Guerrero PC, et al (2014) Phylogenetic perspectives on biome shifts in Leucocoryne (Alliaceae) in relation to climatic niche evolution in western South America. Journal of Biogeography 41:328–338. doi: 10.1111/jbi.12186

Kahmen A, Wanek W, Buchmann N (2008) Foliar δ15N values characterize soil N cycling and reflect nitrate or ammonium preference of plants along a temperate grassland gradient. Oecologia 156:861–870. doi: 10.1007/s00442-008-1028-8

Kerkhoff AJ, Fagan WF, Elser JJ, Enquist BJ (2006) Phylogenetic and Growth Form Variation in the Scaling of Nitrogen and Phosphorus in the Seed Plants. Am Nat. doi: 10.1086/507879?ref=search-gateway:8b9bfcc18447661e3cfc4b9f8f1a8aaf

Klak C, Reeves G, Hedderson T (2004) Unmatched tempo of evolution in Southern African semi-desert ice plants. Nature 427:63–65. doi: 10.1038/nature02243

Kolb KJ, Evans RD (2002) Implications of leaf nitrogen recycling on the nitrogen isotope composition of deciduous plant tissues. New Phytol 156:57–64. doi: 10.1046/j.1469-8137.2002.00490.x

Kraft NJB, Cornwell WK, Webb CO, Ackerly DD (2007) Trait evolution, community assembly, and the phylogenetic structure of ecological communities. Am Nat 170:271–283. doi: 10.1086/519400

Kron KA, Judd WS, Stevens PF, Crayn DM (2002) Phylogenetic classification of Ericaceae: molecular and morphological evidence. The Botanical … 68:335–423.

Lallemand F, Gaudeul M, Lambourdière J, et al (2016) The elusive predisposition to mycoheterotrophy in Ericaceae. New Phytologist 212:314–319. doi: 10.1111/nph.14092

Liu H, Xu Q, He P, et al (2015) Strong phylogenetic signals and phylogenetic niche conservatism in ecophysiological traits across divergent lineages of Magnoliaceae. Nature Publishing Group 1–12. doi: 10.1038/srep12246

Meinzer F, Goldstein G (1985) Some Consequences of Leaf Pubescence in the Andean Giant Rosette Plant Espeletia Timotensis. Ecology 66:512–520. doi: 10.2307/1940399

Münkemüller T, Lavergne S, Bzeznik B, et al (2012) How to measure and test phylogenetic signal. Methods in Ecology and Evolution 3:743–756. doi: 10.1111/j.2041-210X.2012.00196.x

Oren R, Sperry JS, Katul GG, et al (1999) Survey and synthesis of intra- and interspecific variation in stomatal sensitivity to vapour pressure deficit. plant, cell and environment

22:1515–1526. doi: 10.1046/j.1365-3040.1999.00513.x

Osnas JLD, Lichstein JW, Reich PB, Pacala SW (2013) Global leaf trait relationships: mass, area, and the leaf economics spectrum. Science 340:741–744. doi: 10.1126/science.1231574

Pagel M (1999) Inferring the historical patterns of biological evolution. Nature 401:877–884. doi: 10.1038/44766

Revell LJ (2012) phytools: an R package for phylogenetic comparative biology (and other things). Methods in Ecology and Evolution 3:217–223. doi: 10.1111/j.2041-210X.2011.00169.x

Savage JA, Cavender Bares J (2012) Habitat specialization and the role of trait lability in structuring diverse willow (genus Salix) communities.

Sexton JP, McIntyre PJ, Angert AL, Rice KJ (2009) Evolution and ecology of species range limits. Annual Review of Ecology, Evolution, and Systematics 40:415–436. doi: 10.1146/annurev.ecolsys.110308.120317

Smith SE, Read D (2008a) Mycorrhizas in achlorophyllous plants (mycoheterotrophs). In: Mycorrhizal Symbiosis (Third Edition). Academic Press, London, pp 458–XV

Smith SE, Read D (2008b) Ericoid mycorrhizas. In: Mycorrhizal Symbiosis (Third Edition). Academic Press, London, pp 389–418

Smith SE, Read DJ (1997) Mycorrhizal symbiosis. Mycorrhizal symbiosis

Swofford DL (2002) PAUP*. Phylogenetic Analysis Using Parsimony (*and Other Methods). Sinauer Associates, Sunderland, Massachusetts

Tedersoo L, Pellet P, Kõljalg U, Selosse M-A (2006) Parallel evolutionary paths to mycoheterotrophy in understorey Ericaceae and Orchidaceae: ecological evidence for mixotrophy in Pyroleae. Oecologia 151:206–217. doi: 10.1007/s00442-006-0581-2

Tucker GC (2009) Ericaceae. In: Flora of North America North of Mexico. New York and Oxford, pp 364–504

Wiens JJ, Ackerly DD, Allen AP, et al (2010) Niche conservatism as an emerging principle in ecology and conservation biology. Ecol Letters 13:1310–1324. doi: 10.1111/j.1461-0248.2010.01515.x

Wright IJ, Reich PB, Westoby M, et al (2004) The worldwide leaf economics spectrum. Nature 428:821–827. doi: 10.1038/nature02403

Yang J, Zhang G, Ci X, et al (2014) Functional and phylogenetic assembly in a Chinese tropical tree community across size classes, spatial scales and habitats. Funct Ecol 28:520–529. doi: 10.1111/1365-2435.12176

Yoneyama T, Omata T, Nakata S, Yazaki J (1991) Fractionation of Nitrogen Isotopes during the Uptake and Assimilation of Ammonia by Plants. Plant and Cell Physiology 32:1211–1217. doi: 10.1093/oxfordjournals.pcp.a078199

Zachos, J. C., S. M. Bohaty, C. M. John, H. McCarren, D. C. Kelly, and T. Nielsen (2007) The Palaeocene–Eocene carbon isotope excursion: constraints from individual shell planktonic foraminifer records. Philosophical Transactions of the Royal Society of London A: Mathematical, Physical and Engineering Sciences 365. The Royal Society: 1829–1842. doi:10.1098/rsta.2007.2045.

Zimmer K, Hynson NA, Gebauer G, et al (2007) Wide geographical and ecological distribution of nitrogen and carbon gains from fungi in pyroloids and monotropoids (Ericaceae) and in orchids. New Phytologist 175:166–175. doi: 10.1111/j.1469-8137.2007.02065.x

APPENDIX

Appendix 1.1

Table A1.1: Average leaf cellulose $\delta^{13}C$ and $\Delta^{18}O$, and associated integrated metabolic strategy (IMS) for ten Mediterranean plant species. Data are species' means and microhabitat means with standard error in parentheses from Moreno-Gutierrez *et al.* 2012. Asterisks indicate significant differences between mesic and xeric microhabitats determined by one-way analysis of variance. * $p < 0.05$, ** $p < 0.01$.

Species	**Microhabitat**	**$\delta^{13}C$**	**$\Delta^{18}O$**	**IMS**
Anthyllis cytisoides	Xeric	-26.5	42.5	0.46
Chaemaerops humilis	Mesic	-23.0	45.0	0.42
Helianthemum syriacum	Xeric	-28.5	39.0	0.47
Nerium oleander	Mesic	-25.5	43.0	0.45
Olea europaea	Mesic	-22.0	47.7	0.42
Pinus halepensis	Mesic	-21.7	43.9	0.39
Pistacia lentiscus	Mesic	-23.0	47.8	0.44
Rhamnus lycioides	Mesic	-24.0	42.0	0.41
Rosmarinus officinalis	Xeric	-26.2	40.5	0.44
Stipa tenacissima	Mesic	-25.0	39.5	0.41
	Mesic average	-23.5 (0.55)**	44.1 (1.14)	0.42 (0.01)*
	Xeric average	-27.1 (0.72)	40.7 (1.01)	0.46 (0.01)

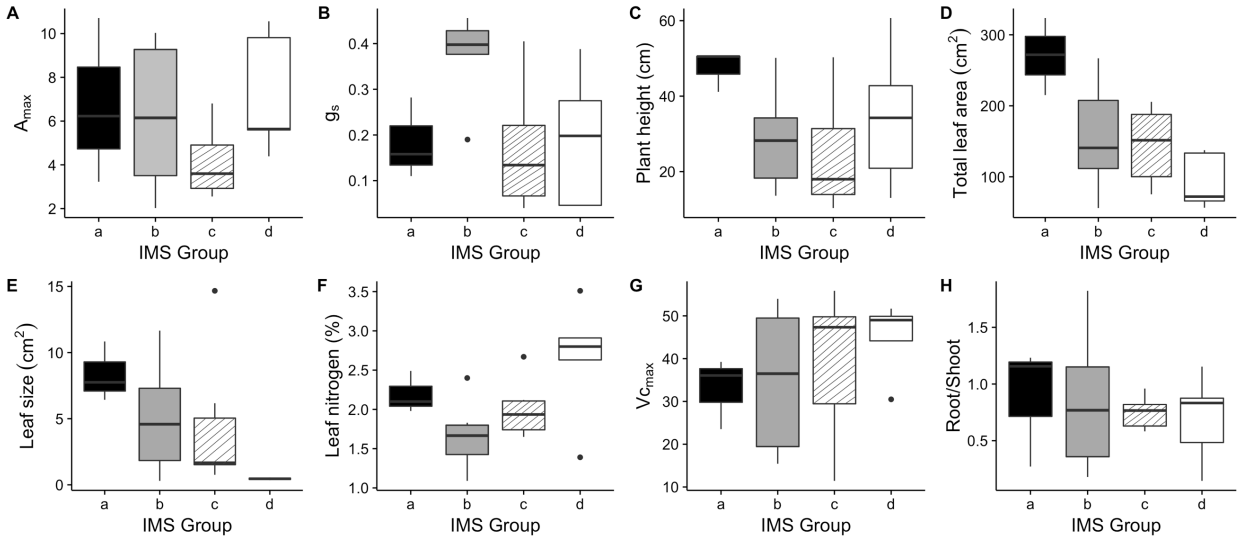

Figure A1.1: Summary of leaf-level and whole-plant traits across 20 *Asclepias* taxa grown under common conditions, grouped by IMS (see Figure 4B for species identities); A) maximum rate of photosynthesis (A_{max}), B) stomatal conductance (g_s), C) plant height, D) total leaf area, E) leaf size, F) leaf nitrogen content root/shoot, G) maximum rate of carboxylation (Vc_{max}), and H) root/shoot. Data are means ± standard error (n=6).

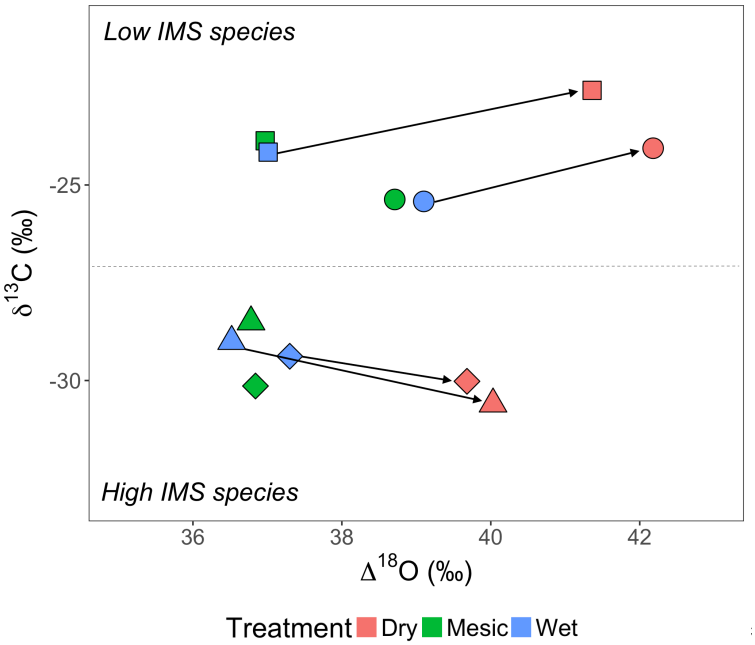

Figure A1.2: Relationships between $\delta^{13}C$ and $\Delta^{18}O$ of leaf cellulose for *A. curassavica* (circles), *A. incarnata* (squares), *A. pumila* (diamonds) and *A. verticillata* (triangles) grown under three different soil water treatments: dry (one-third field capacity), mesic (field capacity), and wet (twice field capacity). Data are means based on six replicates. Arrows indicate the direction of change in $\delta^{13}C$ and $\Delta^{18}O$ between wet and dry treatments.

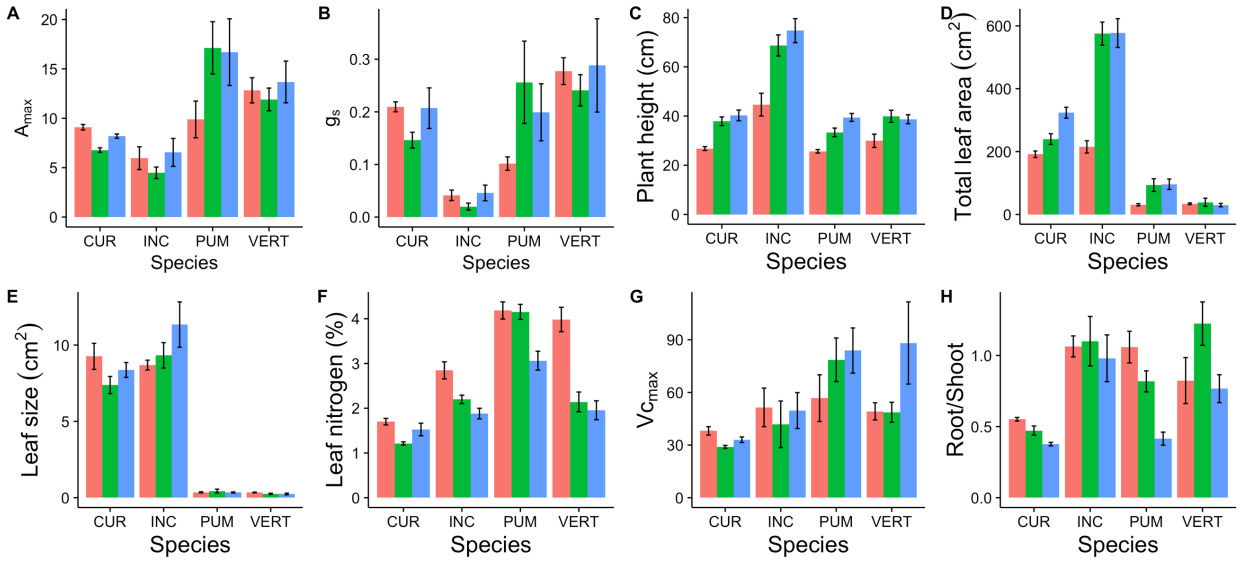

Figure A1.3: Summary of leaf-level and whole-plant traits across four *Asclepias* taxa grown under three soil water treatments: dry (red, one-third field capacity), mesic (green, field capacity), and wet (blue, twice field capacity). A) maximum rate of photosynthesis (A_{max}), B) stomatal conductance (g_s), C) plant height, D) total leaf area, E) leaf size, F) leaf nitrogen content root/shoot, G) maximum rate of carboxylation (Vc_{max}), and H) root/shoot. Data are means ± standard error (n=6).

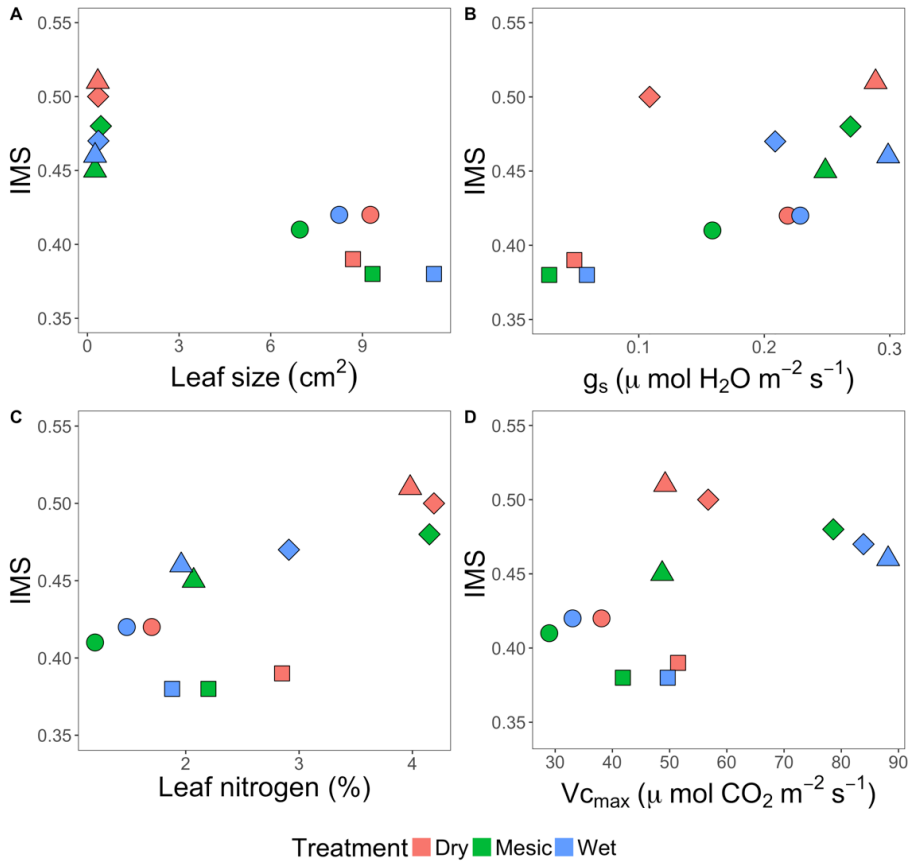

Figure A1.4: Relationships between integrated metabolic strategy (IMS) and A) leaf size, B) stomatal conductance (g_s), C) leaf nitrogen content and D) maximum carboxylation rate (Vc_{max}) for *A. curassavica* (circles), *A. incarnata* (squares), *A. pumila* (diamonds) and *A. verticillata* (triangles) grown under three different soil water treatments: dry (one-third field capacity), mesic (field capacity), and wet (twice field capacity). Data are species means (n=6).

Appendix 2.1

Table A2.1: Pearson correlations between the change in abundance (% cover) between two growing seasons (2017, 2018) and integrated metabolic strategy (IMS) values, leaf carbon isotope ($\delta^{13}C$), and oxygen isotope above source water ($\Delta^{18}O$) obtained from bulk leaf material and leaf cellulose of 18 old field plant species. Additional variables include plant height, leaf nitrogen content (N), and plant source water $\delta^{18}O$. * $p < 0.05$, ** $p < 0.01$, *** $p < 0.0001$.

	Change in abundance	Bulk leaf IMS	Cellulose IMS	Bulk leaf slope	Cellulose slope	Bulk leaf $\delta^{13}C$	Cellulose $\delta^{13}C$	Bulk leaf $\Delta^{18}O$	Cellulose $\Delta^{18}O$	Height	Leaf N
Bulk leaf IMS	-0.42***										
Cellulose IMS	-0.39**	0.74***									
Bulk leaf slope	-0.33**	0.01	-0.05								
Cellulose slope	-0.16	0.26*	0.25*	0.16							
Bulk leaf $\delta^{13}C$	0.47***	-0.86***	-0.79***	0.10	-0.33***						
Cellulose $\delta^{13}C$	0.45***	-0.77***	-0.9***	0.09	-0.27*	0.89***					
Bulk leaf $\Delta^{18}O$	0.43**	-0.36**	-0.45***	0.22	-0.25*	0.73***	0.61***				
Cellulose $\Delta^{18}O$	0.36*	-0.17	0.22*	0.09	-0.05	0.34***	0.58***	0.41***			
Height	-0.24*	-0.01	0.02	0.22	0.08	0.04	0.05	0.06	0.15		
Leaf N	0.06	-0.02	0.1	-0.25*	0.27*	-0.16*	-0.20*	-0.34**	-0.26*	-0.18	
Source water $\delta^{18}O$	-0.02	0.08	0.01	0.02	0.24	-0.12*	-0.17*	-0.11	-0.27*	-0.25*	0.07

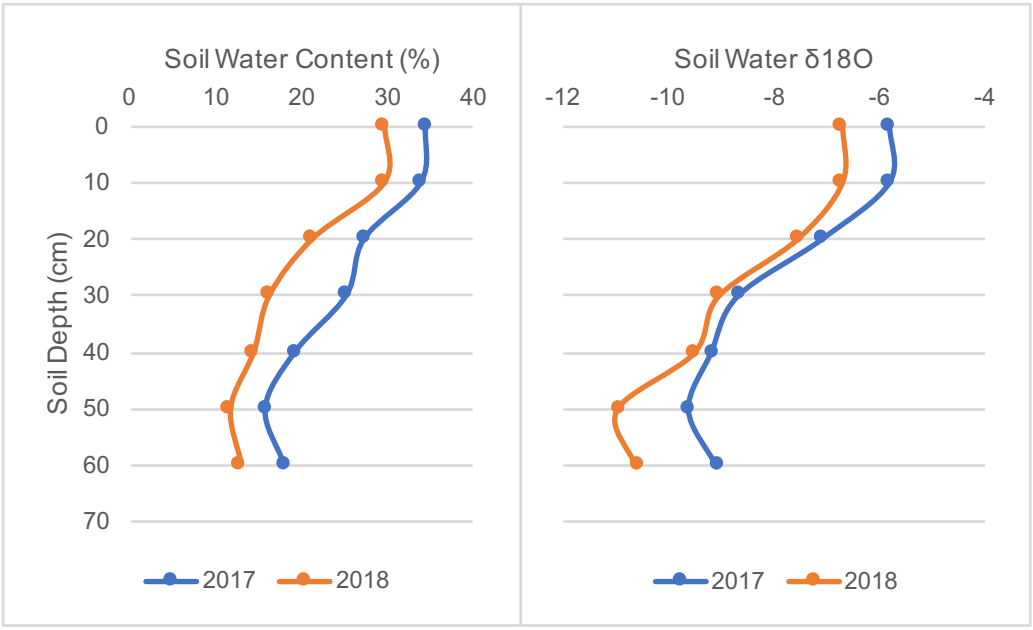

Figure A2.1: Patterns of soil water content (%) and soil water $\delta^{18}O$ (‰) with depth across two growing seasons, 2017 and 2018, in a successional old field in Ithaca, NY. Data are plot means (n=5 per plot, per year).

Appendix 3.1

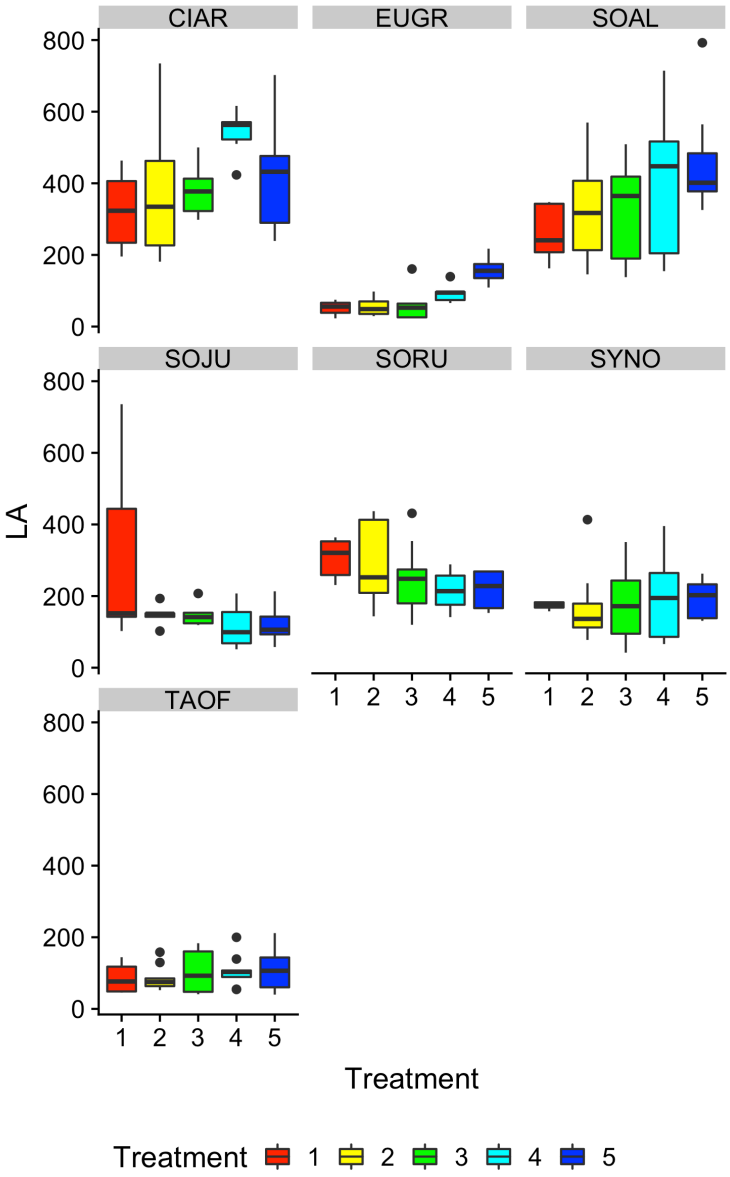

Figure A3.1: Changes in leaf area (LA, cm^2) across five experimental water treatments that span a gradient from the driest ('treatment 1') to the wettest ('treatment 5') year on record from the last 30 years in Ithaca, NY. Data are species means ± standard error for seven co-occurring Asteraceae species (n = 9 per species, per treatment). Species abbreviations are the first two letters of the genus and species epithet given in *Materials and Methods*.

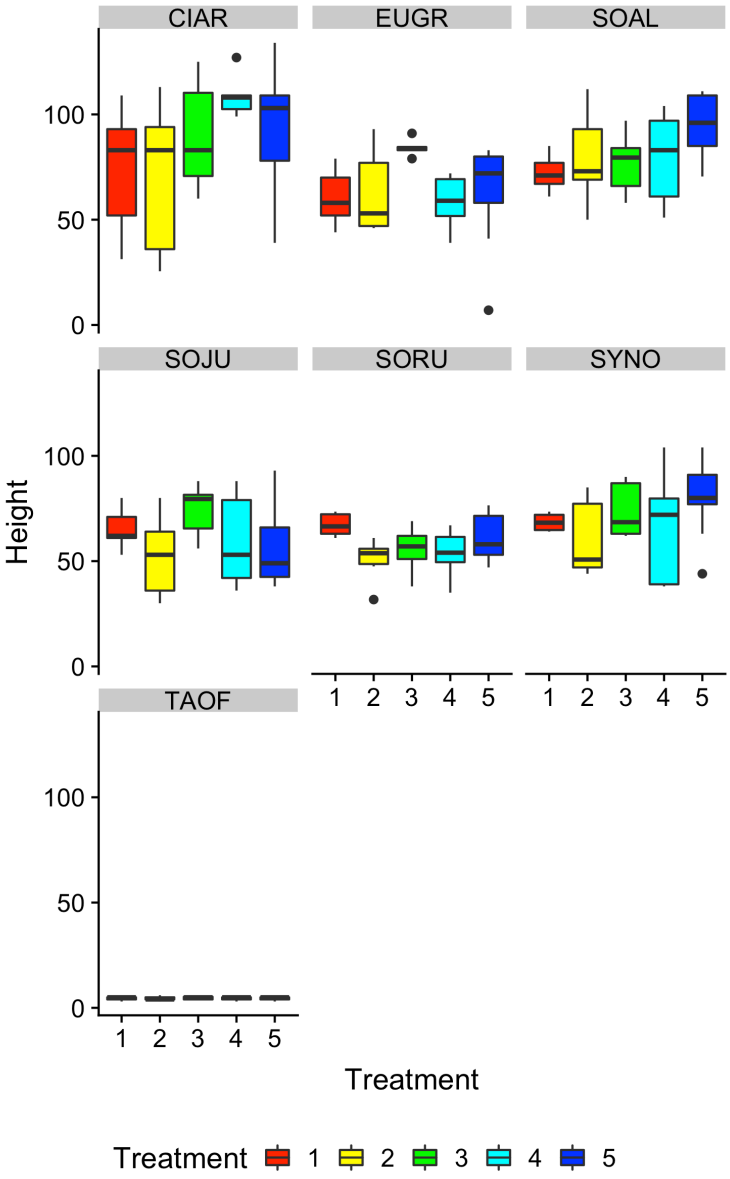

Figure A3.2: Changes in plant height (cm) across five experimental water treatments that span a gradient from the driest ('treatment 1') to the wettest ('treatment 5') year on record from the last 30 years in Ithaca, NY. Data are species means ± standard error for seven co-occurring Asteraceae species (n = 9 per species, per treatment). Species abbreviations are the first two letters of the genus and species epithet given in *Materials and Methods*.

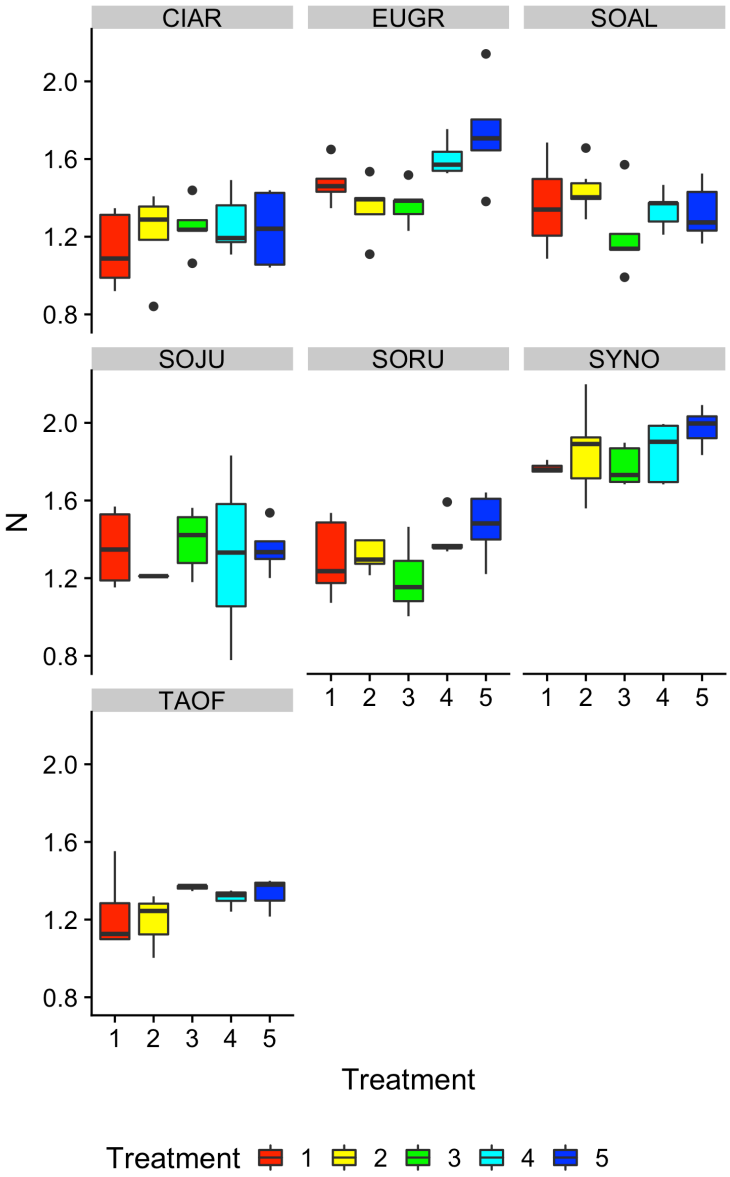

Figure A3.3: Changes in leaf nitrogen content (N, %) across five experimental water treatments that span a gradient from the driest ('treatment 1') to the wettest ('treatment 5') year on record from the last 30 years in Ithaca, NY. Data are species means ± standard error for seven co-occurring Asteraceae species (n = 9 per species, per treatment). Species abbreviations are the first two letters of the genus and species epithet given in *Materials and Methods*.

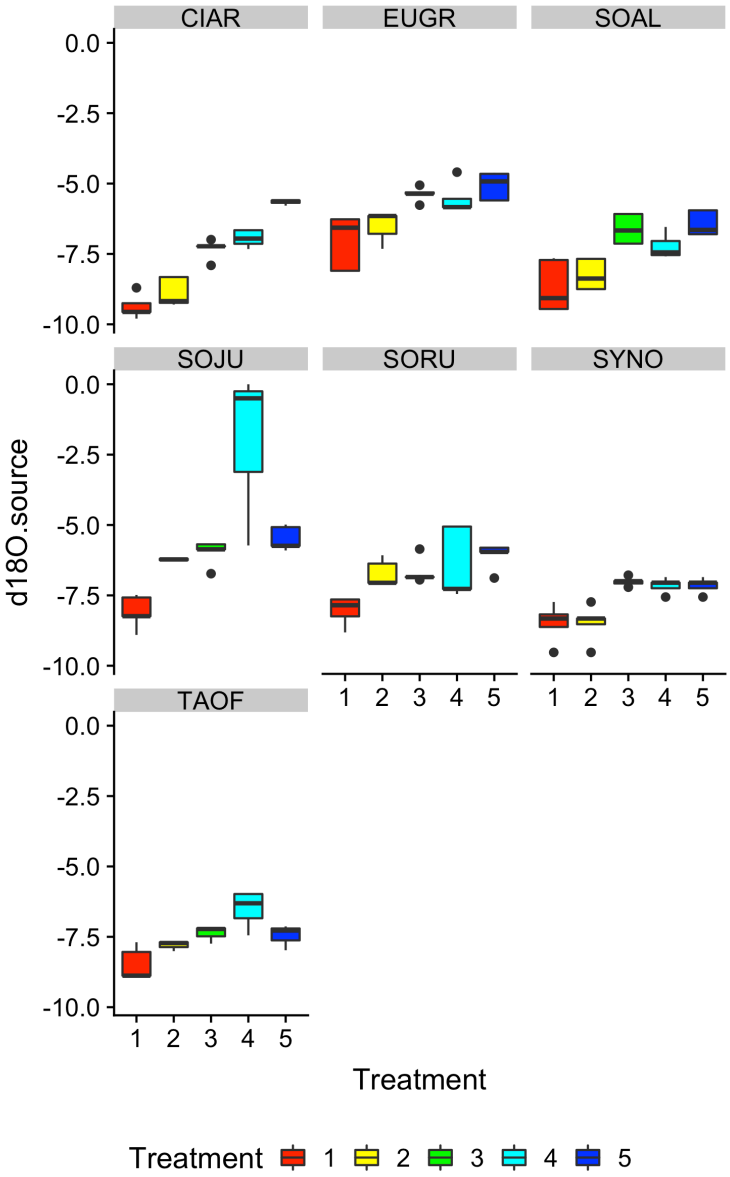

Figure A3.4: Changes in plant source water oxygen isotope composition ($\delta^{18}O$) across five experimental water treatments that span a gradient from the driest ('treatment 1') to the wettest ('treatment 5') year on record from the last 30 years in Ithaca, NY. Data are species means ± standard error for seven co-occurring Asteraceae species (n = 9 per species, per treatment). Species abbreviations are the first two letters of the genus and species epithet given in *Materials and Methods*.

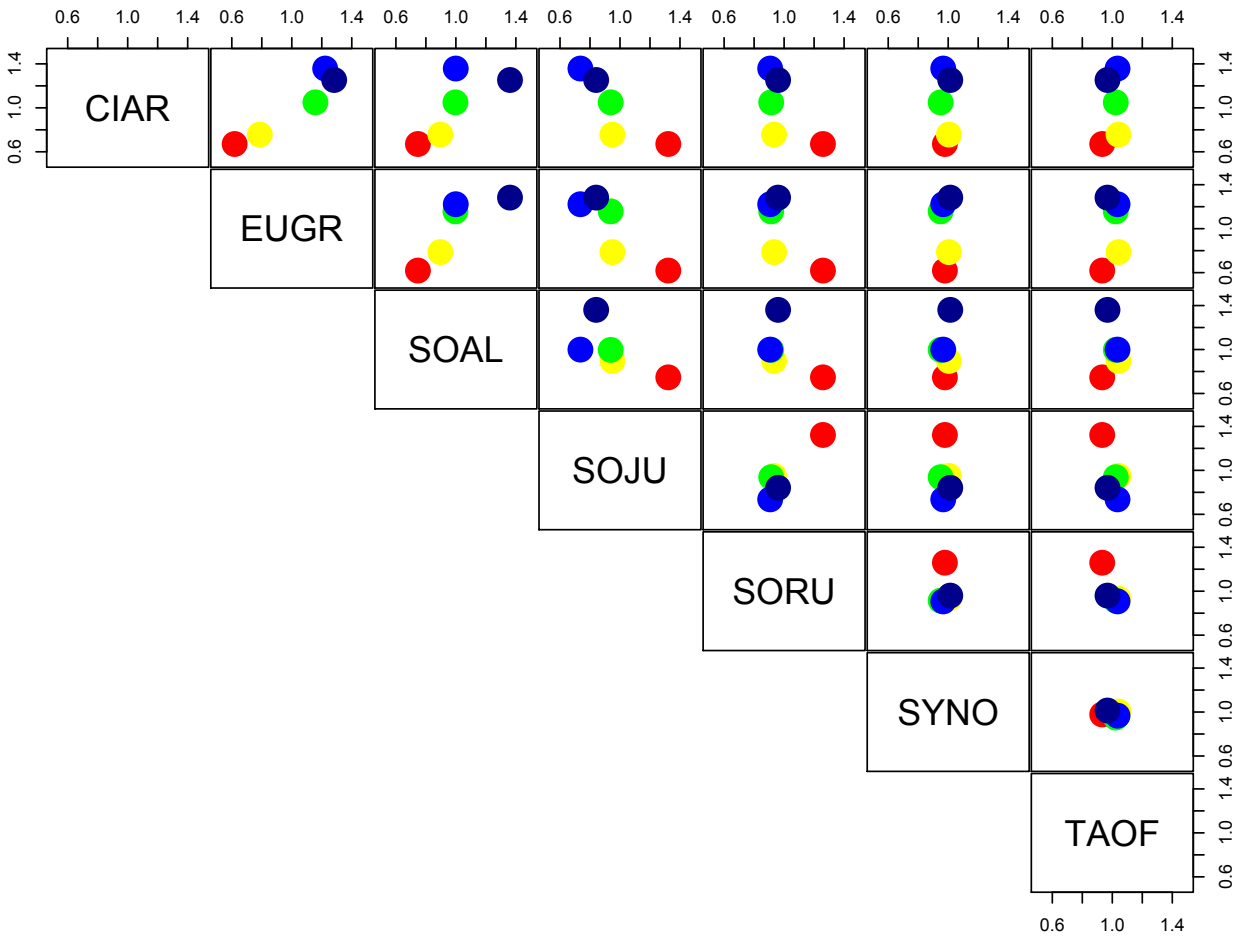

Figure A3.5: Pair-wise species relationships between aboveground biomass (standardized) across five experimental water treatments that span a gradient from the driest ('treatment 1') to the wettest ('treatment 5') year on record from the last 30 years in Ithaca, NY. Data are species means ± standard error for seven co-occurring Asteraceae species (n = 9 per species, per treatment). Species abbreviations are the first two letters of the genus and species epithet given in *Materials and Methods*.